Microbiota-Epithelial-Eosinophil Interactions in the Gut

HARVARD UNIVERSITY
Graduate School of Arts and Sciences

DISSERTATION ACCEPTANCE CERTIFICATE

The undersigned, appointed by the

Division of Medical Sciences

Committee on Immunology

have examined a dissertation entitled

Microbiota-Epithelial-Eosinophil Interactions in the Gut

presented by Yiyun Grace Cao

candidate for the degree of Doctor of Philosophy and hereby certify that it is worthy of acceptance.

Signature: Shiv Pillai
Typed Name: Dr. Shiv Pillai

Signature: Ruaidhrí Jackson
Typed Name: Dr. Ruaidhrí Jackson

Signature: Jose Ordovas-Montanes
Jose Ordovas-Montanes (Apr 30, 2022 12:30 EDT)
Typed Name: Dr. Jose Ordovas-Montanes

Signature: Daniel Mucida
Daniel Mucida (Apr 29, 2022 12:07 EDT)
Typed Name: Dr. Daniel Mucida

Date: April 15, 2022

Microbiota-Epithelial-Eosinophil Interactions in the Gut

A dissertation presented

by

Yiyun Grace Cao

to

The Division of Medical Sciences

in partial fulfillment of the requirements

for the degree of

Doctor of Philosophy

in the subject of

Immunology

Harvard University

Cambridge, Massachusetts

April 2022

Dissertation Advisor: Wendy S. Garrett Yiyun Grace Cao

Microbiota-Epithelial-Eosinophil Interactions in the Gut

Abstract

The gut is a critical interface between the host and its environment that requires a fine balance between nutrient absorption and barrier integrity in the face of exogenous dietary and microbial components. The intestinal epithelium, supported by interactions with intestinal immune cells, plays a central role in maintaining this equilibrium. Given their proximity to the gut lumen, the many specialized cell types of the epithelium sense and integrate external environmental signals. In this dissertation, I explore mechanisms by which intestinal epithelial cells (IECs) sense microbial components and relay signals to immune cells to regulate gut physiology.

Compared to the colon, microbiota-epithelial cell interactions in the small intestine are less well characterized. Using single-cell RNA sequencing of duodenal IECs under germ-free and different conventional microbiota compositions, we show that specific microbiota members alter epithelial homeostasis by increasing epithelial turnover rate, proliferation, and major histocompatibility complex class II expression. Microbiome profiling identified *Faecalibaculum rodentium* as a species that regulates these processes by decreasing retinoic acid-producing enzymes in enterocytes. Retinoic acid is required for the presence of certain intestinal eosinophil populations, which suppress interferon-γ production by intraepithelial lymphocytes that regulates epithelial cell function.

Another context in which IECs receiving microbial inputs influence gut immune cells is tuft cells in the ileum, which activate a type 2 immune response to commensal protozoa via an

interleukin-25, type 2 innate lymphoid cell, and interleukin-13-dependent pathway. We found that TAS1R3, a taste receptor expressed on intestinal tuft cells, is required for the induction of tuft cells in response to the protozoa *Tritrichomonas muris* and succinate. This requirement may be due to a severe reduction in tuft cells in the distal small intestine at homeostasis in *Tas1r3*$^{-/-}$ mice. Overall, this thesis elucidates two mechanisms by which IECs tune gut immune responses to microbial inputs in order to maintain gut homeostasis.

Table of Contents

Acknowledgements

Many people helped me along the path to my dissertation. First, I must thank my advisor, Wendy Garrett, for her faith in and support of me as an independent scientist. From the start, Wendy gave me the space to develop my own project on a strange and difficult cell type that the lab did not have experience in and stuck with me through all the challenges that arose. She is the most responsive person I know and has tirelessly and speedily read through all my drafts and emails, helping me to craft my ideas into a finished product. I would also like to thank my dissertation advisory committee, Vijay Kuchroo, Matt Waldor, and Peter Weller, for their encouragement and sound advice at my committee meetings. Thanks go also to my thesis defense committee, Ruaidhrí Jackson, Daniel Mucida, and Jose Ordovas-Montanes, for their time and feedback on this dissertation and my defense.

I would be remiss not to thank the previous mentors without whom I would not have been prepared to undertake a PhD. Bana Jabri and Cezary Ciszewski, thank you for patiently introducing me to immunology and planting the seeds of my interest in the gut. Carla Rothlin and Lidia Bosurgi, thank you for helping me to develop as an independent scientist and getting me excited about myeloid cells. I owe much of my achievements in graduate school and my decision to pursue a PhD at all to everything I learned from you.

My fellow members of the Garrett Lab have made my PhD a much more enjoyable and productive time. Michael Howitt, my rotation mentor, taught me to work with the gut and inspired my interest in tuft cells and epithelial cells in general. Monia Michaud kept the lab running and helped me and everyone else with great patience. Lior Lobel provided constant mentorship, support, and random fun facts as my baymate and collaborator, and contributed a lot to my scientific and personal growth. Eunyoung Chun, Slater Clay, Jen El Tekle, Kathrin Fenn, Diogo

Fonseca-Pereira, Sydney Lavoie, Daniel Nakatsu, and other past Garrett Lab members all were great sources of scientific advice and kept me sane during my PhD. Finally, thanks go especially to Sena Bae, who has been an amazing friend and cheerleader through the ups and downs of lab.

I would also like to thank my friends and family for their support on this long journey. My parents, Ping Li and Larry Cao, have always believed I could succeed at anything I put my mind to and encouraged me to pursue my dreams. My brother Jeffrey has cheered me on at every step of the way. I am also grateful to friends old and new who have kept me company and reminded me that there is more to life than my PhD. Finally, to my partner Albert, thank you for the love, support, and care you show me every single day and inspiring me to achieve my best.

Chapter 1

Introduction

I. OVERVIEW

The gut is a barrier surface where exogenous substances including dietary and microbial factors must interact with the host in a tightly regulated manner. The gut must endow the host with necessary functions like nutrient uptake while preventing breaches that could lead to injury, infection, or maladaptive inflammation. Epithelial and immune cells are both critical for responding to the challenges of acquiring macronutrients and micronutrients from the environment and maintaining homeostasis in the face of environmental perturbation. While much has been learned about how a host's resident microbiota can shape epithelial and immune interactions, there remain large knowledge gaps regarding the effect of the microbiota of certain immune cell types and specific biogeographical regions of the gastrointestinal tract. In particular, the role of the microbiota in influencing epithelial and immune cells in the proximal small intestine is not fully characterized. Additionally, how the microbiota might influence eosinophils, an abundant but understudied immune cell in the gut, is not known. In this dissertation, I set out to characterize microbiota-epithelial cell-eosinophil interplay in order to understand how such interactions maintain intestinal homeostasis and might be dysregulated in the context of injury and inflammation.

II. MICROBIOTA-HOST INTERACTIONS

The microbiota is a key factor in shaping the physiology of gastrointestinal tract. Decades of research have shown that in addition to a highly appreciated role in immune cell modulation, the microbiota also controls many features of gut development and function. Germ-free (GF) mice, which lack a microbiota, have a thinner intestinal mucus layer; longer, thinner, and less vascularized intestinal villi; increased epithelial permeability; and reduced epithelial turnover rate.[1–5] The microbiota also plays critical roles in host metabolism by increasing nutrient

accessibility, such as by breaking down dietary fiber into short-chain fatty acids that can be used by colonocytes.[6]

The microbiota indelibly shapes the immune system. At a macroscopic level, GF mice have smaller secondary and tertiary lymphoid organs including Peyer's patches, mesenteric lymph nodes and isolated lymphoid follicles.[4] Their immune compartments are also highly altered, with fewer adaptive immune cells including $CD4^+$ T cells and IgA-producing B cells.[7] Some of these effects have been attributed to specific symbionts, such as segmented filamentous bacteria that induce Th17 differentiation[8,9] and *Clostridia* species and *Bacteroides fragilis* that induce regulatory T cells (Tregs).[10,11] Aside from adaptive immunity, the microbiota also shapes innate cells, as demonstrated by fewer CX_3CR1^+ dendritic cells and an altered transcriptional and epigenetic landscape in innate lymphoid cells (ILCs) in GF mice.[12,13] While much has been uncovered about the influence of the microbiota on immune cells, only a small slice of which has been discussed here, much also remains to be done, and it is likely that the microbiota affects the development or function of most immune cell types.

The contribution of different members of the gut microbiota is an area of high interest and importance for attributing causality in microbiota-dependent effects. Major bacterial phyla found in the gut microbiota in humans and mice include Bacteroidetes, Firmicutes, Actinobacteria, Proteobacteria, and Verrucomicrobia, among others.[14] Viruses, fungi, and protozoa are also part of the microbiota and have major contributions, though they have been less well characterized compared to their bacterial counterparts to date.[15–17] Germ-free mice have been crucial in furthering mechanistic understanding of microbiota components by allowing for colonization with a single or defined mix of microbes. Large screens of bacterial monocolonization and immune

phenotyping have shed light on the specific immunomodulatory effects of some bacteria beyond a few well-studied species[18], but many bacteria in the microbiota remain poorly characterized.

One family of bacteria that is abundant in mouse and human gut and beginning to garner attention as immune modulators is *Erysipelotrichaceae*, which are anaerobic bacteria in the phylum Firmicutes. This family is highly coated in IgA in the gut, suggesting a potential immunogenic function.[19] Some notable genera within *Erysipelotrichaceae* include *Allobaculum, Faecalibaculum,* and *Turicibacter*. *Allobaculum* has been associated with resistance to weight gain and Th17 cell induction, as well as increased susceptibility to experimental autoimmune encephalitis.[20,21] *Faecalibaculum* can protect against intestinal tumor growth via short-chain fatty acid-mediated inhibition of tumor cell proliferation.[22] *Turicibacter sanguinis* can take up host-derived serotonin, which helps its colonization of the gut, where it can modulate lipid metabolism.[23] The emerging roles of these *Erysipelotrichaceae* family members suggest they are important regulators of host physiology and immunity worth further study.

Gut and microbiota biogeography

The structure and contents of the gastrointestinal tract change significantly along its length based on the requirements for achieving differing functions. Broadly speaking, the small intestine absorbs macro- and micronutrients, while the colon is a site for bacterial fermentation and fluid and electrolyte reabsorption. Thus, the small intestine has long villi to maximize absorption capacity, as well as much more rapid transit time as a result of contractions that mix digestive juices with food.[24] Each region of the small intestine is also further specialized. The most proximal region of the small intestine, the duodenum, receives bile and pancreatic inputs to facilitate digestion. These inputs as well as chyme from the stomach result in an acidic pH. The duodenum also has a thinner mucus layer to permit absorption of proteins, carbohydrates, and lipids.[25] The

next region, the jejunum, shares many properties of the duodenum and is also a major site of absorption. The final and most distal part of the small intestine, the ileum, has a different functional role in absorbing B vitamins and bile acids secreted into proximal regions. One transcription factor important for maintaining jejunal identity is GATA4, loss of which results in epithelial cells taking on a more ileal-like identity and dysregulation of microbiota and intraepithelial lymphocyte interactions.[26,27]

As a result of these changes in environmental conditions, the gut microbiota also varies significantly in composition and density along the gastrointestinal tract. Bacterial load increases from the proximal to distal small intestine and is highest in the colon, as a gradient of increasing pH, decreasing antimicrobial peptide and oxygen levels, and slower colonic transit time makes the distal small intestine and colon suitable for colonization by more bacteria.[14] Correspondingly, bacterial diversity also increases in distal regions.

The variations in dietary components and microbiota density in different regions of the gut result in changes in immune cell populations. The small intestine has a higher dietary protein antigen load, whereas more antigens in the colon are microbial. Accordingly, $Foxp3^+$ regulatory T cells in the small intestinal lamina propria are reduced in the absence of dietary protein, while in the colon they are reduced in the absence of a microbiota.[10,28] The colon also has a higher proportion of regulatory T cells compared to the small intestine, which is inversely correlated with the abundance of Th17 cells that are enriched in the small intestine.[29,30] This difference may be linked to differences in subsets of dendritic cells (DCs). The small intestine contains more $CD103^+CD11b^+$ DCs, which can induce Th17 differentiation, while the colon contains more $CD103^+CD11b^-$ DCs.[29,31] The increased number of $CD103^+CD11b^+$ DCs is partly due to higher production of the vitamin A metabolite retinoic acid in the small intestine, particularly

proximally.[32,33] Retinoic acid produced by DCs also plays a role in the homing of IgA^+ plasma cells to the small intestine, but not colon, via CCR9 induction.[34] IgA responses themselves differ between the small intestine and colon, with different IgA plasma cell clones expanded in small intestine and colon, as well as overall higher titers of IgA and higher levels of IgA-coated bacteria in the small intestine.[35,36] In addition to the lamina propria, changes are also seen in the epithelial compartment, with the small intestine containing more intraepithelial lymphocytes (IELs) than the colon, with the highest number in the proximal small intestine.[29,30] This gradient may be due to higher retinoic acid levels in the proximal small intestine, as well higher expression of butyrophilin-like molecules on enterocytes, which help recruit IELs.[37] The regional specificity of the immune response influences the diseases that may develop. Celiac disease, characterized by IEL-mediated inflammation targeting dietary gluten, affects the proximal small intestine, while inflammatory bowel diseases, caused in part by a breakdown of microbiota, are more prevalent in the colon and distal small intestine.[29]

The higher density and diversity of bacteria found in the colon has led to a greater focus on colonic microbiota. However, more recent studies have identified distinct roles for small intestinal microbiota in host physiology as well.[25] For instance, the small intestinal (jejunal) microbiota regulates dietary lipid absorption by proximal small intestinal IECs.[38] The ileal microbiota also promotes reabsorption of bile acids[39], as well as inducing a variety of immune cells and antimicrobial peptides.[25] These studies suggest that an improved regional understanding of microbiota composition and function would aid the elucidation of their role in host health and disease.

III. EOSINOPHILS

Eosinophils were identified in the mid-1800s as blood cells containing dense cytoplasmic granules and named based on the staining of these granules by the acidic dye eosin.[40] Over the past two centuries, most eosinophil studies have focused on the cationic proteins that compose these granules and their toxic properties in contexts where eosinophils accumulate, particularly in parasitic and allergic responses.[41]

Inflammatory roles of eosinophils

These cationic granule proteins consist of major basic proteins (MBPs), eosinophil peroxidase (EPX), and ribonucleases (eosinophil cationic protein (ECP) and eosinophil-derived neurotoxin (EDN) in humans; eosinophil-associated ribonucleases (EARs) in mice), all of which have inflammatory functions. MBP1 can cause cell damage by aggregating and disrupting lipid bilayers of the plasma membrane.[42–44] EPX generates extracellularly-directed reactive oxygen species (ROS) using hydrogen peroxide.[45] Eosinophil RNases have cytotoxic properties as well, and can also recruit and activate dendritic cells.[46,47] These proteins can be released through piecemeal degranulation or from cell-free granules after cytolysis, as well as together with extracellular DNA "nets" to trap and kill bacteria.[48,49]

Elucidation of the properties of these granule proteins defined the eosinophil as an inflammatory effector cell.[50] Eosinophil degranulation is associated with epithelial damage in asthma, eosinophilic esophagitis, and ulcerative colitis.[51–53] Eosinophils can also promote inflammation by releasing cytokines including IL-13 and tumor necrosis factor alpha (TNFα), in part from pre-formed stores in granules.[54] However, if their sole function were inducing inflammation for host defense, which leads to disease when dysregulated, then one would expect that a lack of eosinophils would impair parasite expulsion and reduce allergic pathology. Yet studies using eosinophil-deficient mice revealed that worm expulsion was not impaired.[55]

Additionally, anti-IL-5 therapy in patients with mild to moderate asthma decreased blood and sputum eosinophil levels, but did not improve clinical outcomes.[56] These findings suggest that eosinophils, while associated with inflammatory conditions, may have a more nuanced role in immunity.

Homeostatic roles of eosinophils

In support for additional non-inflammatory roles for eosinophils, investigators have begun to identify eosinophils in substantial numbers in certain tissues at steady state. While earlier studies defined the gut, thymus, and uterus as eosinophil-rich organs, further investigation revealed that most organs contain some eosinophils at baseline, though with varying frequencies.[57,58] These tissue eosinophils serve critical homeostatic roles. For example, adipose tissue eosinophils regulate glucose homeostasis by producing IL-4/13 to maintain alternative activation of resident macrophages, and are similarly required for the development of beige fat.[59,60] In the bone marrow and gut, eosinophils support survival of plasma cells and promote IgA class-switching through IL-6, a proliferation-inducing ligand (APRIL), and transforming growth factor beta (TGF-β).[61–63] Small intestinal eosinophils also suppress IL-17 production by Th17 cells through production of IL-1 receptor antagonist (IL-1Ra).[64]

In addition to these homeostatic roles, eosinophils have also been recognized as key mediators of repair after tissue injury or infection. They rapidly accumulate in the liver after partial hepatectomy or carbon tetrachloride-induced injury, in the skeletal muscle after cardiotoxin injury, and in the uterine endometrium after *Chlamydia trachomatis* infection.[65–67] In all of these contexts, eosinophils are the primary producer of IL-4, and mice lacking either eosinophils or IL-4/13 signaling show impaired tissue repair. This impairment is due to the direct action of IL-4 on

hepatocytes, fibro-adipocyte progenitors, and endometrial stromal cells to promote proliferation and does not require IL-4 signaling in macrophages, which have also been implicated in repair. Together, these findings suggest the existence of multiple functional states in eosinophils. Broadly, these might be construed as pro-inflammatory functions mediated by cationic granule proteins and cytokines and pro-homeostatic functions mediated by other cytokines and growth factors. However, the signals that control divergent modes of eosinophil function remain unclear, and what is known is mainly limited to the classical eosinophil-regulating cytokines IL-5, GM-CSF, and CCL11, also known as eotaxin-1.

Intestinal eosinophils

A technically feasible and biologically interesting site in which to study the signals that regulate eosinophil phenotype in homeostasis is the gut, which contains the largest eosinophil population at steady state.[57] Intestinal eosinophils are most abundant in the proximal small intestine (duodenum and jejunum), with fewer in the ileum and especially colon, though these distal regions still contain a substantial fraction of eosinophils.[68] These cells regulate intestinal homeostasis by promoting the mucus barrier, supporting IgA production by plasma cells, and suppressing inflammatory Th1 and Th17 cells.[61,62,64,69] In this context, the roles of IL-5, GM-CSF, and CCL11 have been extensively studied. All three are required for intestinal eosinophil accumulation, although the effects of IL-5 and GM-CSF are secondary to a systemic decrease in eosinophil number.[57,70,71]

While undoubtedly important, the activity of these cytokines is insufficient to explain the diversity of eosinophil function. For example, GM-CSF appears to induce a conflicting array of effects in intestinal eosinophils. In the small intestine, it induces eosinophil production of IL-1Ra, which suppresses IL-17 production to restrain inflammation.[64] Further, after radiation-induced

damage of the small intestine, GM-CSF activates eosinophils recruited to the sub-mucosa to produce TGF-β that promotes fibrosis.[72] These functions could be considered largely anti-inflammatory, if not necessarily both homeostatic. However, during colitis, GM-CSF activates eosinophils to cause inflammatory tissue damage though EPX, IL-13, and TNFα production.[73] This spectrum of activity suggests that other signals in the gut may be integrated to determine the effect of this pleiotropic cytokine.

One such intestinal eosinophil-regulating signal is likely to be the gut microbiota. Although the microbiota is fundamental in shaping the gut immune system, little is known about its effect on eosinophils. The microbiota is not required for eosinophil accumulation in the gut, as intestinal eosinophils are present in both GF and prenatal (E19) mice.[57] Indeed, a recent study found that GF mice have higher intestinal eosinophil levels compared to SPF mice.[74] However, what microbial factors might be involved in eosinophil regulation, and how they affect eosinophil function, remain unknown.

Understanding how eosinophil functional states are controlled would shed light on the biology of eosinophils in homeostasis and how they become aberrantly activated in disease contexts. If signals regulating eosinophils are defined, they could lead to therapeutic targets to ameliorate eosinophil-driven inflammation in conditions like inflammatory bowel disease and eosinophilic esophagitis. Defining the role of eosinophils in epithelial proliferation could also lay the foundation for understanding how dysregulation of this process results in an impaired response to injury or increased tumorigenesis.

Eosinophils in disease

Inflammatory bowel diseases (IBD) are a group of autoimmune conditions which are characterized by inflammation of the intestine and are influenced by both genetic and environmental factors.

The two major subtypes of IBD are Crohn's disease, which is characterized by patchy inflammation that can involve the entire bowel wall and occur in any region of the intestine, and ulcerative colitis, which is characterized by a continuous pattern of inflammation beginning in the rectum and affect parts of the colon.[75] Increased peripheral and intestinal mucosal eosinophilia has long been noted in IBD, but whether they are beneficial or harmful is still not entirely clear.[76] While ileal and colonic biopsies from ulcerative colitis patients with active disease had more numerous and more activated eosinophils compared to healthy controls, patients with inactive disease had even more, suggesting that eosinophils could contribute to both inflammation and repair.[53] In mouse models, the absence of eosinophils can protect against dextran sodium sulfate (DSS) or T cell transfer-induced colitis, potentially due to reduced tissue damaging eosinophil granule proteins.[73,77] In these contexts, eosinophils are recruited and activated by CCL-11 and GM-CSF. Additionally, intestinal eosinophils could contribute to fibrosis seen in IBD, and have been observed in close relation to nerves in intestinal biopsies from IBD patients, raising the possibility they could contribute to enteric neural dysfunction.[78,79] However, other studies have shown a protective role for eosinophils. Mice lacking eosinophils have exacerbated colitis in three mouse models of colitis (DSS, oxazolone, and TNBS), due to an increased infiltration of neutrophils.[80] Eosinophils also promote resolution of inflammation induced by the decoy receptor IL-13Rα2 in DSS colitis.[81] The opposing roles for eosinophils observed in these studies implies that there could be different activation or functional states of eosinophils, which could be regulated by signals like the microbiota or diet, that explain their different roles.

Eosinophils are also a driver of eosinophilic esophagitis. While eosinophils are normally absent from the esophagus, in eosinophilic esophagitis, airborne or food allergens trigger their recruitment and result in allergic inflammation.[82] Although induction of signals mediating

eosinophil recruitment to the esophagus are not completely understood, they appear to include type 2 cytokines like IL-4, IL-5, and Il-13 as well as eotaxins that are chemoattractants for eosinophils.[83] Once recruited, these eosinophils can promote tissue remodeling and epithelial hyperplasia that can lead to fibrosis and strictures observed in the disease.[82] More interest has also emerged in the potential role of microbes in regulating eosinophils and epithelial cells in the development of eosinophilic esophagitis. *Proteobacteria* and *Campylobacter* were elevated in the esophageal microbiome of some patients, but their functional role is unknown.[84] Therefore, eosinophilic esophagitis is another context in which elucidation of interactions between microbiota, epithelial cells, and eosinophils is important for understanding disease pathology.

Finally, the role of eosinophils in colorectal cancer has further emerged in recent years. Increased eosinophils in the blood as well as increased tumor-infiltrating eosinophils are both associated with better colorectal cancer prognosis.[85,86] In mice, eosinophils also have anti-tumorigenic activity in colorectal cancer models, though the T cell-dependency of this activity appears to vary. One study found that eosinophil activation and degranulation can kill tumor cells independently of $CD8^+$ T cells in both genetic (Apc^{Min}) and colitis-associated (AOM-DSS) cancer models.[87] Another demonstrated that GM-CSF-activated eosinophils promote Th1 and $CD8^+$ T responses in genetic (Apc^{Min}) and injected flank tumor (MC38) models.[88] These differences may be due to different methods of eosinophil depletion (genetic vs. antibody-mediated) or tumor model (genetic vs. flank injected). Nonetheless, eosinophils have a crucial anti-tumorigenic role in colorectal cancer and understanding their regulation would also be relevant for cancer therapy.

While study of intestinal eosinophils has expanded greatly in recent years, advances may be limited by the technical challenges of working with eosinophils.[89] Due to the abundant RNases found in eosinophil granules, it is difficult to isolate large amounts of high quality RNA from

eosinophils, making both targeted gene expression analysis and sequencing efforts, particularly single cell RNAseq, challenging. Eosinophils from the intestine also have a more activated phenotype than other tissues at baseline and are not easily culturable *ex vivo* after isolation. These technical limitations point to a need for development of alternative or specialized methods to permit more functional studies of eosinophils.

IV. INTESTINAL EPITHELIAL CELLS

The intestinal epithelium consists of specialized cell types with key functions in nutrient uptake, barrier integrity, and an increasingly recognized role in host defense.[90–92] Intestinal epithelial cells (IECs) differentiate from intestinal stem cells (ISCs) found in the intestinal crypt into either absorptive enterocytes for nutrient uptake, M cells that facilitate luminal antigen sampling above Peyer's patches, or one of the secretory lineages, which include goblet, Paneth, enteroendocrine, and tuft cells. As the cells differentiate and mature, they move from the crypts towards the villus tip and are eventually shed, with a turnover rate of about 3-5 days. Single cell sequencing of mouse and human IECs has provided further granularity on these cell types, with subsets of many cell types being described, as well as regional differences between the small intestine and colon.[93,94]

IECs form a critical interface with the gut microbiota, both forming a barrier to segregate the host from environmental insults as well as integrating signals to be transmitted. Epithelial tight junction proteins turn IECs into a physical barrier with low intestinal permeability at steady state. Additionally, goblet cells secrete mucins to form a mucus layer overlying the epithelium, and Paneth cells produce antimicrobial peptides to create a chemical defense.[95] However, IECs are also direct sensors of dietary and microbial signals in the gut and can relay these signals to immune cells. This communication can involve the passage of antigens, in the case of both M cells which pass antigen to immune cells in Peyer's patches and goblet cells which transmit luminal antigen to

dendritic cells in the lamina propria to promote immune tolerance.[96] It can also involve the sensing of microbial metabolites, such as short chain fatty acids, secondary bile acids, and tryptophan metabolites, which can both directly affect IEC function and regulate intestinal immune cells.[97,98] Additionally, dietary components such as retinol (vitamin A) are taken up by epithelial cells, and can be converted to the immune-modulating metabolite retinoic acid either by IECs themselves or by intestinal dendritic cells.[99] Aside from metabolic signals, the microbiota can also influence intestinal epithelial cell (IEC) function by inducing the expression of antigen-presenting MHCII molecules[100], regulating the frequency of different epithelial subsets, including tuft and goblet cells[101–103], and increasing the rate of homeostatic epithelial turnover.[5]

Epithelial turnover rate

The intestinal epithelium has the highest turnover rate in adult animals, and its rate of turnover is tightly controlled to maintain barrier integrity. Wnt signaling in stem cells and transit amplifying cells in the intestinal crypts is the major regulator of proliferative activity, with signaling decreasing in a gradient up the crypt axis.[104] However, other signal inputs from immune cells and environmental factors like the diet and microbiota can also affect epithelial cell turnover. GF mice have slower epithelial turnover rate compared to conventionally-raised mice, but the microbial inputs are not completely understood.[5] Short chain fatty acids, a microbial metabolite, can increase epithelial turnover rate, as can lactate produced by the microbiota.[105–107] Type 1 interferons produced after viral infection can also promote faster epithelial turnover via a pathway requiring macrophages.[108] Other immune cell inputs include B cells, which can reduce turnover rate, and γδ T cells, which increase it.[109,110] Changes in turnover rate can affect host fitness. For example, an increased epithelial turnover rate can act as a form of resistance to infection by helminth parasites by promoting their expulsion.[111] Regulation of turnover rate is also critical for repair after injury,

whether via infection or damage to proliferation cells via radiation or chemotherapy. However, it is possible that an excessive basal rate of turnover could increase the likelihood of aberrant proliferation leading to cancer. Thus, study of different inputs into epithelial turnover rate and how they are integrated is important for understanding epithelial function in both steady state and disease contexts.

Retinoic acid production by IECs

One way in which IECs can modulate intestinal immune function is via the uptake of retinol and production of retinoic acid (RA). Dietary retinol is absorbed by epithelial cells primarily in the proximal small intestine[32], where it can be esterified for transport and storage or processed into RA. Production of RA involves two enzymatic steps: first, conversion of retinol to retinaldehyde by alcohol or retinol dehydrogenases, followed by the irreversible conversion of retinaldehyde to RA by aldehyde dehydrogenases. Alcohol dehydrogenases are ubiquitously expressed, but aldehyde dehydrogenases have a more limited distribution which restricts the cell types that can produce retinoic acid.[112] In the intestine, the main cells which express aldehyde dehydrogenases are IECs, dendritic cells and macrophages, and stromal cells. Different isoforms are present in each cell type, with IECs primarily expressing *Aldh1a1,* DCs expressing *Aldh1a2,* and stromal cells expressing *Aldh1a1, Aldh1a2,* and *Aldh1a3*.[99] Thus, IECs are also important for passing retinol to other RA-producing cell types. Serum amyloid A proteins produced by the epithelium carry retinol from IECs to $CD11c^+$ myeloid cells, which take up the complex using the surface receptor LRP1.[113]

Retinoic acid has pleiotropic effects on intestinal immunity via signaling through the RAR and RXR receptors.[99,114] One major ability of RA is imprinting gut T cells, IgA-producing B cells, and ILCs with gut homing abilities by upregulation of the chemokine receptor CCR9 and α4β7

integrin[34,115,116], which is critical for the formation of gut immune responses. RA also controls the balance between different T helper cell subsets. It contributes to both Th17 and Treg differentiation, an apparently paradoxical observation that is explained by dose dependency: low levels of RA promote Th17 differentiation while high levels promote Treg differentiation.[117–122] Within the intraepithelial lymphocyte (IEL) compartment, RA together with transforming growth factor beta (TGF-β) promotes the conversion of $CD4^+$ IELs to a less inflammatory state.[123] Additionally, RA promotes ILC3 expansion while reducing ILC2s[124], and supports the survival and maturation of $CD11b^+CD103^+$ dendritic cells (DCs).[33] IEC-derived RA is crucial for promoting IL-22 production by both T cells and ILCs[125], whereas many other effects on T cells are thought to be dependent on DC-derived RA. Thus, further studying the contribution of RA produced by epithelial cells will be important to understanding the roles of this coordinator of many gut immune responses.

Intraepithelial lymphocyte-epithelial interactions

Intraepithelial lymphocytes (IELs) are a population of immune cells, comprising primarily T cells along with some innate lymphocytes, that are interspersed between epithelial cells in the intestine. These cells patrol the epithelium, with roles in both defense against pathogens as well as homeostatic interactions with epithelial cells and the microbiota. They represent one of the largest reservoirs of lymphocytes in the body, with an estimated 1 IEL per 10 IECs.[126] Considering their close proximity to and interactions with IECs, understanding IEL function is highly relevant to a gaining a full picture of IEC regulation.

IELs can be divided into $TCR\alpha\beta^+$ IELs, which mainly develop from naïve T cells encountering foreign antigen in the periphery often in Peyer's patches and are sometimes referred to as peripheral, induced, or conventional IELs; and $TCR\gamma\delta^+$ IELs, which are more innate-like and

develop after recognition of self-ligands, and are thus termed thymic, natural, or unconventional IELs.[126,127] TCRαβ$^+$ IELs can be further sub-divided into CD8αβ$^+$ IELs, which are similar to conventional tissue-resident CD8$^+$ T cells; CD4$^+$ IELs, which depend on MHCII expression by IECs[100,128]; and CD8αα$^+$ IELs, which are more similar to TCRγδ$^+$ IELs that share CD8αα expression and are innate-like. While natural IELs do not require the microbiota for their development, peripheral IELs are significantly reduced in GF mice.[127] In addition to these T cell populations, there are innate (non-T cell) IELs, including CD8αα$^+$ TCR$^-$ IELs and a minor population of ILC1s.

A major function of all IEL populations is the production of type 1 effector molecules such as IFN-γ, tumor necrosis factor (TNF)-α, and granzyme B.[126] These molecules can be induced by IL-12, IL-15, and IL-18 that can be produced by IECs as well as lamina propria antigen-presenting cells. Given that they share many of the same activation signals and effector molecules, there is some functional redundancy between different IEL subsets[126], which is also supported by the observation that TCRαβ$^+$ and TCRγδ$^+$ IELs have many transcriptional similarities.[129] However, differences in their developmental pathways and recruitment may allow for the generation of a multilayered immune defense.

IELs, IECs, and the microbiota interact with each other in a multitude of ways. Signaling through MyD88 downstream of toll-like receptors in IECs regulates multiple outputs of IELs, suggesting that the epithelium transduces microbial signals. These IEC-dependent functions include activation of TCRγδ$^+$ IELs in response to *Salmonella typhimurium*, specifically their production of the anti-microbial peptide RegIIIγ and altered patrolling behavior and metabolic state.[130,131] Production of IL-15 by IECs to recruit and activate IELs in the steady state also requires MyD88 signaling.[132] In turn, IELs can also regulate the turnover rate of IECs[110], and in conditions

such as celiac disease, kill IECs resulting in villous atrophy.[133] The interconnected nature of microbiota-IEL-IEC interactions suggests that considering them together is important for fully understanding their roles in both homeostasis and disease.

Tuft cells

Tuft cells are a type of secretory epithelial cell that comprise around ~1% of epithelial cells at homeostasis. Although long identified as a morphologically distinct epithelial cell type with a "tuft" of apical microvilli[134], their function and molecular characterization remained elusive until recently. They are chemosensory cells that express the canonical taste chemosensory components gustducin, 1-phosphatidylinositol 4,5-bisphosphate phosphodiesterase β-2 (PLCβ2), and transient receptor potential cation channel sub-family M member 5 (TRPM5), which transduce signals from taste chemosensory G protein coupled receptors (GPCRs).[135,136]

Tuft cells are required for the initiation of type 2 immune response to parasites in the gut. When mice are exposed to type 2 stimuli, including helminths and certain commensal protozoa such as *Tritrichomonas muris*, tuft cells produce interleukin (IL)-25 to activate group 2 innate lymphoid cells (ILC2s).[101,135,137] These ILC2s produce IL-13, which induces the differentiation of intestinal stem cells towards mucus-producing goblet cells as well as tuft cells themselves, thereby acting as a feed-forward signal to expand the type 2 immune response. Tuft cells can also produce cysteinyl leukotrienes to induce NFAT-dependent signaling in ILC2s, further enhancing their activation.[138] The initiation of this loop requires taste chemosensory signaling in tuft cells, as TRPM5-deficient animals do not mount a response.[101]

The identification of chemosensation-dependent activation of tuft cells led to a question of which GPCRs might be sensing parasite-derived signals to activate this pathway. Succinate, a Krebs cycle intermediate that can also be produced by microbes as a metabolic by-product, was

identified as one signal involved in this regulation. Tuft cells express the succinate receptor *Sucnr1*, which detects succinate produced by *Tritrichomonas* protozoa and activates a TRPM5-dependent signaling pathway to initiate type 2 immunity.[102,103,139] While helminths, including *Nippostrongylus brasiliensis,* can also produce succinate, *Sucnr1*$^{-/-}$ mice were not impaired in their response to them, suggesting that alternate receptors may be required for helminth sensing.[103] Indeed, Tas2r receptors, which sense bitter tastes, have been reported to be involved in tuft cell response to another helminth, *Trichinella spiralis*.[140] However, Tas2r receptor expression is not restricted to tuft cells. Ghrelin-secreting enteroendocrine cells in the stomach, which regulate hunger and food intake, can be activated by Tas2r agonists.[141] Paneth cells in human jejunum also express TAS2R43 and TAS2R10 and secrete defensins and lysozyme in response to Tas2r agonists.[142] Another taste receptor, Tas1r3, which can dimerize with Tas1r1 or Tas1r2 to sense umami and sweet tastes, was identified as being enriched in tuft cells in single cell RNA sequencing data.[93] These findings demonstrate the importance of chemosensory signaling in tuft and other epithelial cell responses and suggest that different receptors, potentially including other uncharacterized taste receptors, are required for sensing different microbial and dietary products.

Intestinal epithelial cells in disease

A disruption in intestinal epithelial cell homeostasis can lead to multiple different diseases, including IBD, celiac disease, and cancer. In particular, impaired barrier function is associated with IBD. Maintenance of barrier integrity is a major function of the intestinal epithelium, via production of mucus and anti-microbial peptides. Accordingly, genes associated with barrier function, including *MUC19, FUT2,* and *NOD2* have been linked to IBD pathogenesis by genome wide association studies.[143] The function of many of these genes is to maintain segregation of intestinal microbiota from the rest of the host. For example, *FUT2* (a fucosyltransferase) genotype

affects microbial community composition in Crohn's disease patients and in mice, disruption of *Fut2* and epithelial cell fucosylation leads to increased susceptibility to bacterial infection.[144,145] Another polymorphism in *ATG16L1*, a protein involved in autophagy and linked to Crohn's disease, causes dysfunction in Paneth cells, which are major producers of anti-microbial peptides.[146] *LYPD8*, which in mice has been shown to be expressed in colonic epithelial cells and prevent flagellated bacterial invasion into the inner mucus layer and epithelia, is also expressed at lower levels in some ulcerative colitis patients.[147] Thus, breakdown of any of the multifaceted ways in which the epithelium maintains barrier integrity can lead to increased susceptibility to intestinal inflammation and disease.

Injury to epithelial cells is also characteristic of celiac disease, an autoimmune disorder involving the development of an inflammatory T cell response to dietary gluten.[133] Cytotoxic IELs in celiac disease patients express elevated levels of the natural killer activating receptor NKG2D, which recognizes stress-induced ligands such as major histocompatibility complex (MHC) class I chain-related A (MICA) that are upregulated on celiac patients' IECs and kill them.[148] Another non-classical MHCI molecule upregulated on IECs in celiac disease is HLA-E[149], which can be recognized by NKG2C and CD94 on IELs and result in killing. This epithelial cell death leads to villous atrophy and crypt hyperplasia, and can result in deficient nutrient absorption and malnutrition.[133] Thus, an alteration to the finely balanced interaction between IELs and IECs can lead to injury to the intestine. In celiac disease, this altered balance is partly driven by an increased expression of IL-15, which licenses IELs to express activating receptors and kill IECs.[148] IL-21 also synergizes with IL-15 to active $CD8^+$ IELs.[133] A better understanding of what causes epithelial cell alterations in celiac disease would therefore aid in targeting future treatments.

Although the proliferative capacity of the intestinal epithelium is critical for its homeostatic function in barrier maintenance and ability to repair, excessive proliferation is also a danger. Activating mutations in the Wnt signaling pathway that controls epithelial stem cell proliferation are involved in most cases of colorectal cancer.[150] In the absence of signaling, a complex containing APC, CKI, GSK3, and Axin targets β-catenin for proteasomal degradation. Binding of Wnt ligands to Frizzled/LRP receptors inactivates the complex and activates β-catenin to form a transcriptional complex with TCF and results in the expression of Wnt target genes. Thus, mutations that activate Wnt signaling, such as via inactivation of the tumor suppressors APC or Axin2 or activation of β-catenin, are common in colorectal cancer.[104] Understanding how other inputs from immune cells or the microbiota can affect epithelial proliferation, potentially via regulation of Wnt signaling, could therefore help identify pathways that go awry during tumorigenesis.

V. DISSERTATION OBJECTIVES

In this dissertation, I set out to understand how the microbiota interacts with intestinal epithelial cells and eosinophils to maintain gut homeostasis, and how these mechanisms are also involved in inflammation. I focused in particular on the small intestine, where less is known about microbiota-host interactions. In **Chapter 2**, I investigated duodenal microbiota-epithelial-immune cell interactions and their impact on host physiology. Using single-cell RNA sequencing of duodenal IECs under germ-free (GF) and different conventional microbiota compositions, I found that specific microbiota components alter epithelial homeostasis by increasing epithelial turnover rate, crypt proliferation, and MHCII expression. This regulation is driven by *Faecalibaculum rodentium* and is dependent on a retinoic acid (RA)-eosinophil-interferon-γ-dependent pathway. Altogether,

this work reveals a mechanism by which specific microbiota members can regulate intestinal epithelial cell homeostasis via an immune cell-mediated circuit.

I also studied the mechanisms by which epithelial cells can sense microbiota and parasite signals by focusing on one subset of epithelial cells, the tuft cell. In **Chapter 3**, I characterize the function of the taste receptor Tas1r3 in tuft cell homeostasis. I found that *Tas1r3*$^{-/-}$ mice have fewer tuft cells at homeostasis and also have a weaker response to tuft cell-inducing stimuli. These findings identify a novel chemosensory receptor controlling intestinal tuft cells and their function in type 2 immunity.

In **Chapter 4**, I present some concluding views on how microbiota-epithelial-eosinophil interactions shape the homeostatic function of the gut as well as the response to injury or infection.

Chapter 2

Faecalibaculum rodentium Remodels Retinoic Acid Signaling to Govern Eosinophil- and Interferon-γ-dependent Intestinal Epithelial Homeostasis

This chapter is a reproduction of a manuscript in preparation with minor modifications.

Authors: Y. Grace Cao, Sena Bae, Jannely Villarreal, Madelyn Moy, Eunyoung Chun, Jessica K. Lang, Jonathan N. Glickman, Lior Lobel, and Wendy S. Garrett

Author Contributions: YGC, MM, EC, and LL performed experiments and analyzed data. SB and JV assisted with 16S rRNA gene amplicon sequencing. JL assisted with gnotobiotic experiments. JNG performed histological analysis. YGC and WSG designed experiments, interpreted data, and wrote the manuscript.

I. ABSTRACT

The intestinal epithelium plays critical roles in sensing and integrating dietary and microbial signals. How the interactions between the microbiota and intestinal epithelial cells (IECs) regulate host physiology in the proximal small intestine, particularly the duodenum, is unclear. Here, using single-cell RNA sequencing of duodenal IECs under germ-free (GF) and different conventional microbiota compositions, we show that specific microbiota members alter epithelial homeostasis by increasing epithelial turnover rate, crypt proliferation, and major histocompatibility complex class II (MHCII) expression. Microbiome profiling identified *Faecalibaculum rodentium* as a species that regulates these processes by decreasing retinoic acid-producing enzymes *Adh1, Aldh1a1,* and *Rdh7* in enterocytes. We found that retinoic acid is required for the presence of certain intestinal eosinophil populations, which suppress interferon-γ production by intraepithelial lymphocytes that regulates epithelial cell function. Thus, we identify a retinoic acid-eosinophil-interferon-γ-dependent circuit by which the microbiota modulates duodenal epithelial homeostasis.

II. INTRODUCTION

The intestinal epithelium consists of specialized cell types that function in nutrient uptake, barrier integrity, and host defense.[90–92] These cells are direct sensors of dietary and microbial signals in the gut, and can relay these signals, such as short chain fatty acids, secondary bile acids, and tryptophan metabolites, to intestinal immune cells.[97,98] The microbiota can also influence intestinal epithelial cell (IEC) function by inducing the expression of antigen-presenting MHCII molecules

[100], regulating the frequency of different epithelial subsets, including tuft and goblet cells[101–103], and increasing the rate of homeostatic epithelial turnover.[5]

Most host-microbiota studies of the intestinal epithelium have focused on the distal small intestine (ileum) or colon and often do not distinguish between different regions of the intestine, which vary dramatically in their physiological function and microbiota composition.[25,29] However, comparison of proximal and distal small intestinal epithelia has demonstrated regional specialization in gene expression, particularly in absorptive enterocytes.[93,94] The small intestinal microbiota also regulates dietary lipid absorption by proximal small intestinal IECs.[38] These studies suggest that proximal small intestinal microbiota and IECs have important differences as compared to more distal regions. In particular, the duodenum plays a pivotal role in host physiology and nutrient absorption. Given its location immediately distal to the stomach where it receives additional inputs from the pancreas and bile ducts, it is a special ecosystem for gut micro-organisms.[151] Despite the duodenum's susceptibility to injury, infection, chronic inflammation, and malignancy[152], it remains surprisingly under-explored in mucosal immunity.

Herein, using single cell RNA sequencing, we found microbiota-dependent differences in duodenal IEC gene expression, most notably in intestinal stem cells and enterocytes. The presence of certain bacteria in specific pathogen-free (SPF) mice increased epithelial cell proliferation and turnover by suppressing enterocyte retinoic acid production. This reduction in retinoic acid led to a loss of eosinophil populations, which constrain epithelial turnover via suppression of intraepithelial lymphocyte interferon (IFN)-γ production. These alterations in epithelial turnover and proliferation are associated with an impaired response to injury. Thus, we have identified a mechanism by which specific microbiota members including *F. rodentium* regulate duodenal epithelial homeostasis via a retinoic acid-eosinophil-IFN-γ circuit.

III. RESULTS

Certain microbiota members regulate intestinal stem cell proliferation and epithelial turnover

To begin to understand how the microbiota may regulate the duodenal epithelial cell compartment, we performed single cell RNA sequencing on duodenal IECs. As we and others have found differences in intestinal immune responses in mice from different vivaria[8,101,153], we harvested samples from germ-free (GF) and two different SPF groups of C57BL6/J mice – either purchased from Jackson Labs (Jax) or bred and maintained in our in-house (IH) facility. We identified all expected IEC cell types from the duodenum in all three microbiota conditions (**Fig. 2.1A**), with the exception of a low recovery of Paneth cells likely due to the increased difficulty of recovering cells with high granularity, and assigned identities based on previously described gene signatures.[93]

Figure 2.1. Certain microbiota features regulate intestinal stem cell proliferation and epithelial turnover

(A) UMAP representation of scRNAseq of sorted live $EpCAM^{+}CD45^{-}Ter119^{-}CD31^{-}$ epithelial cells. TA, transit amplifying; EEC, enteroendocrine. **(B)** GO categories for differentially expressed genes enriched in IH vs GF and Jax ISCs (dashed line indicates threshold for p value = 0.05). **(C)** Top differentially expressed genes in IH vs GF and Jax ISCs ranked by significance. **(D)** Representative histograms and quantification of MHCII MFI in ISCs. **(E)** Representative images (scale bar 50 μm) and **(F)** quantification of $Ki67^{+}$ cells across microbiota conditions. **(G)** Representative images (scale bar 50 μm) and **(H)** quantification of epithelial turnover after 48h continuous BrdU labeling via drinking water. Each symbol (D, F, H) represents data from an individual mouse. Data are pooled from 3 experiments (D, F, H). Data are shown as mean with individual data points. *$p < 0.05$, **$p < 0.01$, ***$p < 0.001$, Mann-Whitney U test (D), one-way ANOVA with Holm-Sidak's post-test (F, H).

Figure 2.1 (Continued)

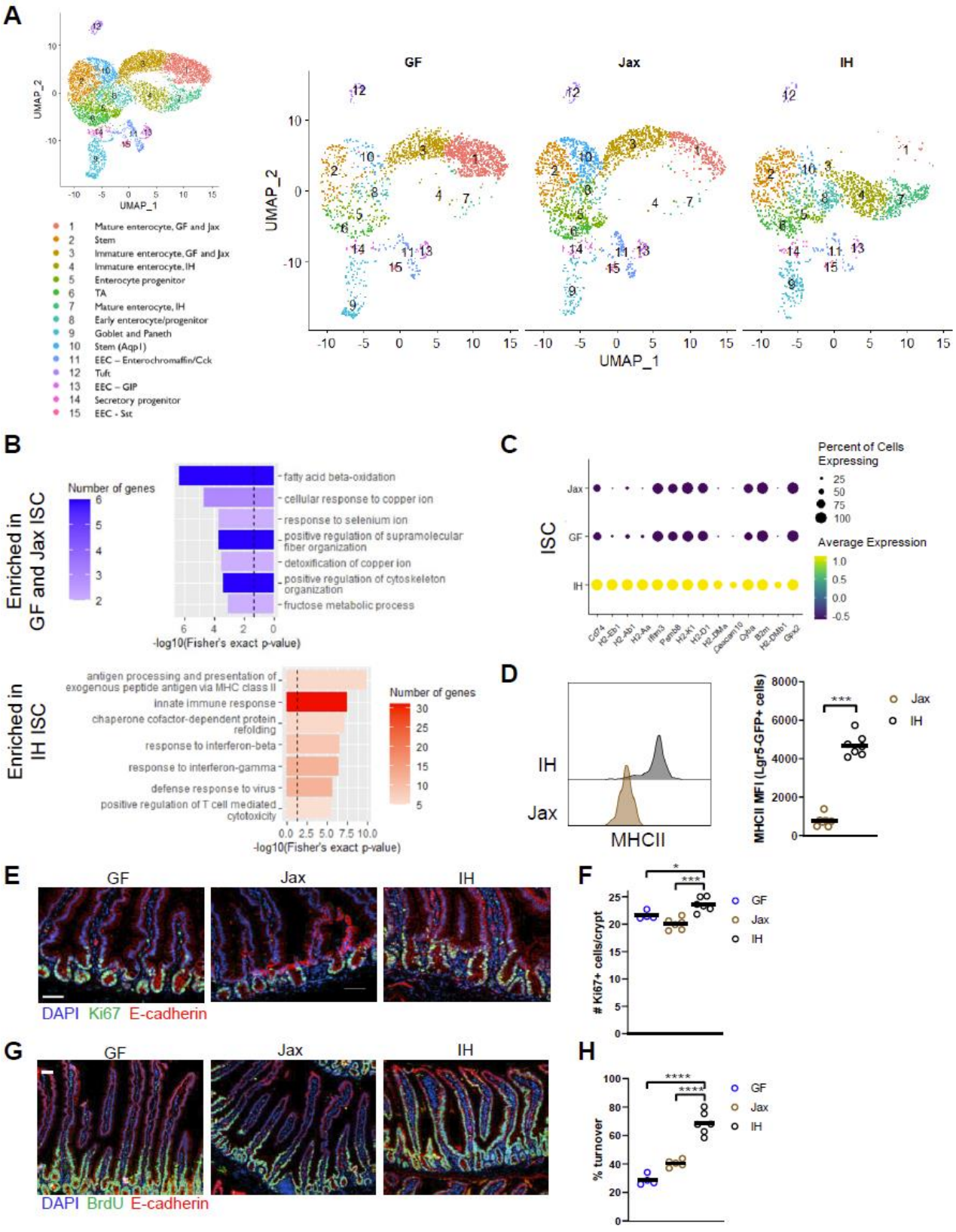

Initially, we focused our investigation on intestinal stem cells (ISCs), which give rise to all differentiated mature IECs. IH ISCs differed more from Jax/GF ISCs overall, with 209 significantly different genes between IH and Jax/GF ISCs, and only 60 genes when comparing Jax/IH to GF ISCs and 44 genes comparing Jax to GF ISCs. Gene ontology (GO) analysis of genes differentially expressed between GF and Jax vs. IH ISCs identified an enrichment in metabolic processes (including fatty acid and metal ion metabolism) in GF/Jax ISCs, while enriched categories in IH ISCs mostly related to immune responses (**Fig. 2.1B**). Most of the top differentially expressed genes, as ranked by significance, were related to major histocompatibility complex class II (MHCII) expression in IH ISCs (**Fig. 2.1C**). This finding is in line with the "response to interferon (IFN)-γ" category in IH ISCs (**Fig. 2.1B**), as IFN-γ can induce MHCII expression.[154] These differences in immune response genes were specific to IH ISCs, as differentially expressed genes in Jax versus GF ISCs were also mainly related to lipid and metal ion metabolism (**Fig. S2.1A-B**). These characteristics of IH ISCs also represent the most pronounced response to the microbiota, as comparing Jax/IH ISCs vs GF ISCs resulted in enrichment in immune response and MHCII transcriptional signatures similar to that seen in the IH vs GF/Jax comparison. These analyses support that most of the transcriptional differences attributable to the presence of a microbiota are driven by IH ISCs (**Fig. S2.1C-D**). To study the ISC compartment *in vivo*, we derived *Lgr5-GFP-creERT2* reporter mice, which express GFP in $Lgr5^+$ ISCs, onto a Jax or IH microbiota background. We did not observe a significant difference in the proportion of ISCs in Jax and IH mice by flow cytometry (**Fig. S2.1E-F**) but confirmed increased MHCII expression in IH ISCs (**Fig. 2.1D**). *Gpx2*, a gene with both pro- and anti-proliferative effects in stem cells and cancer[155–157], was also highly upregulated in IH ISCs (**Fig. 2.1C**), prompting us to investigate the proliferation of ISCs and epithelial turnover rate under the

different microbiota conditions. We measured crypt Ki67 expression, which marks all non-G0 phase cells, and performed 48 hours of continuous bromodeoxyuridine (BrdU) labeling, which is incorporated during DNA replication in the S phase, to measure epithelial turnover. IH mice had increased numbers of $Ki67^+$ cells in the crypts as well as a higher epithelial turnover rate compared to GF and Jax mice (**Fig. 2.1E-H**). Overall, we found that rather than the presence or absence of microbiota, it is microbiota composition that is critical for regulation of ISC proliferation and epithelial turnover. In particular, the IH but not Jax microbiota is able to induce MHCII expression, crypt proliferation, and increased epithelial turnover rate, indicating that only certain microbiota members possess this regulatory capacity.

The microbiota modulates intestinal immune populations via enterocyte retinoic acid production

We next examined the distinct mature IEC subsets that can arise from these differing ISCs, with a focus on absorptive enterocytes, where we observed the most pronounced differences. Unexpectedly, even though Jax and IH both possess SPF microbiota, their enterocytes had strikingly different gene expression profiles, with Jax enterocytes closely resembling the enterocytes derived from GF mice, resulting in their categorization into a separate cluster from IH enterocytes (**Fig. 2.1A**). GO analysis of differentially expressed genes in GF/Jax vs IH enterocytes revealed a similar pattern as seen in ISCs, with GF/Jax enterocytes enriched in fatty acid metabolism and IH enterocytes enriched in immune response pathways (**Fig. 2.2A**). The top differentially expressed genes enriched in IH enterocytes as ranked by significance included MHCII-related genes and defense response genes such as the anti-microbial peptide *Reg3g*, the mucin *Muc13*, and the microbiota-epithelial cell segregation-promoting *Lypd8* (**Fig. 2.2B**). As in

ISCs, the differences in immune response-related genes were specific to IH enterocytes, for comparison of Jax versus GF enterocytes from cluster 1 did not identify activation of immune pathways (**Fig. S2.2A-B**). Similarly, as expected due to the clustering of IH and Jax/GF enterocytes separately, most of the differences due to the microbiota identified when comparing Jax and IH vs GF enterocytes are driven by expression changes in IH enterocytes, with similar enriched categories and genes as observed when comparing IH to GF and Jax (**Fig. S2.2C-D**). We confirmed high MHCII expression in total epithelial cells from IH mice and low MHCII expression in GF and Jax IECs by flow cytometry (**Fig. 2.2C**). Among genes highly expressed in GF and Jax enterocytes, three are related to retinoic acid (RA) production (**Fig. 2.2B**): *Aldh1a1*, a aldehyde dehydrogenase that catalyzes the final conversion of retinaldehyde to retinoic acid, as well as the alcohol dehydrogenase *Adh1* and retinol dehydrogenase *Rdh7*, which can catalyze the upstream conversion of retinol to retinaldehyde.[158] Overall, IH enterocytes exhibited an immune activation phenotype, whereas GF and Jax enterocytes were enriched in expected metabolic processes and RA production, demonstrating that the specific composition of the microbiota is important in shaping epithelial cell function.

Figure 2.2. The microbiota modulates enterocyte phenotypes and retinoic acid production
(A) GO categories of differentially abundant genes in GF/Jax and IH enterocytes (clusters 1 and 7, dashed line indicates threshold for p value = 0.05). **(B)** Top differentially expressed genes in GF/Jax and IH enterocytes ranked by significance. **(C)** Quantification of MHCII MFI in total epithelial cells. **D)** mRNA expression in epithelial fraction. **(E-F)** Measurement of Aldh enzyme activity via Aldefluor assay in epithelial cells ($EpCAM^+CD45^-$) or dendritic cells ($CD45^+CD11c^+MHCII^+CD64^-$). Control samples included an Aldh inhibitor (DEAB) as baseline for fluorescent background. Gating strategy as in Fig. S1E and Fig. S3A.
Each symbol (C-F) represents data from an individual mouse. Data reflect at least 2 independent experiments (C-F). Data are shown as mean with individual data points. *$p < 0.05$, **$p < 0.01$, ***$p < 0.001$, ****$p < 0.0001$, one-way ANOVA with Holm-Sidak's post-test (C-F).

Figure 2.2 (Continued)

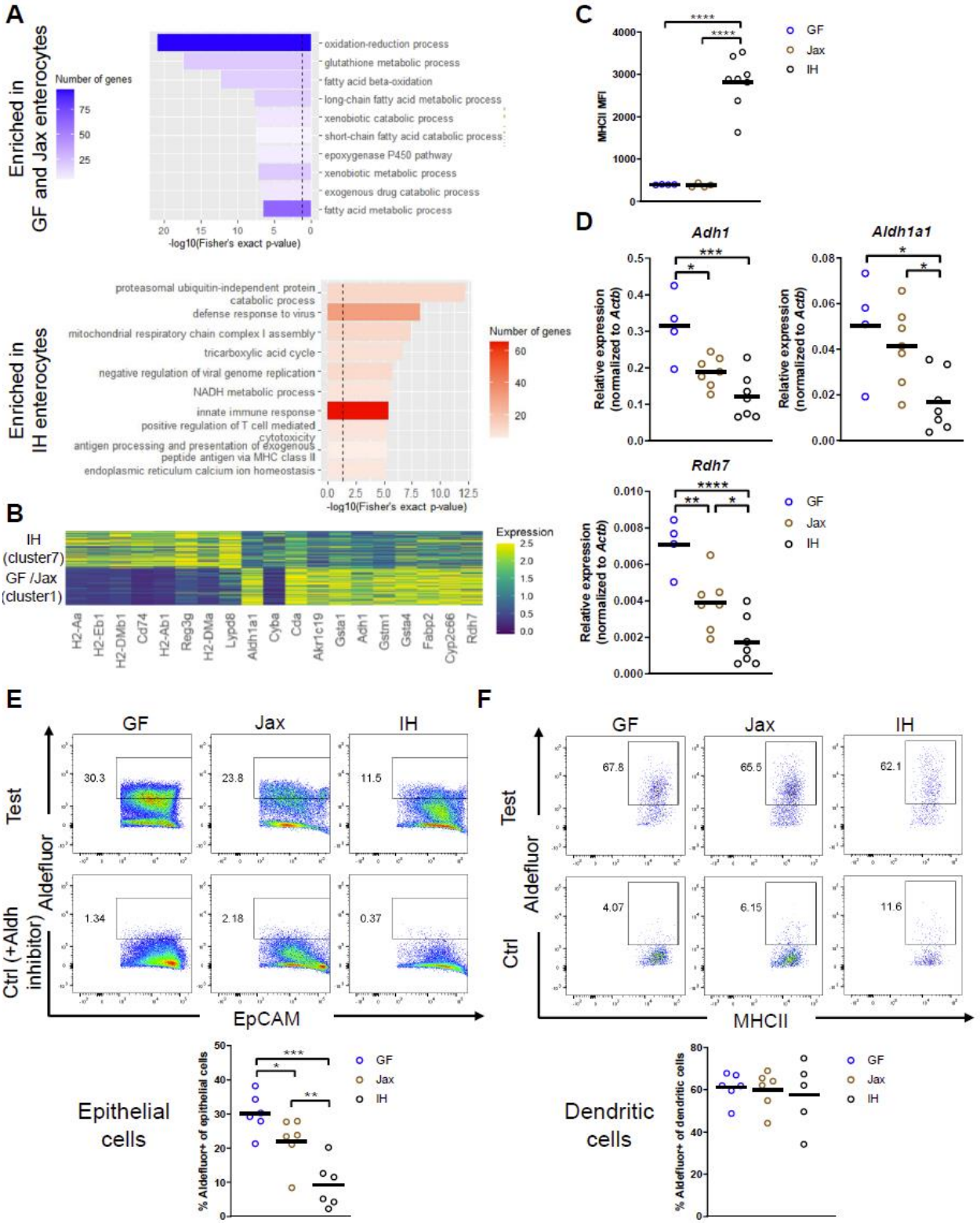

Dietary retinol (vitamin A) is absorbed by epithelial cells primarily in the proximal small intestine and then processed to RA[32], which affects intestinal immunity via signaling through the RAR and RXR receptors.[99,114] Some of these effects include: imprinting gut T, IgA-producing B, and innate lymphoid cells (ILCs) with gut homing abilities by upregulating the chemokine receptor CCR9 and α4β7 integrin[34,115,116], controlling the balance between different T helper cell as well as ILC subsets, and supporting the survival and maturation of $CD11b^{+}CD103^{+}$ dendritic cells (DCs).[112] We confirmed the decreased mRNA expression of the RA-producing enzymes *Adh1*, *Aldh1a1*, and *Rdh7* in IH mice by quantitative reverse-transcription polymerase chain reaction (qRT-PCR) (**Fig. 2.2D**). Next, we assessed whether differences in enzyme expression levels led to differential RA production using the Aldefluor assay, which measures Aldh activity. We found that GF IECs have the highest Aldh activity, and both GF and Jax IECs have higher Aldh activity than IH IECs ("Test" samples) (**Fig. 2.2E**). All IECs lacked Aldh activity in the presence of the Aldh inhibitor DEAB ("Ctrl" samples). The other major source of RA in the gut is DCs in the intestinal lamina propria, which also produce RA in a gradient fashion in the gut, with the highest levels in the duodenum.[32] Duodenal GF, Jax, and IH DCs produced similar levels of RA (**Fig. 2.2F**), suggesting that any differential levels of RA production or activity are likely due to epithelial-derived RA. Additionally, we found that while epithelial Aldh activity was also decreased in the jejunum and ileum of IH mice compared to Jax mice (**Fig. S2.2E-F**), overall Aldh

activity was highest in duodenal epithelial cells (about twice as high as jejunal and 4 times as high as ileal), consistent with previous reports.[32]

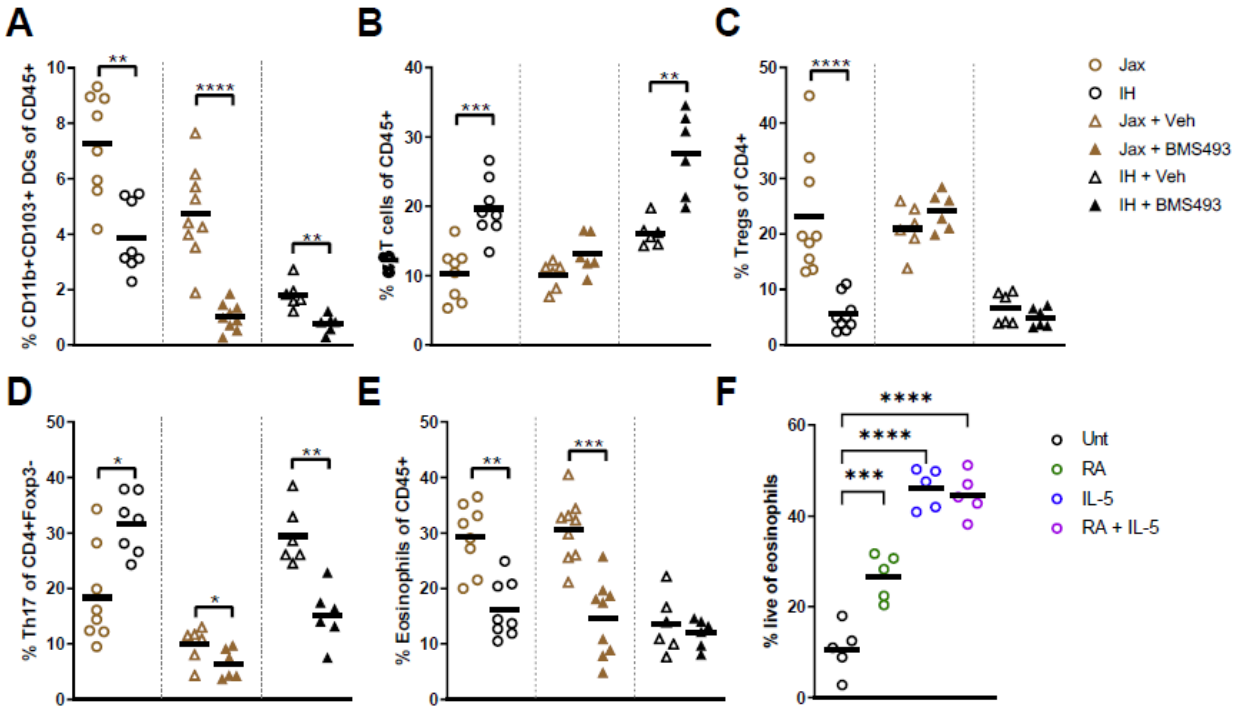

Figure 2.3. Differential epithelial cell production of retinoic acid in Jax and IH mice regulates intestinal immune populations

(A-E) Flow cytometric profiling of lamina propria immune populations at steady state, or after treatment with 220µg RAR inhibitor BMS493 or vehicle (DMSO) for 8 days. **(F)** Live eosinophils measured by flow cytometry after sorted bone marrow eosinophils were cultured for 24h with 10ng/mL IL-5, 100nM RA, or both.

Each symbol represents data from an individual mouse. Data reflect at least 2 independent experiments. Data are shown as mean with individual data points. *$p < 0.05$, **$p < 0.01$, ***$p < 0.001$, ****$p < 0.0001$, Mann-Whitney U test (A-E), one-way ANOVA with Holm-Sidak's post-test (F).

Given RA's roles in regulating intestinal immunity and its higher abundance in the proximal small intestine, we profiled duodenal lamina propria immune cell populations to determine the effect of epithelial-derived RA in Jax and IH mice (**Fig. 2.3, Fig. S2.3, Fig. S2.4A-M**). To determine which differences in Jax and IH immune cells are specific to RA, we administered the retinoic acid receptor inhibitor BMS493.[159] We found that compared to Jax mice, IH mice (with lower RA levels) had a lower proportion of $CD11b^{+}CD103^{+}$ DCs, which are known

to be dependent on RA[33] (**Fig. 2.3A**). As expected, inhibiting retinoic acid receptor signaling also decreased $CD11b^+CD103^+$ DCs in both Jax and IH mice. Intestinal Tregs and Th17 cells are also regulated by either high or low levels of RA.[117–121] IH mice had a higher proportion of total αβT cells and Th17 cells but lower Tregs than Jax mice (**Fig. 2.3B-D**). However, these differences do not seem to mainly depend on RA, as BMS493 treatment did not cause Jax αβT cells, Th17 cells, or Tregs to resemble IH proportions. Other cell types, including Th1, Th2, and ILC populations, also differed between Jax and IH mice, but again, these differences were not directly regulated by RA as BMS493 administration did not replicate the effect on their proportions (**Fig. S2.4A-M**).

Eosinophils, which are regulated by RA *in vitro* when isolated from human peripheral blood[160], were also significantly higher in Jax compared to IH mice (**Fig. 2.3E**). Retinoic acid receptor signaling inhibition decreased the eosinophils in Jax mice to IH proportions but had no effect on IH eosinophils. Unlike other immune cells dependent on RA such as $CD11b^+CD103^+$ DCs, Th17 cells, or ILC3s that decrease in both Jax and IH mice after BMS493 administration, only eosinophils exhibited this pattern of being decreased in Jax but not IH mice after treatment. To confirm that retinoic acid receptor (RAR) signaling occurs in eosinophils and is blocked by BMS493, we sorted proximal small intestinal eosinophils and measured the expression of select RAR and RAR target genes. Intestinal eosinophils express the RARs *Rara* and *Rarb*, and inhibiting RAR signaling decreased expression of the RA target gene *Tgm2*[161] (**Fig. S2.4N-O**). Using an *in vitro* system with eosinophils isolated from the bone marrow, we directly tested the effect of RA on eosinophil survival. Incubation with RA increased the survival of bone marrow eosinophils, though not to the same extent as observed with the classical eosinophil survival signal interleukin (IL)-5[162] (**Fig. 2.3F**). These results suggest that increased RA production in Jax mice increases eosinophil levels, potentially via enhanced survival, and is the main driver behind differential

eosinophil frequencies in Jax versus IH mice. Following inhibition of RAR signaling, we noted that some eosinophils remain in both groups, potentially suggesting an RA-independent cell state or subset of eosinophils. Thus, we demonstrate a new role for RA in regulating certain intestinal eosinophils and raise the possibility of different eosinophil cell states or subsets with varying dependence on RA.

Eosinophils regulate epithelial cell turnover and MHCII expression by suppressing IFN-γ-producing intraepithelial lymphocyte (IEL) subsets in a microbiota-dependent manner

The proximal small intestine, where we determined that eosinophils are regulated by RA, contains the highest levels of eosinophils in the gut, with fewer eosinophils found in the ileum and colon.[68] Eosinophils in other tissues have been implicated in promoting proliferation during the tissue repair process after injury or infection[65–67], and the intestinal epithelium is a highly proliferative tissue at steady state. Thus, we wondered if eosinophils may be responsible for the distinct epithelial proliferation phenotypes we observed in IH and Jax mice. To test this hypothesis, we used eosinophil-deficient PHIL mice derived onto either a Jax or IH microbiota background. As we initially observed, IH wild-type (WT) mice had a higher rate of epithelial turnover and more proliferating $Ki67^+$ crypt cells than Jax WT mice (**Figs. 2.1E-H, 2.4A-B**). On a Jax microbiota background, eosinophils had no effect on turnover or $Ki67^+$ cells (**Fig. 2.4A-B**). However, on an IH microbiota background, PHIL mice had increased epithelial turnover and $Ki67^+$ cells compared to WT mice. A similar pattern was observed in MHCII expression, with very low expression in both Jax WT and PHIL mice, higher expression in IH WT mice, and highest expression in IH PHIL mice (**Fig. 2.4C**). These results suggest that when there is little proliferative signal, as in Jax mice, eosinophils have no regulatory effect. However, when an increased proliferative signal is present,

eosinophils can act as a negative regulator to dampen excess proliferation. To determine if this difference in proliferation and turnover resulted in an impaired ability to respond to injury, we employed a model of small intestinal injury by injecting an anti-CD3 antibody that results in T cell-mediated damage to the epithelium.[163] Similar to the patterns in turnover, IH and especially IH PHIL mice had more extensive intestinal damage as evaluated in histological injury scores that was characterized by villous atrophy and crypt injury (**Fig. 2.4D-F**). Thus, excess proliferation in IH and IH PHIL mice might result in an increased sensitivity to inflammatory injury.

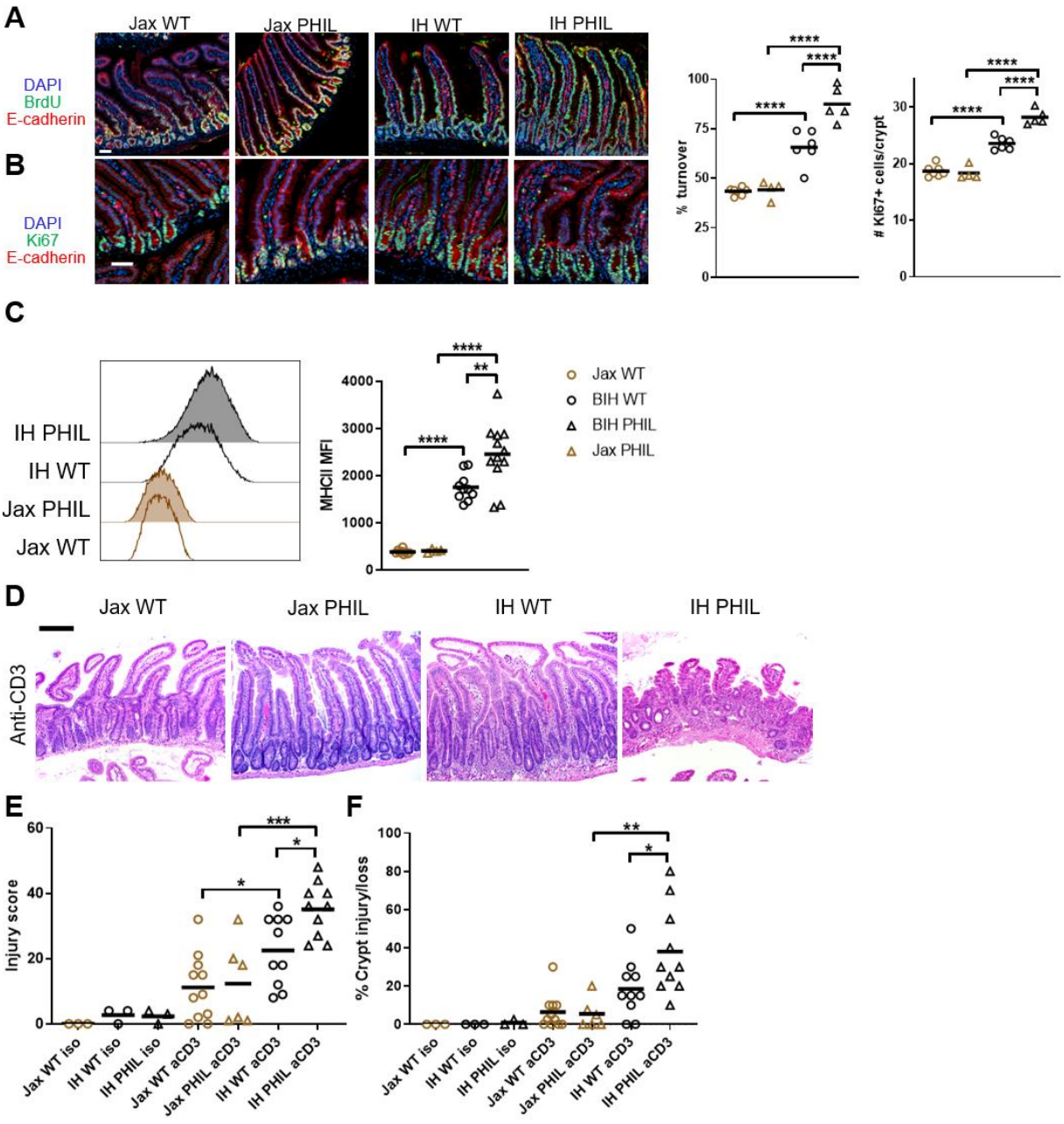

Figure 2.4. Eosinophils regulate epithelial cell turnover, MHCII expression, and response to injury

Representative images (scale bar 50 μm) and quantification of **(A)** Epithelial turnover after 48h continuous BrdU labeling via drinking water and **(B)** $Ki67^{+}$ cells measured by immunofluorescence. **(C)** MHCII expression on epithelial cells by flow cytometry. **(D)** Representative hematoxylin and eosin staining (scale bar 200 μM), **(E)** Histological injury score, and **(F)** Percent crypt injury/loss in duodenum on day 3 after injection of anti-CD3.

Each symbol represents data from an individual mouse. Data reflect at least 3 independent experiments. Data are shown as mean with individual data points. *p <= 0.05, **p < 0.01, ***p < 0.001, ****p < 0.0001, two-way ANOVA with Holm-Sidak's post-test.

Interferon (IFN)-γ can regulate IEC proliferation[164] and is also a well-known stimulator of MHCII expression, including in epithelial cells.[154] Eosinophils suppress IFN-γ production by lamina propria T cells in the colon and stomach[69] and response to IFN-γ was an enriched GO category in IH ISCs when compared to Jax and GF ISCs (Fig. 1B). Therefore, we measured *Ifng* mRNA levels in the epithelial and lamina propria fractions of Jax and IH WT and PHIL mice. In the epithelial fraction, which contains both epithelial cells and immune cells (most of which are intraepithelial lymphocytes (IELs)), we found that IH PHIL had the highest *Ifng* expression (**Fig. 2.5A**), mirroring the patterns in epithelial turnover and MHCII expression. No differences were observed in the lamina propria (**Fig. 2.5B**). This epithelial *Ifng* likely comes from IELs, which are the majority of immune cells in the epithelium and known IFN-γ producers[126], whereas epithelial cells do not produce IFN-γ under homeostatic conditions. Thus, we next characterized IEL subsets and their IFN-γ production. IELs can be divided into TCRαβ$^+$ IELs, which mainly develop from naïve T cells encountering foreign antigen in the periphery often in Peyer's patches, and TCRγδ$^+$ IELs, which are more innate-like and develop after recognition of self-ligands[126]. TCRαβ$^+$ IELs can be further sub-divided into CD8αβ$^+$ IELs, which are similar to conventional tissue-resident CD8$^+$ T cells; CD4$^+$ IELs, which depend on MHCII expression by IECs[100,128]; and CD8αα$^+$ IELs, which are similar to TCRγδ$^+$ IELs that share CD8αα expression. A majority of IELs in IH WT mice were TCRαβ$^+$, whereas Jax WT mice had a majority of TCRγδ$^+$ IELs (**Figs. 2.5C, S2.5**). Jax PHIL mice had a similar ratio of TCRαβ$^+$ to TCRγδ$^+$ IELs as Jax WT mice, but IH PHIL mice had even more TCRαβ$^+$ and fewer TCRγδ$^+$ IELs than IH WT mice. Within the TCRαβ$^+$ IEL subsets, IH mice had fewer CD8αα$^+$ IELs, more CD8αβ$^+$ IELs, and more CD4$^+$ IELs than Jax WT and PHIL mice (**Fig. 2.5D**), the latter of which correlates with increased MHCII expression in IH mice. IH PHIL mice had similar profiles to IH WT mice, with a particular additional increase in CD4$^+$

IELs, again correlated with highest MHCII expression in IH PHIL mice. Overall, these findings reflect a shift away from innate-like IELs towards more conventional, peripherally educated IELs in IH and especially IH PHIL mice compared to Jax mice. Analysis of IFN-γ production by flow cytometry showed that in IH PHIL mice, most IEL subsets produced more IFN-γ than in Jax WT and PHIL mice (**Fig. 2.5E**). Additionally, certain subsets, including total TCRαβ$^+$ IELs, CD8αβ$^+$ IELs, and CD4$^+$ IELs, produced more IFN-γ overall across all conditions compared to TCRγδ$^+$ and CD8αα$^+$ IELs. Therefore, increased IFN-γ production in IELs in IH PHIL mice is due to both a per cell increase in IFN-γ production as well as a shift in overall IEL populations to higher IFN-γ-producing subsets. Overall, we concluded that IH microbiota increases IFN-γ production in IELs and that eosinophils can suppress this change in IFN-γ production.

To determine if the increased IFN-γ production in IH and IH PHIL mice was a driver of differences in epithelial phenotype, we used a neutralizing antibody against IFN-γ. Blockade of IFN-γ abrogated the difference in epithelial turnover between IH WT and IH PHIL mice without affecting Ki67$^+$ crypt cells and also decreased MHCII expression (**Fig. 2.5F-H**). This difference in cell turnover versus Ki67$^+$ cells could be because Ki67 marks all non-G0 phase cells. ISCs often remain in a quiescent G1 phase[165], so a change in IFN-γ-dependent proliferation could occur without detection by Ki67 expression. Overall, these findings demonstrate that eosinophil restraint of epithelial turnover depends on suppression of IFN-γ.

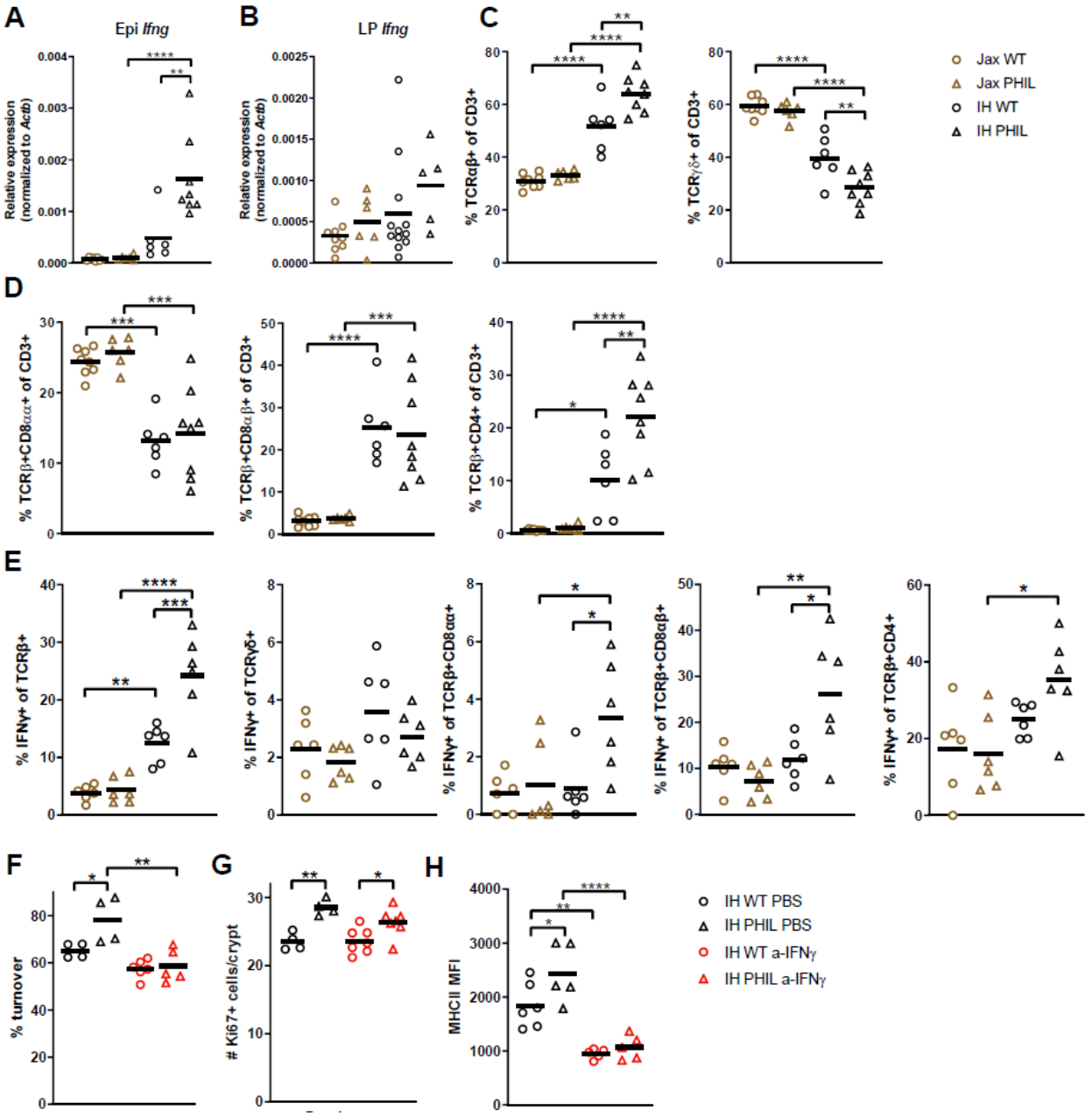

Figure 2.5. Eosinophils suppress IFN-γ-producing IEL subsets to regulate epithelial cell turnover and MHCII expression in a microbiota-dependent manner

(A) *Ifng* mRNA expression in epithelial fraction and **(B)** lamina propria. **(C-D)** Flow cytometric profiling of IEL populations. **(E)** IFN-γ production by IEL populations. **(F)** Epithelial turnover after 48h continuous BrdU labeling via drinking water, **(G)** Ki67^{+} cells, and **(H)** Epithelial cell MHCII expression in mice treated every other day for 8 days with 200μg anti-IFN-γ neutralizing antibody or PBS.

Each symbol represents data from an individual mouse. Data reflect at least 2 independent experiments. Data are shown as mean with individual data points. *p<0.05, **p < 0.01, ***p < 0.001, ****p < 0.0001, two-way ANOVA with Holm-Sidak's post-test.

IH microbiota member *Faecalibaculum* regulates RA-eosinophil-epithelial cell circuit

After observing that decreased RA production by IECs in IH mice results in fewer eosinophils, increased IFN-γ production, and increased turnover rates and MHCII expression in IECs, we sought to determine if these differences are inherent to Jax and IH mice or if they could be modulated by microbiota transfer. Because IH epithelial cells differed more from both Jax and GF IECs, we chose to transfer IH microbiota to Jax mice. A one-time gavage of IH stool or cecal contents in Jax mice resulted in reduced IEC *Adh1*, *Aldh1a1*, and *Rdh7* expression, decreased eosinophil proportion, and shifts in IEL composition toward more TCRαβ$^+$, CD8αβ$^+$, and CD4$^+$ IELs and increased IFN-γ production (**Fig. 2.6A-D**). As a result, MHCII expression and Ki67$^+$ crypt cells also increased after transfer, with a greater increase in Jax PHIL mice receiving IH contents compared to Jax WT recipients (**Fig. 2.6E-G**). The turnover rate was only slightly different between Jax WT and PHIL mice receiving the transfer, possibly because the newly-introduced IH microbiota induced a very high turnover rate reminiscent of baseline IH PHIL mice in both groups. Pre-treatment of IH mice with broad-spectrum antibiotics prior to transfer of their microbiota to Jax mice eliminated the regulatory activity of the transfer (**Fig. S2.6A**). Co-housing Jax and IH mice in the same cage also resulted in Jax mice taking on an IH phenotype (**Fig. S2.6B**). Collectively, these results indicate that antibiotic-sensitive member(s) of the IH microbiota responsible for RA-eosinophil-epithelial regulation can be transferred to Jax mice and confer immunomodulatory effects.

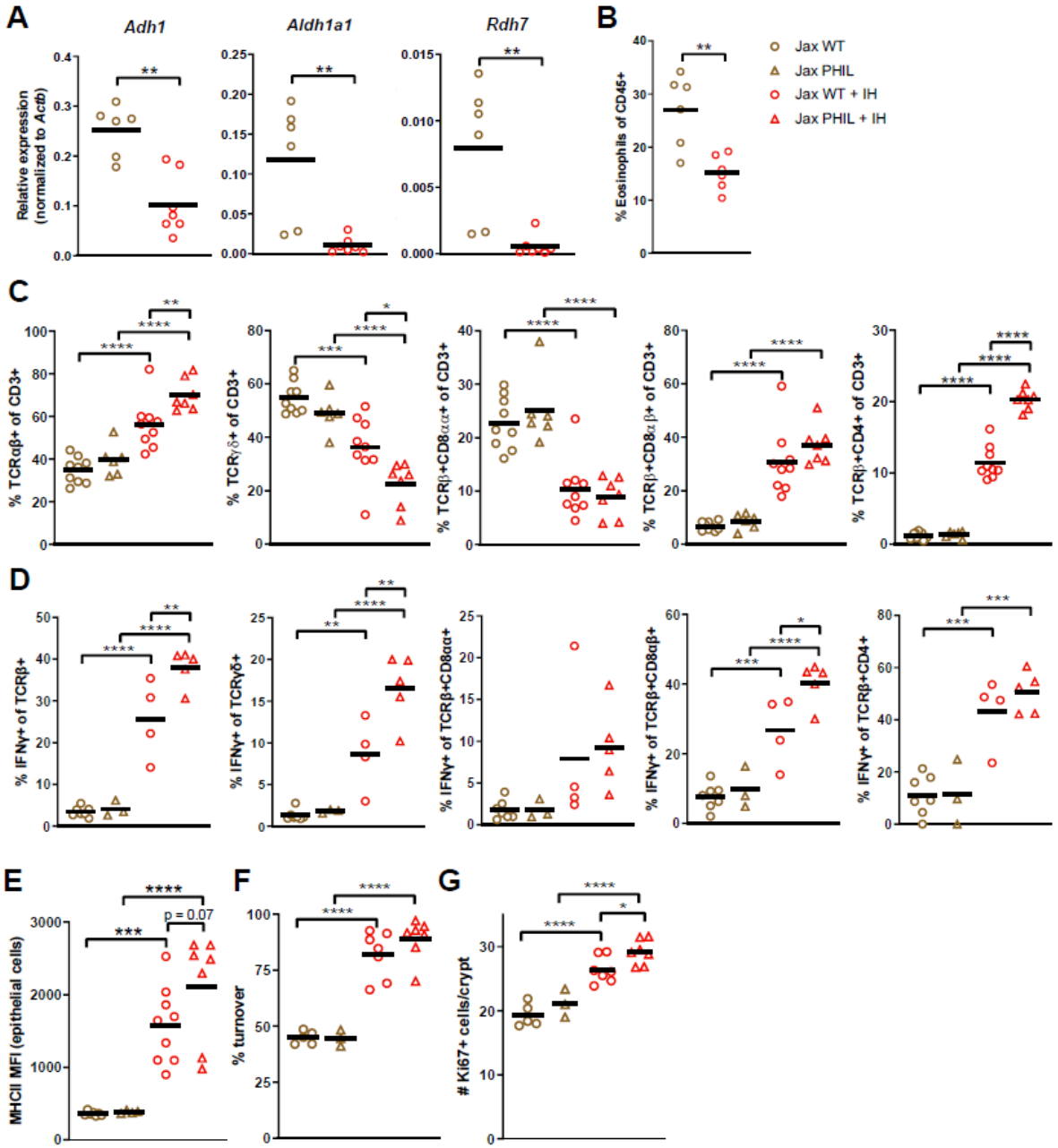

Figure 2.6. IH microbiota regulates epithelial-eosinophil crosstalk
Jax mice received transfer of IH microbiota contents and experiments were conducted at the indicated time-points. **(A)** mRNA expression in epithelial fraction 3 weeks post-transfer. **(B)** Eosinophils assessed by flow cytometry 2 weeks post-transfer. **(C)** IEL subsets and **(D)** IFN-g production by IEL populations assessed by flow cytometry 3 weeks post-transfer. **(E)** MHCII expression on epithelial cells 3 weeks post-transfer. **(F)** Epithelial turnover after 48h continuous BrdU labeling via drinking water and **(G)** Ki67^{+} cells 4 weeks post-transfer.
Each symbol represents data from an individual mouse. Data reflect at least 2 independent experiments. Data are shown as mean with individual data points. *p < 0.05, **p < 0.01, ***p < 0.001, ****p < 0.0001, Mann-Whitney U test (A-B), two-way ANOVA with Holm-Sidak's post-test (C-G).

To pinpoint which component of the IH microbiota is responsible for the microbiota's regulatory capacity, we performed 16S rRNA gene amplicon sequencing of stool from Jax and IH mice from various experimental conditions previously tested: Jax and IH alone, Jax and IH after co-housing, Jax after transfer of IH microbiota, and Jax after transfer of microbiota of IH mice pre-treated with antibiotics. Since both cohousing and direct microbiota transfer recapitulated the IH-like RA-eosinophil-epithelial regulatory capacity in Jax mice, we focused our attention on any bacterial species that were absent in Jax mice and Jax mice receiving antibiotic-treated IH microbiota but present in the other groups. Principal coordinates analysis revealed that the microbiome communities clustered into two groups, with one group comprising samples from high RA/high eosinophil/low epithelial turnover mice (Jax and Jax with Abx-treated IH transfer) and the second comprising low RA/low eosinophil/high epithelial turnover mice (IH, IH cohoused, Jax cohoused, and Jax with IH transfer) (**Fig. S2.7A**). Differentially abundant bacterial genera that distinguish these two groups were identified using linear discriminant analysis effect size (LEfSe) analysis, which identifies features likely to explain the biological differences between groups[166] (**Fig. 2.7A**). In particular, *Bifidobacterium, Faecalibaculum,* and *Lachnospiraceae A2* genera were enriched in IH mice and Jax mice with IH cohousing/transfer compared to Jax, which was confirmed by qPCR on stool samples (**Fig. 2.7B**). *Bifidobacterium* and *Faecalibaculum* were also detected in the duodenal lumenal contents of IH mice (**Fig. 2.7B**), raising the possibility of a direct local effect on the epithelial-immune interactions we observed.

To investigate if any of these identified bacteria can regulate epithelial cell phenotypes, we monocolonized GF mice with strains of these genera that we isolated from IH mice: *Bifidobacterium pseudolongum*, *Faecalibaculum rodentium*, and *Lachnospiraceae A2. B. pseudolongum* and *F. rodentium* but not *Lachnospiraceae A2* successfully monocolonized GF

mice (**Fig. S2.7B**). *F. rodentium* alone was able to reduce *Aldh1a1* expression and eosinophil proportions compared to GF mice, thereby increasing epithelial turnover and $Ki67^+$ crypt cells (**Fig. 2.7C-F**). *B. pseudolongum* reduced *Adh1* expression but did not affect eosinophils or epithelial turnover, perhaps because other enzymes are able to compensate for *Adh1* activity, whereas only *Aldh1a1* in epithelial cells can catalyze the conversion of retinaldehyde to retinoic acid. Thus, *F. rodentium* is one IH microbiota member which is sufficient to recapitulate its RA-eosinophil-epithelial regulation, though other components, including *B. pseudolongum*, likely also play a role in a full SPF microbiota.

Figure 2.7. 16S rRNA gene amplicon survey analysis identifies *Faecalibaculum* as a regulator of a retinoic acid-eosinophil-epithelial circuit

(A) Heatmap of differentially abundant genera identified by LefSE analysis of 16S rRNA gene amplicon sequencing of stool from different IH and Jax housing and transfer conditions. **(B)** Colonization levels in different gut regions determined by qPCR. **(C-F)** GF mice were mono-colonized for 2 weeks. **(C)** mRNA expression in epithelial fraction. **(D)** Eosinophil levels measured by flow cytometry. **(E)** Epithelial turnover after 48h continuous BrdU labeling via drinking water. **(F)** $Ki67^+$ cells. Each symbol (B-F) represents data from an individual mouse. Data reflect at least 2 independent experiments. Data are shown as mean with individual data points. *$p < 0.05$, Mann-Whitney U test (B), one-way ANOVA with Holm-Sidak's post-test (C-F).

Figure 2.7 (Continued)

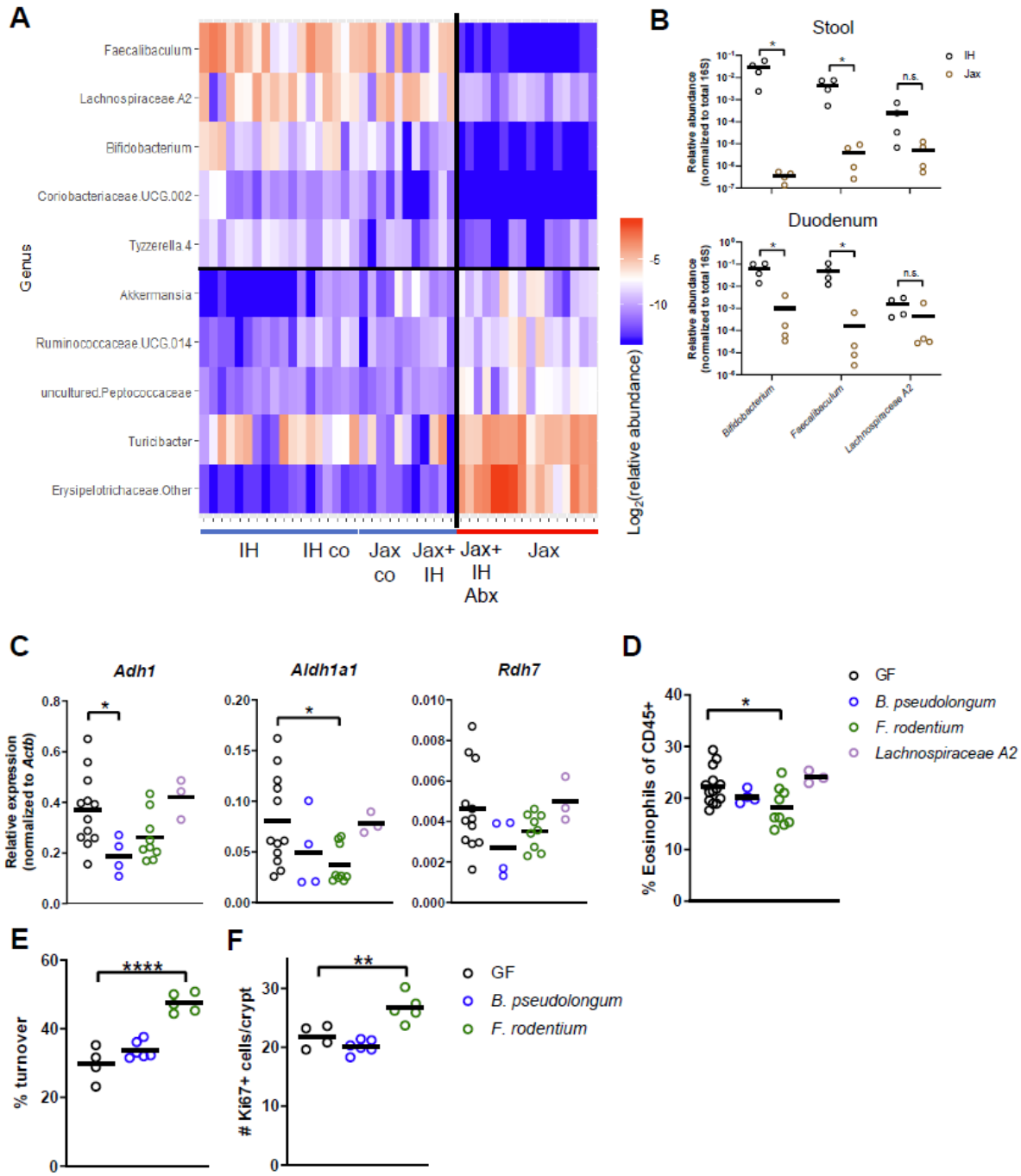

IV. DISCUSSION

In this study, we uncovered a retinoic acid-eosinophil-IFN-γ circuit by which the microbiota can regulate duodenal IEC turnover and MHCII expression. Specific microbiota members including

F. rodentium can activate this circuit, thereby altering both intestinal epithelial and immune homeostasis. Thus, we identify multiple points of regulation for epithelial turnover rate, modulation of which is critical for maintaining baseline barrier function and allowing repair after injury or infection, as we observed in the impaired response to injury in mice with elevated baseline turnover. Furthermore, this finding emphasizes the interconnected nature of microbiota-epithelial-immune interactions, with epithelial cells as both sensors and readouts of changes in microbiota composition and function.

Our work highlights the impact of different SPF microbiota and the importance of certain microbiota members. Although both Jax and IH mice possess complex microbiota with many bacterial species, in many aspects of epithelial and immune cell function, we found that Jax mice more closely resembled GF mice than IH mice. GF mice have long been known to have a slower small intestinal epithelial turnover rate compared to SPF mice.[5] However, we further demonstrate that a specific microbiota component, *F. rodentium*, which is present in many mouse microbiotas [22,167,168], can accelerate epithelial turnover. The IH microbiota can also induce epithelial MHCII expression, which has also been attributed to segmented filamentous bacteria (SFB, also known as *Candidatus savagella*) and their attachment properties.[100] Our IH mice lack SFB (data not shown), and further work is needed to determine if *F. rodentium* could act similarly. Additionally, ablation of MHCII on epithelial cells can increase $Lgr5^{+}$ ISC numbers.[169] We did not find a difference in Jax and IH ISC frequency, but this may be due to the biological difference in genetic ablation in their context versus the lack of inducing signal we observed. SPF mice also produce less RA than GF mice due to suppression of *Rdh7* expression.[125] In our study, we extend this work to show that only IH microbiota, and specifically *F. rodentium*, was able to suppress IEC RA production. We also found that in addition to *Rdh7*, *Adh1* and *Aldh1a1* expression was also reduced in IH IECs,

perhaps because of differing microbiota compositions. Recent work has also shown that certain microbiota members, such as SFB, can produce RA.[170] Although our mice lack SFB, it is possible that there are RA-producing species that could represent another source of RA regulation.

Additionally, our observations reveal an immunomodulatory role of *F. rodentium*, an understudied member of the microbiota. *F. rodentium* is a Gram-positive, strictly anaerobic member of the family *Erysipelotrichaceae.*[167,168] It is found predominantly in the murine gut, through a closely related species, *Holdemanella biformis*, is present in humans.[22] *F. rodentium* in the ileum and colon reduces tumor growth in mice through production of short-chain fatty acids. In the ileum, *F. rodentium* was found in the mucus layer.[22] We also found that *F. rodentium* can colonize the duodenum. Further work is needed to determine if *F. rodentium* regulates RA production and MHCII expression through metabolites or direct contact with epithelial cells.

We also uncovered a pivotal role for the microbiota and RA in regulating intestinal eosinophils. Jax mice with high RA had more intestinal eosinophils than IH mice with low RA, and inhibiting RAR signaling reduced Jax eosinophils to IH levels. This finding is in accordance with previous observations that SPF mice have fewer intestinal eosinophils than GF mice[74], and provide a mechanism for that regulation. Furthermore, the remaining presence of a subset of eosinophils in Jax mice after inhibiting RAR signaling and the lack of an effect in IH mice suggest that there are different eosinophil functional states or subsets in the duodenum with different requirements for RA. Consistent with previous observations in human eosinophils[160], we found that eosinophils express RAR and RXR receptors, and that RAR signaling is active in intestinal eosinophils. Future work will also determine if RA-dependent and RA-independent eosinophils have different functional properties, and if this contributes to differences in Jax and IH eosinophil function.

Additionally, we demonstrated that intestinal eosinophils suppress production of IFN-γ by IELs to restrict excessive epithelial turnover. Heightened turnover in IH PHIL mice was associated with an increased sensitivity to inflammatory injury. This anti-proliferative role contrasts with the pro-proliferative function of eosinophils in injury and repair contexts[65,66], which may be due to the homeostatic nature of the intestinal interaction and presence of resident eosinophils, whereas pro-proliferative eosinophils are rapidly recruited after an insult. Gastric and colonic eosinophils can modulate lamina propria IFN-γ production by T cells via a PD-L1-dependent pathway.[69] It remains to be determined if intestinal eosinophils directly interact with IELs to regulate IFN-γ production and if that regulation is mediated by a similar pathway. We found that neutralization of IFN-γ abrogates increased epithelial turnover in IH WT and PHIL mice. Both type I (IFN-α/β) and type II (IFN-γ) IFNs can promote epithelial proliferation.[108,171] We further demonstrate that specific SPF microbiota can alter IFN-γ production by IELs, similar to what has previously been shown for lamina propria CD8 T cells.[172] This second microbiota signal in addition to suppression of RA production and eosinophil levels is required to increase epithelial turnover, as the absence of eosinophils in Jax PHIL mice does not itself result in faster turnover rates as seen in IH PHIL mice. These findings point to eosinophils as an important regulator of intestinal homeostasis by fine-tuning microbiota inputs, a role which is slowly gaining traction after eosinophils have long been pigeonholed as merely functioning in anti-parasite immunity or contributing to the pathophysiology of atopic and allergic diseases.[173]

In summary, we identified a mechanism by which microbiota components including *F. rodentium* can constrain epithelial proliferation through a retinoic acid-eosinophil-IFN-γ-dependent pathway. This role for the microbiota in controlling duodenal IECs illustrates the importance of deeper exploration of microbiota-host interactions in the proximal small intestine,

which could open up new therapeutic avenues for upper gastrointestinal tract diseases like celiac disease, eosinophilic esophagitis, and environmental enteric dysfunction. Further study of how eosinophils contribute to intestinal epithelial homeostasis could also identify targets for modulating epithelial proliferation and preventing tumor initiation. Finally, this study highlights the importance of understanding the differing bioactivities of members in a complex microbiota and how they interact with the epithelium and immune cells to promote different biological states.

V. METHODS

Experimental Model and Subject Details

Mice

Wild-type C57BL/6J mice (called in-house, IH) were bred and housed in microisolator cages in the specific-pathogen-free (SPF) barrier facility at the Harvard T.H. Chan School of Public Health. These mice are distinct from other mice in our facility that we have previously described in Howitt et al., 2016, in that the IH mice in this paper are maintained free of the protozoan *Tritrichomonas muris*. C57BL/6 WT (called Jax) and *Lgr5-GFP-creERT2* mice were obtained from the Jackson Laboratory, Bar Harbor, Maine. PHIL mice[174] were obtained from Dr. Elizabeth Jacobsen at the Mayo Clinic (Scottsdale, Arizona). All genetically modified mouse lines were bred on a C57BL6/J background and were bred as heterozygotes to generate littermate controls. Both male and female mice were used. Mice were used experimentally between 6-12 weeks of age.

Germ-free WT C57BL/6J mice were bred and maintained in semi-rigid gnotobiotic isolators in the Harvard T. H. Chan Gnotobiotic Center for Mechanistic Microbiome Studies.

To rederive genetically modified lines onto a Jax microbiota background, pups were taken on the day of birth or one day after and raised by a dam of the desired microbiota background.

These Jax mice were maintained in SPF facility caging but all SPF cages were changed by the investigators to prevent mixing of microbiota. Microbiota status was monitored by qPCR and Jax background mice were regularly rederived onto freshly ordered Jax mice.

Animal studies and experiments were approved and carried out in accordance with Harvard Medical School's Standing Committee on Animals and the National Institutes of Health guidelines for animal use and care.

Bacterial strains and gnotobiotic colonization

Bifidobacterium pseudolongum was isolated from BIH mice from our facility by plating stool on selective *Bifidobacterium* iodoacetate medium agar plates.[175] *Lachnospiraceae A2* was isolated from BIH mice by plating stool on brain-heart infusion (BHI) plates supplemented with 1 g/L inulin. 48 colonies of each condition were screened by colony polymerase chain reaction (PCR) using *Bifidobacterium* genus or *Lachnospiraceae A2* primers. *Faecalibaculum rodentium* was obtained from the DSMZ collection (#103405) and was also isolated from our IH mice by plating on Eggerth-Gagnon plates (ATCC medium 2840) and screening by colony PCR with *F. rodentium* primers. All of these strains were cultivated under anaerobic conditions at 37°C.

For gnotobiotic experiments, *B. pseudolongum* was grown in MRS medium (BD) supplemented with 0.5 g/L L-cysteine for 24 hours, *F. rodentium* in DSMZ medium 104 (modified PYG medium) for 24 hours, and *Lachnospiraceae A2* in BHI (BD) supplemented with 5 g/L yeast extract, L-cysteine, and hemin (Sigma) for 48 hours. Cultures were observed to be turbid and concentrated 10x for gavage in GF mice. Monocolonization was confirmed by Sanger sequencing of stool DNA, and germ-free status was confirmed by qPCR with universal bacterial 16S primers.

Method Details

scRNA-seq

Cell isolation and sorting

Epithelial cells for sequencing were isolated similarly to as described in Biton et al., 2018. The duodenum was excised, opened longitudinally, rinsed in PBS, and sliced into fragments about 2-5mm in length. The tissue was incubated in 20 mM EDTA (VWR) in PBS on ice for 45 min with occasional inversion, then shaken vigorously. The tissue was then transferred to subsequent EDTA-PBS solutions for a total of 4 times, for 5 minutes each, and then shaken. Fractions were examined under a light microscope and crypt-enriched fractions were collected and combined. This crypt fraction was passed through a 70 μM filter, centrifuged, dissociated with pre-warmed TrypLE express (Invitrogen) for 1 min at 37 °C, centrifuged, and resuspended in 1% BSA (Roche), 5 mM HEPES (Corning), 1 mM EDTA. Cells from each condition were stained with a distinct barcoded antibody (Cell-Hashing antibody, TotalSeq-A, Biolegend). Epithelial (live $EpCAM^{+}CD45^{-}Ter119^{-}CD31^{-}$) cells were sorted on a FACSAria (BD).

Sequencing and analysis

Single cell RNA-seq experiments were performed by the Brigham and Women's Hospital Single Cell Genomics Core. ~7,500 cells from each condition were resuspended in 0.4% BSA in PBS at a concentration of 2,000 cells per μl, pooled together, then loaded onto a single lane (Chromium Next GEM Chip G, 10X Genomics) followed by encapsulation in a lipid droplet (Chromium Next GEM Single Cell 3' GEM, Library & Gel Bead Kit v3.1, 10X Genomics) followed by cDNA and library generation according to the manufacturer's protocol.

mRNA libraries were sequenced to an average of 30,000 reads per cell and HTO (Cell Hashing antibodies) libraries sequenced to an average of 5,000 reads per cell on an Illumina Novaseq. scRNA-seq reads were processed with Cell Ranger v3.1, which demultiplexed cells

from different samples and quantified transcript counts per putative cell. Quantification was performed using the STAR aligner against the mm10 transcriptome.

Further processing and visualization was performed using the Seurat v3 R package.[176] Cells with either less than 200 or more than 6,000 detected genes or >0.12 mitochondrial fraction were excluded from further analysis. Cell expression was normalized followed by selection of highly variable features, data scaling and cell clustering. We identified genes that are differentially expressed (had an adjusted P value lower than 0.05 and fold change >1.5 or <0.5) using the MAST test[177] implemented in Seurat v3. Enrichment of differentially expressed genes in gene ontology categories was determined using the topGO package.[178] P values were calculated using Fisher's exact test.

Intestinal lamina propria and epithelial cell isolation

The small intestine and/or colon were removed and flushed with ice-cold sterile PBS using a 19-gauge feeding needle. The duodenum (defined as the first 7 cm following the stomach), jejunum (the 10 cm following the duodenum), and ileum (the last 10 cm of the small intestine, immediately proximal to the cecum) were excised and Peyer's patches were removed. Intestines were then opened longitudinally and gently agitated at 4˚C in PBS, 2% FBS (Gibco), 5mM HEPES (Corning), 1mM DTT (Sigma) for 10 min. The tissue was then transferred into prewarmed PBS, 2% FBS, 5mM HEPES, 5mM EDTA and rotated at 37˚C for 15 minutes followed by vigorous shaking to remove epithelial cells. This was repeated and epithelial cells from both fractions were combined and washed with PBS prior to epithelial digestion. The remaining non-epithelial tissue was used for lamina propria cell isolation. The tissue was rinsed twice in PBS, placed into an Eppendorf tube with RPMI, minced with scissors, and digested in RPMI containing 5% FBS, 5mM HEPES, 1% penicillin/streptomycin (Corning), 0.5 units/ml Dispase II (StemCell Technologies),

50 μg/ml DNase (Roche), and 0.25 mg/mL collagenase A (Roche) for 45 minutes at 37˚C. For epithelial cell isolation, the epithelial fraction was digested in RPMI containing 5% FBS, 5mM HEPES, 1% penicillin/streptomycin, 0.5 units/ml Dispase II, and 50 μg/ml DNase for 10 minutes at 37˚C. Both the epithelial and lamina propria fraction were then passed through 40 μm filters and washed with PBS, 2% FBS, 1mM EDTA.

Flow cytometry

Single cell suspensions were initially Fc blocked with anti-CD16/CD32 (clone 93, Biolegend) and then stained with surface antibodies and viability dye (20 min on ice). For transcription factor staining, after surface staining, cells were fixed for 45 min with eBioscience Transcription Factor Staining Set and then stained intracellularly for 1h at room temperature. For cytokine (IFN-γ) staining, 1 million isolated epithelial fraction cells were stimulated with eBioscience Cell Stimulation Cocktail (with protein transport inhibitors) for 4h at 37°C in RPMI with 10% fetal bovine serum and penicillin/streptomycin. Cells were then washed, blocked, surface stained, and fixed in BD Cytofix/Cytoperm for 20 minutes. Intracellular staining was performed for 45 min on ice. Samples were acquired on an LSRII or FACS Symphony (BD). Antibodies used are listed in the Key Resources Table.

Histology and fluorescence microscopy

The duodenum was opened longitudinally and rolled before overnight fixation in 4% paraformaldehyde (Sigma). The tissue was then embedded in paraffin and cut into 5μm thick sections at the Harvard Medical School Rodent Histopathology Core. For immunofluorescence staining, sections were initially deparaffinized and rehydrated. Heat-mediated antigen retrieval was performed in Target Retrieval Solution, Citrate pH 6.1 (Agilent) for 20 minutes. Afterwards, the slides were washed in PBS and blocked in PBS containing 3% BSA (Roche), 3% donkey serum

(Jackson Immunoresearch), 0.1% Triton X-100 (Sigma), 0.1% saponin (Sigma) for 1 hour at room temperature. Primary antibodies were incubated overnight at 4˚C and secondary antibodies were applied for 1.5 hours at room temperature. Primary antibodies included: rat anti-BrdU (1:200 dilution, ab6326, Abcam), rat anti-Ki-67 (1:300 dilution, 14-5698-82, ThermoFisher Scientific), mouse anti-E-Cadherin (1:400 dilution, 36/E-Cadherin, BD Biosciences). DNA was labeled with DAPI (0.5 μg/ml).

Image analysis was performed in Fiji (a version of ImageJ). Epithelial turnover was quantified by dividing the length of the crypt-villus axis labeled by BrdU by the total crypt-villus length labeled by DAPI. $Ki67^+$ cells were counted in the crypts. For both epithelial turnover and $Ki67^+$ cell quantification, 15-20 villi/crypts were usually counted per mouse and averaged for a final value.

Eosinophil isolation and sorting

For intestinal eosinophils, the lamina propria was processed as described for flow cytometry and cells were sorted with a two-step MACS process according to the manufacturer's instructions, first by labeling with MHCII-PE antibody (Biolegend) and using Anti-PE Microbeads (Miltenyi Biotech) to deplete $MHCII^+$ cells, and then sorting $SiglecF^+$ cells with Anti-Siglec-F MicroBeads (mouse) (Miltenyi Biotech). The purity of $SiglecF^+MHCII^-$ eosinophils was usually >95%.
For bone marrow eosinophils, the tibia and femur were harvested, cleaned of muscle, one end of the bone cap was cut off, and bone marrow was collected by centrifuging at 12,000 rpm for 2 minutes. Red blood cells were removed with Ammonium Chloride solution (STEMCELL Technologies). $SiglecF^+$ cells were sorted from the remaining bone marrow cells Anti-Siglec-F MicroBeads (mouse) (Miltenyi Biotech). The purity of $SiglecF^+$ eosinophils was usually >75%.

***In vitro* eosinophil culture**

Sorted bone marrow eosinophils were cultured in RPMI with Glutamax, 10% FBS, penicillin/streptomycin, sodium pyruvate, and 50 μM beta-mercaptoethanol for 24h. In some conditions, 10 ng/mL IL-5 (Biolegend) and/or 100 nM all-trans retinoic acid (Sigma) was included in the culture. After 24h, cell viability was measured by flow cytometry.

RNA/DNA isolation and RTq-PCR

For RNA isolation from total intestinal tissue, tissue was snap frozen and lysed in Qiazol (Qiagen) for RNA extraction following manufacturer's instructions. For RNA isolation from eosinophils, sorted cells were lysed in Qiazol and processed with the Direct-zol RNA Miniprep Kit (Zymo Research). cDNA was synthesized using the iScript cDNA Synthesis Kit (Bio-Rad). Bacterial DNA isolation from stool or intestinal contents was performed using the QIAamp Fast DNA Stool Mini Kit (Qiagen). qPCR was performed using the Kapa SybrFast mastermix. The following primers were used:

Actin	Fw	TACCACCATGTACCCAGGCA
	Rv	CTCAGGAGGAGCAATGATCTTGAT
Adh1	Fw	GCAAAGCTGCGGTGCTATG
	Rv	TCACACAAGTCACCCCTTCTC
Aldh1a1	Fw	ATACTTGTCGGATTTAGGAGGCT
	Rv	GGGCCTATCTTCCAAATGAACA
Ifng	Fw	ATGAACGCTACACACTGCATC
	Rv	CCATCCTTTTGCCAGTTCCTC
Rara	Fw	TTCTTTCCCCCTATGCTGGGT
	Rv	GGGAGGGCTGGGTACTATCTC
Rarb	Fw	CTGCTCAATCCATCGAGACAC
	Rv	CTTGTCCTGGCAAACGAAGC
Rarg	Fw	GGAGCAGGCTTCCCATTCG
	Rv	CATGGCTTATAGACCCGAGGA
Rdh7	Fw	GTGTCTTTGTGTGGTGGTGGTTAC
	Rv	CCACAGCTTCTCTATGCTGTGTGA
Tgm2	Fw	GACAATGTGGAGGAGGGATCT
	Rv	CTCTAGGCTGAGACGGTACAG

16S universal	Fw	TCCTACGGGAGGCAGCAGT
	Rv	GGACTACCAGGGTATCTAATCCTGTT
Bifidobacterium genus	Fw	CTCCTGGAAACGGGTGG
	Rv	GGTGTTCTTCCCGATATCTACA
F. rodentium	Fw	CCGGGAATACGCTCTGGAAA
	Rv	GCCAACCAACTAATGCACCG
Lachnospiraceae A2	Fw	GCCGGCAGCATATGCAACG
	Rv	TTTACCTGCTGGCTACTGAGGG

BrdU

Mice were injected intraperitoneally (i.p.) with 100 µl of a 3mg/mL BrdU (Sigma) solution in PBS and simultaneously started on drinking water containing 0.8 mg/mL BrdU and 0.5% glucose. Drinking water was continued for 48 hours to measure epithelial turnover.

Aldefluor assay

Epithelial and lamina propria cells were isolated as described. The assay was performed using the ALDEFLUOR Kit (StemCell Technologies) according to the manufacturer's instructions, at a concentration of 500,000 cells/mL with 30 min incubation time.

Retinoic acid receptor inhibitor

Mice were injected i.p. with 220 µg of the pan-retinoic acid receptor inverse agonist BMS493 (Tocris) or vehicle control DMSO (Corning) daily for 8 days, in a volume of 25 µl.

Anti-CD3 injury

Mice were injected i.p. with 50 µg anti-CD3ε or Armenian hamster IgG isotype control (Biolegend). On day 3 after injection, the duodenum was excised, opened longitudinally, and prepared for paraffin embedding as described above in the histology section. Hematoxylin and eosin stained slides were evaluated by a blinded pathologist and histological injury was scored on a scale of 0-4 for the parameters of villus to crypt ratio, crypt injury/loss, and monocyte and

polymorphonuclear cell infiltration. The summed score was multiplied by a conversion factor of 1-4 based on the percent of intestine length involved by injury/abnormality.

IFN-γ neutralization

Mice were injected i.p. with 200 μg of anti-IFN-γ (BioXCell clone XMG1.2) neutralizing antibody or PBS every other day for 8 days. BrdU treatment started on day 6, 48h before the endpoint.

Transfer of intestinal contents

Stool or cecal contents were collected into 1 mL of sterile PBS. Usually 2 stool pellets (approximately 10-20% of total liquid volume) were used. Contents were homogenized by mashing with a pestle and vortexing, and 100 μl of liquid was orally gavaged into recipient mice.

Antibiotic treatment

IH mice were provided with 0.5g/L vancomycin (Alfa Aesar), 1 g/L metronidazole (Sigma), 1 g/L neomycin (Alfa Aesar), 1 g/L ampicillin (Corning), and 0.2 g/L amphotericin B (Alfa Aesar) in their drinking water *ad libitum* with water changes every 3 days. For experiments with antibiotic pre-treatment of donor mice prior to cecal content transfer, antibiotic treatment was for 2 weeks.

Cohousing experiments

In general, unless otherwise noted, mice were cohoused with littermates at weaning and all mice on a Jax background were maintained in cages separate from in-house mice. For experiments in which Jax and IH mice were cohoused, equal numbers of Jax and IH mice were placed in the same cage for 2 weeks.

16S rRNA gene amplicon sequencing

DNA was isolated from stool pellets by phenol-chloroform extraction after bead beating as previously described.[179] The 16S rRNA gene sequencing protocol was adapted from the Earth Microbiome Project.[180] The 16S rRNA V4 region was amplified from the extracted DNA by PCR

and sequenced by using the 2 150–base pair paired-end reading on a MiSeq instrument (Illumina, San Diego, CA). Analysis of 16S rRNA sequence data was performed using Microbiome Helper scripts and QIIME v1.9.[181,182] Sequences were clustered into operational taxonomic units (OTUs) at a similarity threshold of 97% by using the sortmerna_sumaclust method of open-reference OTU picking. OTUs were subsequently mapped to a subset of the SILVA 132 database containing only sequences from the V4 region of the 16S rRNA gene to determine taxonomies.[183] To account for variations in sequencing depth, OTU tables were rarified to the lowest sequence depth among samples. Data were visualized in R using the phyloseq package.[184] Differentially abundant OTUs between groups at the genus level were identified using LefSE.[166]

Quantification and Statistical Analysis

Data were analyzed with GraphPad Prism (version 9.0). Data are shown as mean with individual data points as noted. For comparison between two independent experimental groups, a two-tailed Mann-Whitney U test was used. For comparison between more than two groups, one-way ANOVA followed by Holm-Sidak's test was performed. For comparison in experiments with two independent variables, two-way ANOVA followed by Holm-Sidak's test was performed. Details of statistical analysis and sample size are provided in the figure legends. No samples were excluded from any experiments performed in this study unless in the case of technical failure. Experimenters were not blinded to experimental conditions. Differences of $P < 0.05$ were considered statistically significant.

Chapter 3

The taste receptor TAS1R3 regulates small intestinal tuft cell homeostasis

Authors: Michael R. Howitt[1,2], Y. Grace Cao[1], Matthew B. Gologorsky, Jessica A. Li, Adam L. Haber, Moshe Biton, Jessica Lang, Monia Michaud, Aviv Regev, and Wendy S. Garrett[2]

[1]These authors contributed equally

[2]Corresponding authors

Author Contributions: MRH, YGC, MBG, JAL, and MM performed experiments and analyzed data. ALH, MB, and AR performed and oversaw RNA sequencing analysis. JL assisted with gnotobiotic experiments. MRH, YGC, and WSG designed experiments, interpreted data, and wrote the manuscript.

I. ABSTRACT

Tuft cells are an epithelial cell type critical for initiating type 2 immune responses to parasites and protozoa in the small intestine. To respond to these stimuli, intestinal tuft cells use taste chemosensory signaling pathways, but the role of taste receptors in type 2 immunity is poorly understood. Here we show that the taste receptor TAS1R3, which detects sweet and umami in the tongue, also regulates tuft cell responses in the distal small intestine. BALB/c mice, which have an inactive form of TAS1R3, as well as *Tas1r3*-deficient C57BL6/J mice both have severely impaired responses to tuft cell-inducing signals in the ileum including the protozoa *Tritrichomonas muris* and succinate. In contrast, TAS1R3 is not required to mount an immune response to the helminth *Heligmosomoides polygyrus*, which infects the proximal small intestine. Examination of uninfected *Tas1r3*$^{-/-}$ mice revealed a modest reduction in the number of tuft cells in the proximal small intestine but a severe decrease in the distal small intestine at homeostasis. Together, these results suggest that TAS1R3 influences intestinal immunity by shaping the epithelial cell landscape at steady state.

II. INTRODUCTION

Barrier defenses constitute the first arm of the innate immune system at mucosal surfaces. Via its sensing of mechanical injury, metabolites, or secreted molecules, the intestinal epithelium with its many cell sub-types is both an active defender and a signal broker to the innate and adaptive immune system. A chemosensory epithelial cell subset called tuft cells have recently emerged as critical sensors of intestinal helminths and protists and initiators of anti-parasite immunity in the gut.[101,135,137] Tuft cells produce IL-25, resulting in the accumulation of type 2 innate lymphoid cells (ILC2s) within the intestinal lamina propria and ILC2 production of IL-13.[101,135,137] This local

increase in IL-13 biases the differentiation of epithelial progenitor/stem cells to become goblet cells, known for their production of mucins and anti-helminthic resistin-like molecules, and tuft cells.[101,135,137,185] The cross-talk between tuft cells and ILC2s creates a positive-feedback loop amplifying the numbers of these cell types and culminating in productive anti-parasite immunity.

Tuft cells utilize chemosensory signaling pathways to respond to parasites and initiate anti-parasite immunity. Intestinal tuft cells express the canonical taste chemosensory components gustducin, 1-phosphatidylinositol 4,5-bisphosphate phosphodiesterase beta-2 (PLCB2), and transient receptor potential cation channel subfamily M member 5 (TRPM5).[101] In lingual type II taste cells, these chemosensory components facilitate signaling from G protein-coupled receptors (GPCRs) that transduce sweet, umami, or bitter tastes from food[186], while in the gut, they function to clear helminth infections and drive anti-parasite immunity in response to *Tritrichomonas* protists.[101] Small intestinal tuft cells also express the GPCR *Sucnr1* (*Gpr91*), which detects the metabolite, succinate and initiates intestinal anti-parasite immunity in a TRPM5-dependent manner.[102,103,139] Mice lacking SUCNR1 do not respond to *Tritrichomonas* protists yet mount an effective immune response to the helminths *Heligomosomoides polygyrus* and *Nippostrongylus brasiliensis*.[102,103,139] In addition, bitter taste GPCRs were recently implicated in the tuft cell response to infection with the helminth *Trichinella spiralis*.[140] Collectively, these observations suggest that tuft cells utilize multiple taste-associated GPCRs to initiate intestinal anti-parasite immunity. Given the immense diversity of microbial and non-microbial signals that stimulate the anti-parasite immune response at barrier surfaces, we hypothesized that there may be additional uncharacterized tuft cell receptors that modulate intestinal anti-parasite immunity.

Here we show that the taste receptor, TAS1R3, which mediates responsiveness to sweet and umami in the tongue, also contributes to anti-parasite immunity in the distal small intestine.

Stimuli that induce a tuft cell response in the ileum, such as *Tritrichomonas muris* or succinate, are severely diminished in *Tas1r3*$^{-/-}$ mice. Our results reveal important roles for TAS1R3 in regulating tuft cell homeostasis in the small intestine, thereby modulating sensitivity to luminal stimuli during the initiation of type 2 immunity.

III. RESULTS

C57BL6/J and BALB/c mice differ in tuft cell response to the protozoa *Tritrichomonas muris* but not the helminth *Heligmosomoides polygyrus*

Given the critical role of chemosensation in tuft cell-mediated anti-parasite immunity in the gut, we considered if inbred mouse strains with their well-characterized genetics and immune responses to parasites could be utilized to further elucidate the potential connection between parasite surveillance and taste receptors. Inbred mouse strains such as BALB/c and C57BL/6J can differ in their immune responses to parasites, which results in marked differences in clearing these infections.[187,188] Furthermore, BALB/c and C57BL/6J mice carry genetic polymorphisms in the taste receptor *Tas1r3*, with C57BL/6J having a high preference for the TAS1R3 ligand saccharin and BALB/c low.[189,190] To investigate if these differences between mouse strains could alter the tuft cell response to parasites, we colonized both C57BL/6J and BALB/c mice with the protozoa *Tritrichomonas muris. T. muris* induced a significant increase in tuft cell frequency at the site of colonization, the distal small intestine (ileum), of C57BL6/J mice, which contrasted with an absence of tuft cell expansion in *T. muris*-colonized BALB/c mice **(Fig. 3.1A-B)**. This difference in tuft cell responses was not due to variation in *T. muris* colonization, as protozoal loads were similar between C57BL/6J and BALB/c mice **(Fig. 3.1C)**.

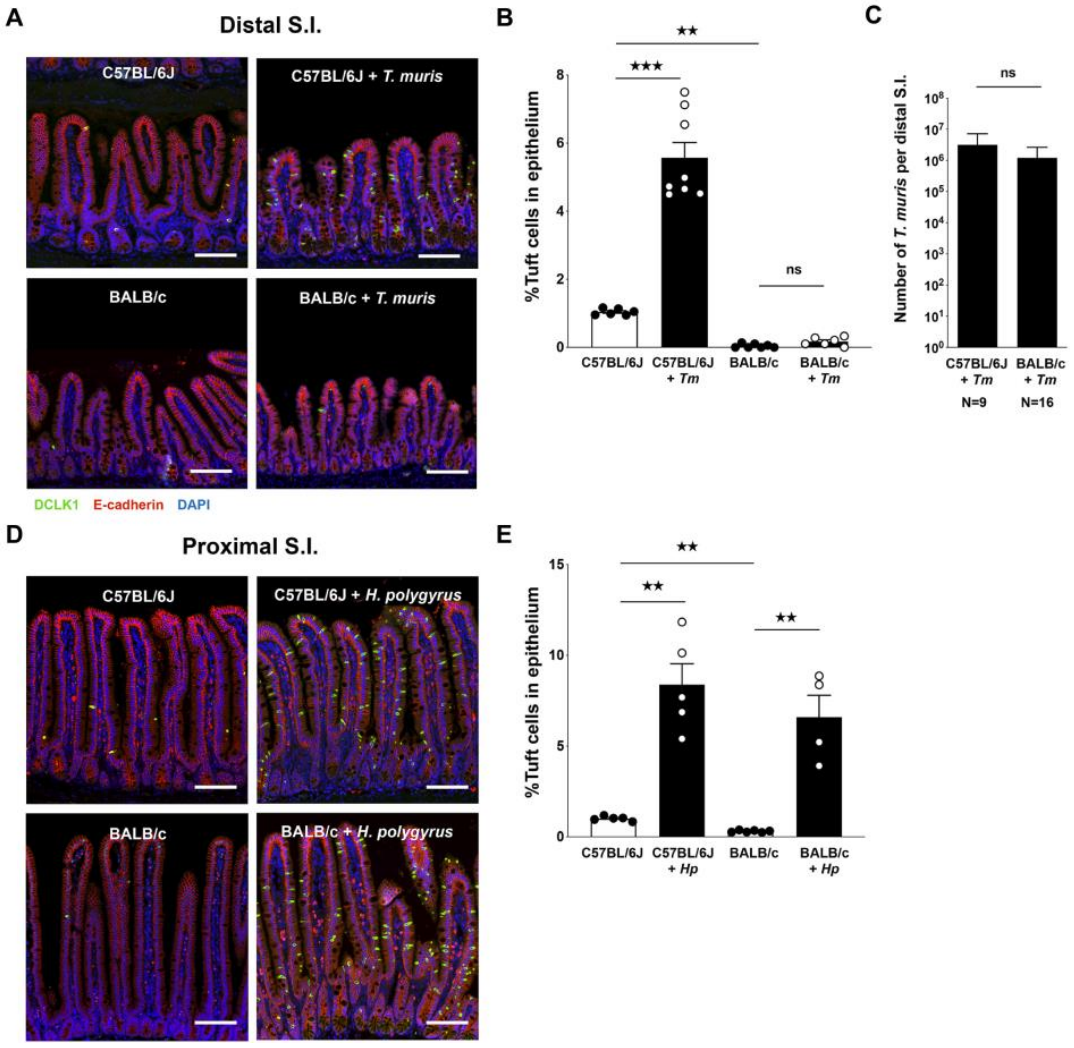

Figure 3.1. Tuft cell responses differ in C57BL/6J and BALB/c mice to the protozoa *Tritrichomonas muris* but not the helminth *Heligmosomoides polygyrus.* **(A)** Representative distal small intestine (SI) images from uninfected and *T. muris*-colonized C57BL/6J and BALB/c mice (scale bars, 100 μm) and **(B)** tuft cell frequency at day 18 post-infection. **(C)** *T. muris* abundance in distal SI contents determined by qPCR. **(D)** Representative proximal SI images from uninfected and *H. polygrus*-infected C57BL/6J and BALB/c mice (scale bars, 100 μm) and **(E)** tuft cell frequency at day 14 post-infection. Each symbol represents an individual mouse, and all data are representative of 2 independent experiments. Data are plotted as means with SEM. Three stars, $P < 0.001$; two stars, $P < 0.01$; n.s., not significant using the Mann-Whitney U test.

Intestinal helminth-induced immunity is also accompanied by a significant increase in tuft cell frequency.[101,135,137] Consistent with these prior results, BALB/c and C57BL/6J mice both showed robust expansion of tuft cells in the proximal small intestine during *Heligmosomoides*

polygyrus infection **(Fig. 3.1D-E)**, confirming that BALB/c mice can generate tuft cells in response to some parasitic stimuli. To determine if the defect in response to *T. muris* was specific to the protozoa or a more general feature of the ileum, we injected BALB/c mice with recombinant interleukin-25 (IL-25). This cytokine bypasses microbial signal-dependent pathways to directly expand tuft cells via induction of IL-13 production by ILC2s.[101,135,137] IL-25 injection resulted in tuft cell expansion in the distal small intestine **(Supplemental Fig. 3.1)**, suggesting that the lack of BALB/c response to *T. muris* was not due to an inability to increase tuft cells in the ileum.

Tuft cells express the type 1 taste receptor TAS1R3 which affects their response to expansion stimuli

To understand the mechanism underlying the lack of tuft cell response to *T. muris* in BALB/c mice, we returned to the observation that polymorphisms in *Tas1r3* severely reduce the sensitivity of this receptor in BALB/c mice.[189,190] In lingual taste, TAS1R3 activates a signal transduction pathway involving PLCβ2 and TRPM5, which are chemosensory components used by tuft cells to respond to *T. muris*.[101] Previous reports found that tuft cells in the stomach, trachea, thymus, gallbladder, and urethra express *Tas1r3*, but the level of *Tas1r3* expression by intestinal tuft cells was unclear.[103,191,192] We sorted ileal tuft cells from C57BL/6J mice and used RNA-sequencing to measure the expression of type 1 and type 2 taste receptors, which signal through the transduction components PLCβ2 and TRPM5. *Tas1r3* had the highest expression, while most other receptor genes were not detected **(Fig. 3.2A)**. Reverse transcription quantitative polymerase chain reaction (RT-qPCR) analysis confirmed this result **(Fig. 3.2B)**, consistent with single cell sequencing analysis of small intestinal epithelial cells that identified *Tas1r3* as a tuft cell marker.[93]

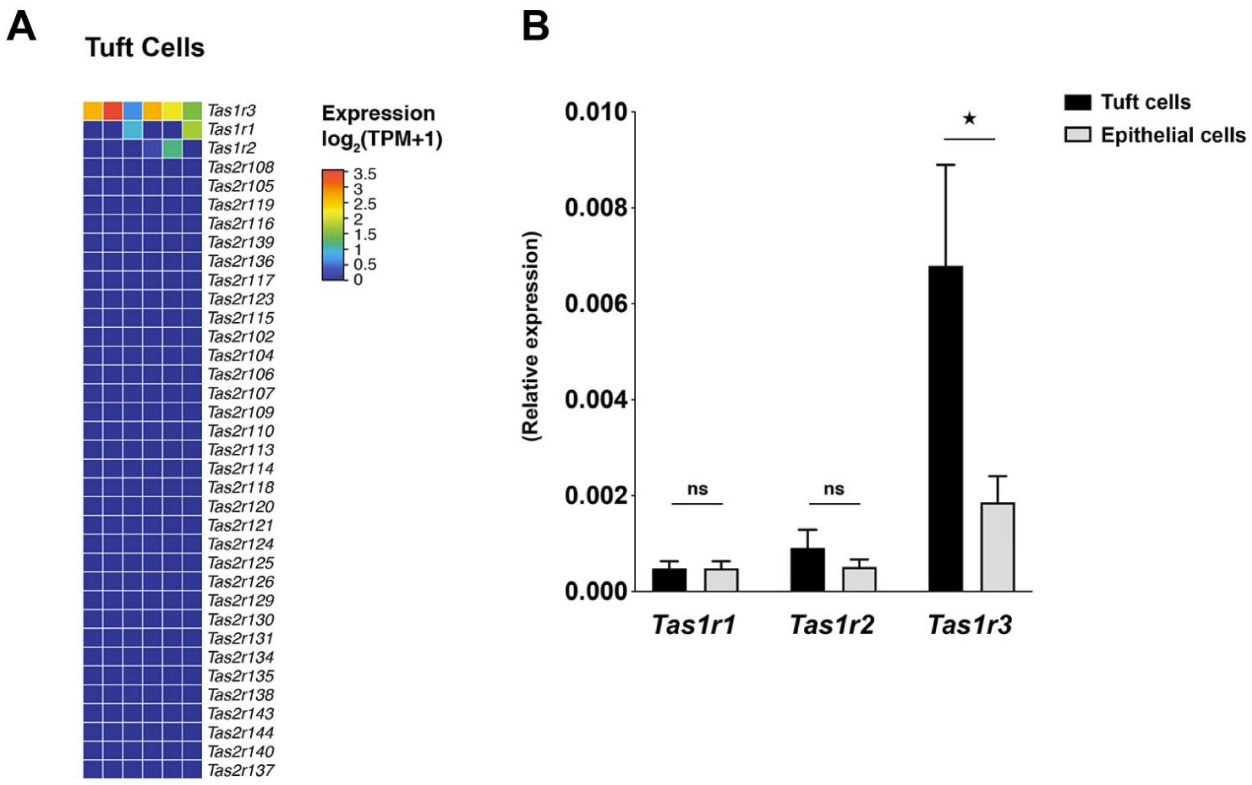

Figure 3.2. Small intestinal tuft cells express the type 1 taste receptor *Tas1r3*. (A) Type 1 and 2 taste receptor expression in sorted C57BL/6J distal small intestinal tuft cells determined by RNA-seq. **(B)** Type 1 taste receptor gene expression in sorted distal SI tuft cells determined by qPCR, compared with the non–tuft cell epithelium. Data represent 6 independent samples **(A)** or 2 independent experiments **(B)**. Data are plotted as means with SEM. One star, $P < 0.05$; ND, not detected. Mann-Whitney U test.

We hypothesized that if the inactive BALB/c TAS1R3 contributed to impaired BALB/c responses to *T. muris*, then *Tas1r3*$^{-/-}$ C57BL/6J mice should recapitulate this lack of response. Indeed, tuft cell frequency in *Tas1r3*$^{-/-}$ mice did not significantly increase after *T. muris* colonization **(Fig. 3.3A-B)**. Similar to what we observed in BALB/c mice, this defect was not due to lower *T. muris* colonization **(Fig. 3.3C)**. Furthermore, the effect of TAS1R3 was restricted to *T. muris*, as *Tas1r3*$^{-/-}$ mice had a similar ability to expel *H. polygyrus* as WT mice, while *Trpm5*$^{-/-}$ mice had an increased worm burden as previously described **(Fig. 3.3D)**.[101]

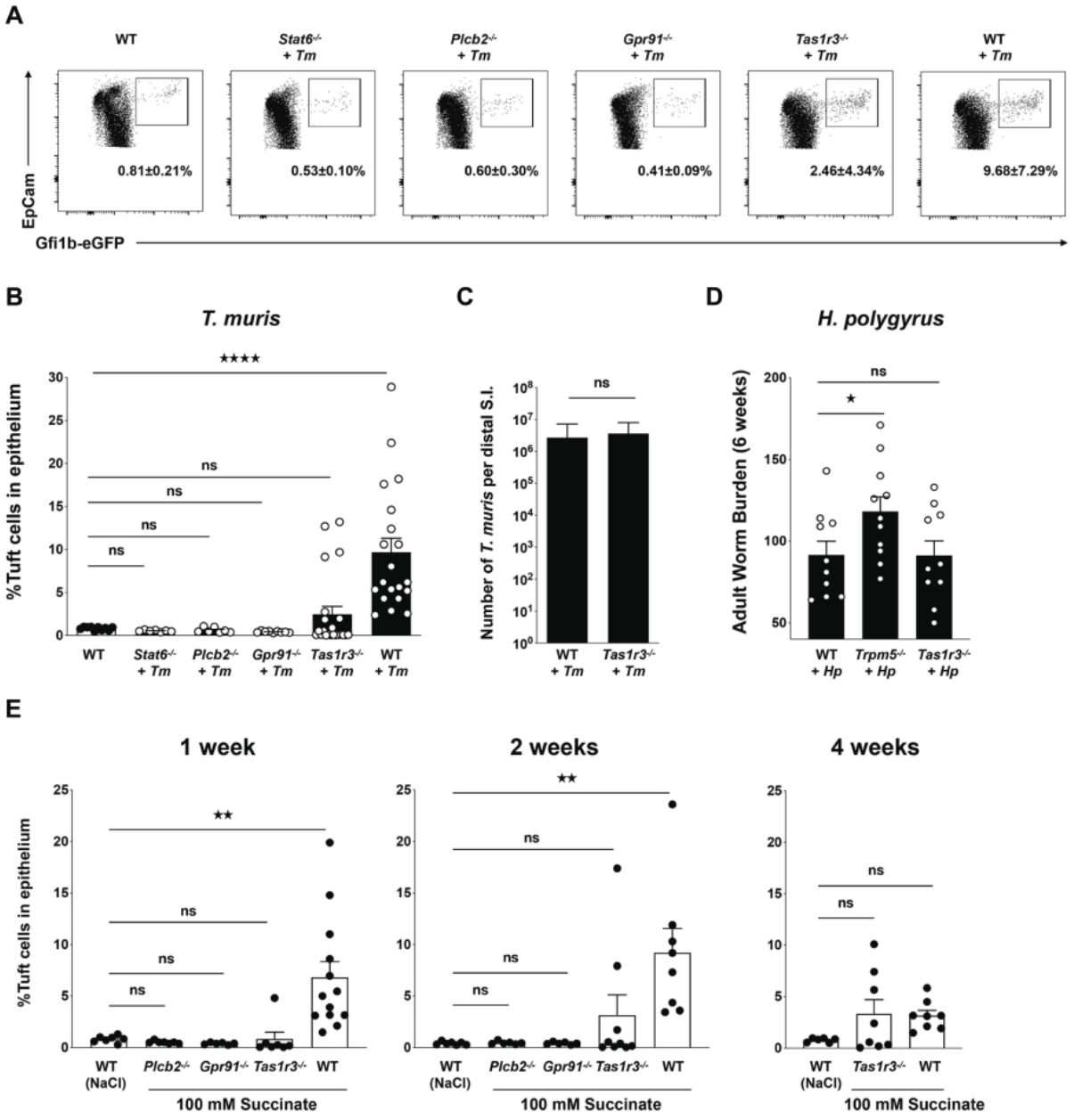

Figure 3.3. TAS1R3 affects distal small intestinal tuft cell response to expansion stimuli. **(A)** Representative flow cytometry plots of live, CD45^{-}EpCAM^{+} intestinal epithelial cells from uninfected or *T. muris*-colonized WT (*Gfi1b*$^{eGFP/+}$) C57BL/6J, *Gfi1b*$^{eGFP/+}$ *Stat6*$^{-/-}$, *Gfi1b*$^{eGFP/+}$ *Plcb2*$^{-/-}$, *Gfi1b*$^{eGFP/+}$ *Gpr91*$^{-/-}$, and *Gfi1b*$^{eGFP/+}$ *Tas1r3*$^{-/-}$ mice and **(B)** tuft cell frequency. **(C)** *T. muris* abundance in distal SI contents determined by qPCR. **(D)** *H. polygrus* worm burden in proximal SI at 6 weeks post-infection. **(E)** Tuft cell frequency determined by flow cytometry after 1, 2, or 4 weeks of feeding succinate or NaCl in the drinking water. Each symbol represents an individual mouse, and all data are representative of at least 2 independent experiments. Data are plotted as means with SEM. Four stars, $P < 0.0001$; two stars, $P < 0.01$; one star, $P < 0.05$; n.s., not significant. one-way analysis of variance (ANOVA) with Holm-Sidak's test or Mann-Whitney U test.

Although tuft cell frequency remained unchanged in the majority of *Tas1r3*$^{-/-}$ mice after *T. muris* colonization, we noted that a subset of mice exhibited a strong tuft cell response. This bimodal response was not observed in mice lacking other tuft cell-regulating components, including PLCβ2; STAT6, a transcription factor downstream of IL-13 receptor signaling; and GPR91, a succinate receptor reported to be involved in sensing of *Tritrichomonas* species **(Fig. 3.3A)**.[102,103] These observations led us to question whether TAS1R3 regulates tuft cell expansion through sensing of a *T. muris*-associated signal such as succinate or potentially another mechanism.

Feeding mice succinate in the drinking water induces a significant expansion of tuft cells in the distal small intestine, which highly resembles the tuft cell response to *Tritrichomonas* colonization.[102,103,139] Wild-type (WT) mice fed 100 mM succinate in the drinking water for 1 week exhibited tuft cell hyperplasia **(Fig. 3.3E)**. However, similar to *Gpr91*$^{-/-}$ and *Plcb2*$^{-/-}$ mice, feeding succinate to *Tas1r3*$^{-/-}$ mice for 1 week failed to increase tuft cell levels in the distal small intestine **(Fig. 3.3E)**. To assess the kinetics of tuft cell response to succinate, we also fed mice 100 mM succinate for 2 weeks and 4 weeks. In contrast to 1 week of succinate feeding, these longer succinate exposures increased the proportion of *Tas1r3*$^{-/-}$ mice with enhanced tuft cell abundance. These findings suggest that TAS1R3 is not required to sense succinate but may act to increase the response kinetics of tuft cells to expansion stimuli.

TAS1R3 regulates homeostatic tuft cell abundance

Tuft cells function in a feed-forward loop, where tuft cell-derived IL-25 leads to increased IL-13 production by ILC2s and expansion of Th2 cells, which results in additional tuft cells and further production of IL-25. Therefore, we hypothesized that the response kinetics of tuft cells to a stimulus would be affected by the number of tuft cells that are available to initiate the feed-forward

loop. To determine if TAS1R3 influences tuft cell frequency at steady state, we profiled tuft cell populations across different regions of the gut and found that *Tas1r3*$^{-/-}$ mice had fewer tuft cells compared to WT, with the most pronounced defect in the ileum **(Fig. 3.4A)**. We further verified the relative reduction of tuft cells in the ileal epithelium of *Tas1r3*$^{-/-}$ animals by measuring RNA expression of the tuft cell markers *Dclk1* and *Trpm5* and by immunofluorescence microscopy, which revealed markedly fewer DCLK1^{+} positive tuft cells in the absence of TAS1R3 **(Figs. 3.4D and S3.2**). Because IL-13 stimulates epithelial progenitor cells to differentiate into both tuft cells and goblet cells[101,135,137,185], we also examined the number of goblet cells in the ileum of WT and *Tas1r3*$^{-/-}$ mice at steady state but found no significant difference **(Fig. 3.4B-C)**. We confirmed that other epithelial populations remained largely unchanged in *Tas1r3*$^{-/-}$ mice by measuring the expression of representative gene markers for intestinal epithelial cell subsets **(Fig. 3.4D)**.[93] One notable exception was the stem cell-regulating gene *Ascl2*. Although *Ascl2* is a signature gene associated with intestinal epithelial stem cells, it is also expressed by tuft cells[193] and therefore the decrease in *Ascl2* expression in the epithelium of *Tas1r3*$^{-/-}$ mice may reflect the reduced number of tuft cells rather than changes in the stem cell population. We therefore surmised that TAS1R3 is required for maintenance of homeostatic levels of tuft cells, and that the few ileal tuft cells present in *Tas1r3*$^{-/-}$ mice cannot trigger the IL-25 and IL-13-dependent feedback loop required for expansion with the same kinetics seen in WT mice.

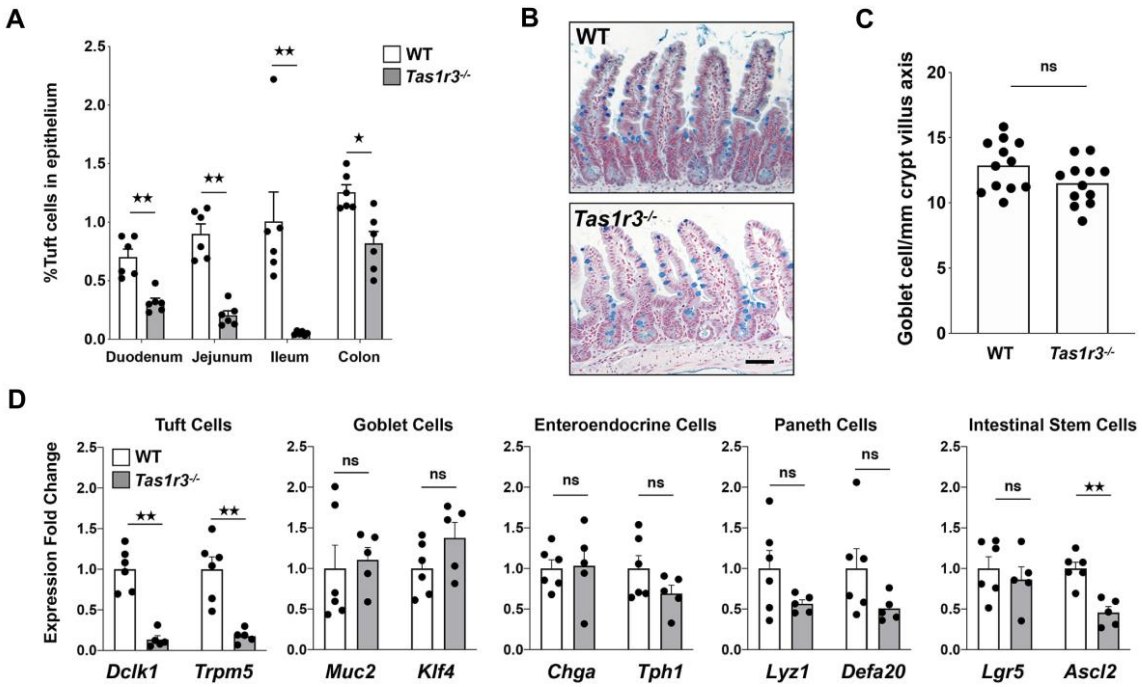

Figure 3.4. TAS1R3 regulates homeostatic tuft cell abundance. (A) Tuft cell frequency determined by flow cytometry in the duodenum, jejunum, ileum, and colon of C57BL/6J WT (*Gfi1b*$^{eGFP/+}$) and *Tas1r3*$^{-/-}$ (*Gfi1b*$^{eGFP/+}$ *Tas1r3*$^{-/-}$) at steady state. **(B)** Representative distal small intestine images of Alcian blue and nuclear red staining (scale bar, 50 μm) and **(C)** goblet cell frequency at steady state. **(D)** Expression of epithelial cell subset marker genes determined by qPCR in the epithelial fraction of the distal small intestine of WT and *Tas1r3*$^{-/-}$ mice at steady state. Each symbol represents an individual mouse, and all data are representative of 3 independent experiments. Data are plotted as means with SEM. Two stars, $P < 0.01$; one star, $P < 0.05$; n.s., not significant. One-way analysis of variance (ANOVA) with Holm-Sidak's test or Mann-Whitney U test.

To understand how TAS1R3 regulates intestinal tuft cells, we next measured the expression of *Tas1r3*, *Dclk1*, and *Trpm5* in epithelial cells harvested from the duodenum, jejunum, ileum, and colon of WT mice. While the expression of the tuft cell markers *Dclk1* and *Trpm5* was relatively consistent across the small intestine, *Tas1r3* expression was elevated in the ileum **(Fig. 3.5)**. This pattern of *Tas1r3* expression inversely correlated with the severity of the tuft cell defect in *Tas1r3*$^{-/-}$ mice. To identify intestinal TAS1R3 ligands that alter tuft cell frequency, we generated organoids from the ileal epithelium of *Gfi1b-eGFP* and *Gfi1b-eGFP x Tas1r3*$^{-/-}$ mice. In this system, TAS1R3 did not affect baseline tuft cell abundance or the IL-13-induced increase in tuft

cell frequency **(Fig. 3.6A)**. This observation led us to consider potential sources of TAS1R3 ligands in vivo. The microbiota is a rich source of ligands for host receptors, so we compared the number of tuft cells in the ileum of conventionally raised specific pathogen-free (SPF) WT and *Tas1r3*$^{-/-}$ mice with germ-free (GF) mice. GF mice had a similar frequency of tuft cells as conventional WT mice but significantly more tuft cells than *Tas1r3*$^{-/-}$ mice **(Fig. 3.6B)**, suggesting that the microbiota is not an important source of TAS1R3 ligands in the ileum.

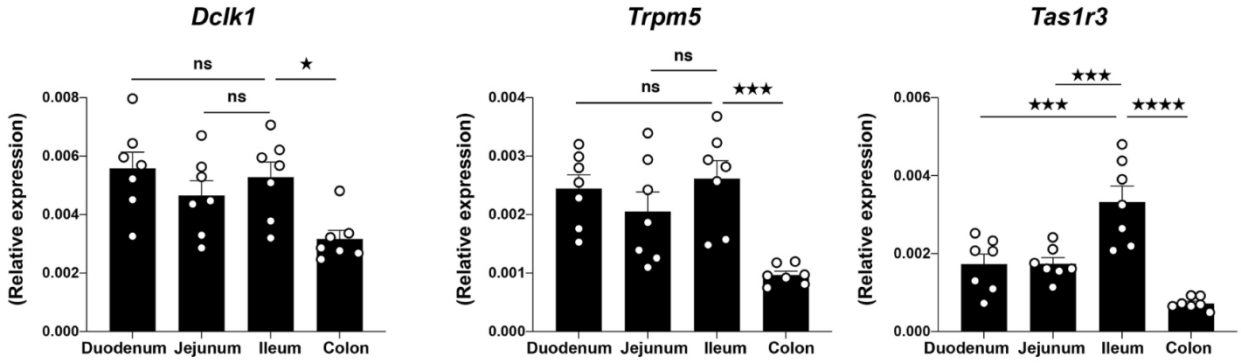

Figure 3.5. Epithelial expression of TAS1R3 is highest in the ileum. Expression of *Dclk1, Trpm5, and Tas1r3* determined by qPCR in the epithelial fraction of the indicated intestinal region in WT C57BL/6J mice. Data are plotted as means with SEM. Four stars, P < 0.0001; three stars, P<0.001; one star, P < 0.05; n.s., not significant. One-way analysis of variance (ANOVA) with Holm-Sidak's test.

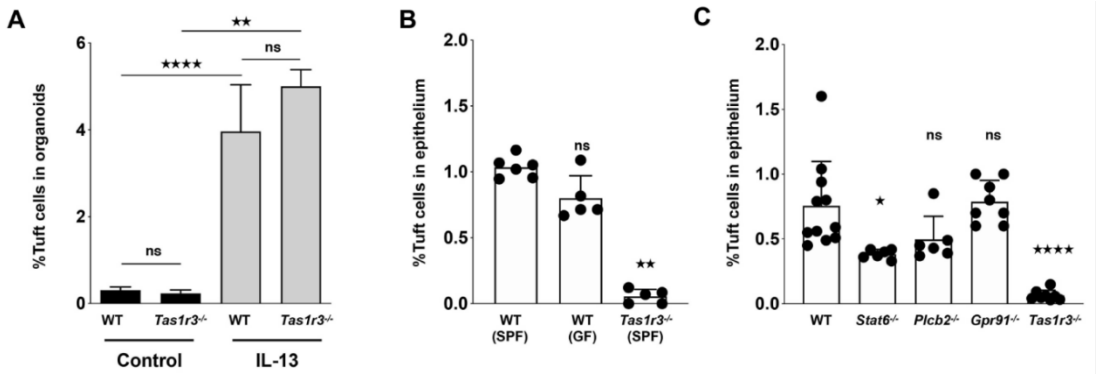

Figure 3.6. Analysis of potential TAS1R3 ligands and signaling pathways. (A) GFP^{+} tuft cell abundance determined by flow cytometry of WT and *Tas1r3*$^{-/-}$ distal SI organoids with or without 48h recombinant IL-13 treatment. **(B)** Distal SI tuft cell abundance determined by immunofluorescence in SPF and GF mice. **(C)** Distal SI tuft cell abundance determined by flow cytometry at steady state. Each symbol represents an individual mouse, and all data are pooled from at least 2 independent experiments. Data are plotted as means with SEM. Four stars, P < 0.0001, two stars, P < 0.01; one star, P < 0.05; n.s., not significant. Mann-Whitney U test.

In lingual taste cells, TAS1R3 forms a heterodimer either with TAS1R1 to detect umami flavor or TAS1R2 to detect sweet flavor[194]. However, in the ileum, we observed considerably lower expression of *Tas1r1* and *Tas1r2* compared to *Tas1r3* **(Fig. 3.2A)**, suggesting that many common sweet and umami taste agonists may not stimulate intestinal tuft cells. Therefore, to mimic a dietary agonist of TAS1R3, we fed mice the artificial sweetener sucralose, which has been reported to target TAS1R3 directly.[195] After feeding mice 2 mM, 20 mM, or 100 mM sucralose in the drinking water for 8 days, we did not observe a significant change in tuft cell abundance in either the duodenum or the ileum **(Supplemental Fig. 3.3)**. Similarly, rebaudioside A, a steviol glycoside that potentiates TRPM5 signaling[196], did not increase tuft cell frequency **(Supplemental Fig. 3.3)**. Because the TAS1R3 receptor putatively activates the canonical taste signal transduction pathway involving PLCβ2, we measured the frequency of tuft cells in the ileum of *Plcb2*$^{-/-}$ mice at homeostasis. Surprisingly, there were significantly fewer tuft cells in *Tas1r3*$^{-/-}$ mice than *Plcb2*$^{-/-}$ mice **(Fig. 3.6C)**. This defect was not observed in mice lacking another tuft cell-regulating GPCR, GPR91. Additionally, there were fewer tuft cells in *Tas1r3*$^{-/-}$ than in *Stat6*$^{-/-}$ mice **(Fig. 3.6C)**. Together, these findings imply that TAS1R3 may not regulate tuft cell abundance through currently established taste chemosensory pathways or through IL-13/IL-4 activation of STAT6 signaling.

IV. DISCUSSION

In this study, we found that the canonical taste receptor TAS1R3 regulates homeostatic tuft cell abundance, particularly in the ileum, where the frequency of tuft cells is reduced by approximately 95% in *Tas1r3*$^{-/-}$ mice. The loss of tuft cells significantly decreases the sensitivity of *Tas1r3*$^{-/-}$ mice to anti-parasite immunity-inducing stimuli like *T. muris* and succinate. In contrast to previous

work on tuft cell receptors, which focused on the direct sensing of parasite products[102,103,140], our study revealed that TAS1R3 indirectly affects intestinal immunity by shaping epithelial cell subset composition at baseline. The bimodal distribution of high and low tuft cell levels in *Tas1r3*$^{-/-}$ mice fed succinate, with an increasing proportion of mice with high-levels of tuft cells after longer treatment, suggests that the lower baseline levels of tuft cells in *Tas1r3*$^{-/-}$ mice delays the feed-forward expansion loop. Although the tuft cell response to succinate in *Tas1r3*$^{-/-}$ mice can be partially compensated for over time, even after four weeks of succinate treatment, approximately 50% of *Tas1r3*$^{-/-}$ mice display no change to tuft cell abundance. This observation is consistent with several possibilities. The relatively low frequency of tuft cells at baseline in *Tas1r3*$^{-/-}$ mice may slow the response kinetics in some animals, while others may never reach the threshold necessary to engage the tuft cell feed forward-loop. Alternatively, the kinetics may suggest a role for other cell populations expressing *Tas1R3*.

We confirmed that tuft cells in the ileum express *Tas1r3*, but we cannot exclude the influence of *Tas1r3* expression by other cell types on tuft cell frequency. For example, a subtype of enteroendocrine cell, the L-cell, also expresses *Tas1r3*.[197] L-cells are particularly abundant in the distal small intestine and colon and are characterized in part by the secretion of the hormones GLP-1 and GLP-2. These peptides function as incretin hormones but can also remodel the gut through increased small intestinal growth and epithelial proliferation.[198,199] GLP-1 secretion by duodenal L-cells is decreased in *Tas1r3*$^{-/-}$ mice[200], but the effect of these peptides on the differentiation or stability of tuft cells is unknown. Nonetheless, our data support that amongst the epithelial subsets, tuft cells are uniquely reduced in *Tas1r3*$^{-/-}$ mice. However, intestinal tuft cells are heterogeneous[93,201], and future work is needed to determine if TAS1R3 supports the differentiation or stability of all tuft cells or only specific tuft cell subpopulations.

To identify endogenous ligands for TAS1R3, we investigated the role of both the gut microbiota and specific dietary sugars on tuft cell frequency. The ilea of germ-free and conventionally raised SPF mice contained a similar abundance of tuft cells and significantly more tuft cells than conventionally raised SPF *Tas1r3*$^{-/-}$ mice. This observation suggests that microbial stimuli do not stimulate TAS1R3 to sustain normal tuft cell frequency. Mice fed the artificial sweetener sucralose also failed to expand tuft cells in either the duodenum or the ileum. Future efforts to identify intestinal TAS1R3 ligands may be aided by determining whether intestinal TAS1R3 functions as a homodimer or a heterodimer with another class C GPCR. Additionally, our study highlights a potential opportunity to understand intestinal tuft cell regulation in humans. TAS1R3 is expressed within the human intestine[202,203], and natural genetic variation in *TAS1R3* accounts for significant differences in sweet perception amongst the population[204]. Whether genetic differences in TAS1R3 can regulate human intestinal tuft abundance and type 2 immunity awaits further investigation.

V. METHODS

Mice

Wild-type C57BL/6J mice were bred and housed in microisolator cages in the specific-pathogen-free (SPF) barrier facility at the Harvard T.H. Chan School of Public Health and at Stanford University. BALB/c, *Gfi1b*$^{eGFP/+}$, *Plcb2*$^{-/-}$, and *Stat6*$^{-/-}$ mice were obtained from The Jackson Laboratory, Bar Harbor, Maine. C57BL/6J *Tas1r3*$^{-/-}$, and *Trpm5*$^{-/-}$ mice were generously provided by Dr. Robert Margolskee (Monell Chemical Senses Center), and *Gpr91*$^{-/-}$ mice were generously provided by Dr. Janos Peti-Peterdi with permission from Amgen.[205–207] All genetically modified mouse lines were bred on a C57BL6/J background and were co-housed for at least two weeks prior

to the experiments. *Gfi1b*$^{eGFP/+}$ *Gpr91*$^{-/-}$, *Gfi1b*$^{eGFP/+}$ *Plcb2*$^{-/-}$, *Gfi1b*$^{eGFP/+}$ *Stat6*$^{-/-}$, *Gfi1b*$^{eGFP/+}$ *Tas1r3*$^{-/-}$, and *Gfi1b*$^{eGFP/+}$ *Trpm5*$^{-/-}$ mice were generated by breeding *Gfi1b*$^{eGFP/+}$ mice to the relevant knock-out mice. Germ-free WT C57BL/6J mice were bred and maintained in semi-rigid gnotobiotic isolators in the Harvard T. H. Chan Gnotobiotic Center for Mechanistic Microbiome Studies. Mice were used experimentally between 6-12 weeks of age. Animal studies and experiments were approved and carried out in accordance with Harvard Medical School's Standing Committee on Animals, Stanford's Institutional Animal Care and Use Committee, and the National Institutes of Health guidelines for animal use and care.

Infection with protozoa and helminths

Tritrichomonas muris was isolated and cultured from bred-in-house mice as described previously.[101] 5x10^6 *T. muris* were orally administered to mice. Mice were then sacrificed 16-18 days post-infection.

Heligmosmoides polygyrus maintenance and infection was performed as previously described.[208] Mice were orally infected with 200 L3 larvae and sacrificed 6 weeks later. The proximal 15 cm of small intestine was excised and worms were counted with a dissection microscope.

***T. muris* enumeration**

T. muris load in the distal small intestine was enumerated as previously described.[101] The distal 10 cm of small intestine was removed and flushed with ice-cold sterile PBS using a 19-gauge feeding needle. The intestinal contents were then pelleted by centrifugation and stored at -20˚C. Genomic DNA was isolated from the stool with QIamp Fast DNA Stool mini kit (Qiagen) according to the manufacturer's directions. To detect and enumerate *T. muris*, quantitative PCR (qPCR) was performed using KAPPA SYBR fast Universal PCR (KAPPA Biosystems) with the following

primers recognizing the *T. muris* 28S rRNA gene: 5'-GCTTTTGCAAGCTAGGTCCC-3'and 5'-TTTCTGATGGGGCGTACCAC-3'. These qPCR values were converted to *T. muris* numbers using a standard curve generated using known amounts of *T. muris*.

Metabolite/taste receptor ligand feeding

For succinate treatment, mice were provided with 100 mM disodium succinate (Sigma #224731) in the drinking water for 1, 2, or 4 weeks as indicated. 200 mM sodium chloride was used as a control to match sodium molarity. Sucralose was fed at concentrations of 2, 20, or 100 mM in the drinking water, and rebaudioside A was fed at a concentration of 1 mM for 8 days.

IL-25 injection

Mice were intraperitoneally (i.p.) injected daily with 0.5μg of recombinant IL-25 (R&D, Endotoxin level < 1.0 EU per 1 μg) or equivalent volume of sterile PBS for 7 days before harvesting the distal small intestine.

Epithelial cell isolation and flow cytometry

The small intestine and/or colon were removed and flushed with ice-cold sterile PBS using a 19-gauge feeding needle. The small intestine was further subdivided into the duodenum (proximal 7 cm), jejunum (next 10 cm), and ileum (distal 10 cm) and Peyer's patches were removed. Both small intestinal regions and colons were then opened longitudinally and gently agitated at 4˚C in PBS, 2% FBS, 5mM HEPES, 1mM DTT for 10 min. The tissue was then transferred into prewarmed PBS, 2% FBS, 5mM HEPES, 5mM EDTA and rotated at 37˚C for 15 minutes followed by vigorous shaking to remove epithelial cells. This was repeated and epithelial cells from both fractions were combined and washed with PBS. The epithelium was then digested in DMEM containing 10% FBS, 0.5 units/ml Dispase II (StemCell Technologies), 50 μg/ml DNase (Roche) for 10 minutes at 37˚C. The resulting solution was passed through 40 μm filters and washed with

PBS, 2% FBS, 1mM EDTA. The resulting single cell suspension was initially Fc blocked with anti-CD16/CD32 (clone 93, Biolegend) and then stained with the following antibodies: PacBlue-conjugated anti-CD45 (clone 30-F11, Biolegend), APC-conjugated anti-EpCam (clone G8.8, Biolegend). Cell viability was assessed by propidium iodide (PI) (Biolegend) staining.

Histology and fluorescence microscopy

The small intestine was removed and divided into proximal and distal sections before overnight fixation in 4% paraformaldehyde. The tissue was then embedded in paraffin and cut into 5µm thick sections. For both histology and immunofluorescence, sections were initially deparaffinized and rehydrated. Goblet cells were identified by alcian blue/nuclear red staining and enumerated along the crypt-villus axis by quantitative microscopy. For immunofluorescence, heat-mediated antigen retrieval was performed in Tris-EDTA buffer 0.05% Tween-20 pH 9.0 for 20 minutes. Afterwards, the slides were washed in PBS and blocked in PBS containing 3% BSA, 3% donkey serum, 0.1% Triton X-100, 0.1% saponin for 1 hour at room temperature. Primary antibodies were incubated overnight at 4˚C and secondary antibodies were applied for 1.5 hours at room temperature. Primary antibodies included: rabbit anti-DCLK1 (1:250 dilution, ab37994, Abcam), mouse anti-E-Cadherin (1:400 dilution, 36/E-Cadherin, BD Biosciences) and DNA was labeled with DAPI (0.5 µg/ml).

RNA isolation and RT-PCR

Epithelial cells from *Gfi1b*$^{eGFP/+}$ mice were isolated and stained for Fluorescence Activated Cell Sorting (FACS) as previously detailed. Tuft cells were sorted based on $GFP^{+}EpCam^{+}CD45^{-}PI^{-}$ while the remaining epithelial cells were $GFP^{-}EpCam^{+}CD45^{-}PI^{-}$. RNA was then extracted from tuft cells and the remaining epithelium using RNeasy Micro Kit (Qiagen). For RNA isolation from total epithelium, the epithelial fraction was collected after EDTA wash (as described above) and

lysed in Qiazol (Qiagen) for RNA extraction following manufacturer's instructions. cDNA was synthesized using the iScript cDNA Synthesis Kit (Bio-Rad) and RT-qPCR was performed using the PowerUp SYBR Green master mix qPCR Kit (Applied Biosystems). The following primers were used:

Dclk1: 5'-CAGCCTGGACGAGCTGGTGG-3' ; 5'-TGACCAGTTGGGGTTCACAT-3',

Trpm5: 5'-CCTCCGTGCTTTTTGAACTCC-3' ; 5'-CATAGCCAAAGG TCGTTCCTC-3',

Klf4: 5'-ATCCTTTCCAACTCGCTAACCC-3' ; 5'-CGGATCGGATAGCTGAAGCTG-3',

Muc2: 5'-CCATTGAGTTTGGGAACATGC-3' ; 5'-TTCGGCTCGGTGTTCAGAG-3',

Chga: 5'-CAGGCTACAAAGCGATCCAG-3' ; 5'-GCCTCTGTCTTTCCATCTCC-3',

Tph1: 5'-AACAAAGACCATTCCTCCGAAAG-3' ; 5'-TGTAACAGGCTCACATGATTCTC-3',

Def20: 5'-TGTAGAAAAGGAGGCTGCAATAG-3' ; 5'-AGAACAAAAGTCGTCCTGAGC-3',

Lyz1: 5'-GCCAAGGTCTACAATCGTTGTGAGTTG-3' ; 5'-CAGTCAGCCAGCTTGACACCACG-3',

Lgr5: 5'-CCTACTCGAAGACTTACCCAGT-3' ; 5'-GCATTGGGGTGAATGATAGCA-3',

Ascl2: 5'-GCCTACTCGTCGGAGGAA-3' ; 5'-CCAACTGGAAAAGTCAAGCA-3',

Gapdh: 5'-CCTCGTCCCGTAGACAAAATG-3' ; 5'-TCTCCACTTTGCCACTGCAA-3',

Tas1r3: 5'-AGGTGGCTCACAGTTCTGCT-3' ; 5'-GAGGTGAGCCATTGGTTGTT-3',

Data are presented as relative expression normalized to Gapdh.

Small intestine organoid culture and flow cytometry

Distal small intestinal organoids were prepared as previously described.[209] When indicated, IL-13 (10ng/ml, Biolegend, Endotoxin level <0.01ng/μg) was added to organoid media for 48 hours. To

perform flow cytometry, organoids were liberated from the matrigel matrix as described by Miyoshi et al.[209] and digested in DMEM containing 10% FBS, 0.5 units/ml Dispase II (StemCell Technologies), 50 μg/ml DNase (Roche) for 8 minutes at 37˚C. The resulting solution was filtered through 40 μm mesh and stained for flow cytometry with APC-conjugated anti-EpCam (clone G8.8, Biolegend) with cell viability assessed with PI (Biolegend).

RNA sequencing

Experimental procedure

Epithelial cells from *Gfi1b*$^{eGFP/+}$ mice were isolated and stained for Fluorescence Activated Cell Sorting (FACS) as previously detailed. Tuft cells were sorted based on GFP^{+}EpCam^{+}CD45^{-}PI^{-} directly into lysis buffer from the RNeasy Mini Kit (Qiagen). RNA was isolated according to the manufacturer's protocol and RNA integrity was confirmed using a 2100 Agilent BioAnalyzer.

Library preparation

Libraries were prepared using a modified SMART-Seq2 protocol as previously reported.[210] RNA lysate cleanup was performed using RNAClean XP beads (Agencourt), followed by reverse transcription with Maxima Reverse Transcriptase (Life Technologies) and whole transcription amplification (WTA) with KAPA HotStart HIFI 2× ReadyMix (Kapa Biosystems) for 18 cycles. WTA products were purified with Ampure XP beads (Beckman Coulter), quantified with Qubit dsDNA HS Assay Kit (ThermoFisher), and assessed with a high sensitivity DNA chip (Agilent). RNA-seq libraries were constructed from purified WTA products using Nextera XT DNA Library Preparation Kit (Illumina). The libraries were sequenced on an Illumina NextSeq 500.

Computational analysis

BAM files were converted to merged, de-multiplexed FASTQs using the Illumina provided Bcl2Fastq software package v2.17.1.14. Paired-end reads were mapped to the UCSC mm10 mouse

transcriptome using Bowtie[211] with parameters "-q --phred33-quals -n 1 -e 99999999 -l 25 -I 1 -X 2000 -a -m 15 -S -p 6", which allows alignment of sequences with one mismatch. Expression levels of genes were quantified as transcript-per-million (TPM) values calculated by RSEM v1.2.3 in paired-end mode.[212] Negative binomial models were fitted to the data and likelihood-ratio tests used to assess differential expression, implemented using the DESeq2 package in R.[213] All data is deposited in GEO (GSE140395).

Statistics

The Mann-Whitney U test was used to compare two samples. One-way analysis of variance (ANOVA) was used for multiple-group comparisons followed by Holm-Sidak post-hoc testing. P-values are indicated in the figure legends.

Chapter 4

Conclusion and Future Directions

The intestinal epithelium is a focal point for communication between the environment and the host. In this dissertation, I identify two examples of how epithelial cells transduce an external signal to the host immune system and the resulting effects on gut physiology. First, epithelial cells in the duodenum responding to *F. rodentium* produce less retinoic acid. This retinoic acid sustains certain intestinal eosinophil populations, which restrict epithelial turnover and MHCII expression via regulation of intraepithelial lymphocyte-derived IFN-γ. Second, tuft cells in the ileum lacking the taste receptor TAS1R3 are unable to activate a type 2 immune response to the protozoa *T. muris*, perhaps due to a tuft cell defect under homeostatic conditions. These findings demonstrate the role of the intestinal epithelium as a critical mediator between the immune system and microbiota and suggest that further work elucidating the interactions between the three components will be important to understanding gut immunity and function.

Our work illustrates the profound effect of the microbiota on the epithelium and immune system in the duodenum. The role of the microbiota is often considered less in the proximal small intestine compared to more distal regions, as it has a lower microbial density than the ileum or colon. However, we demonstrated that the microbiota does affect many aspects of epithelial, eosinophil, and IEL function. Nonetheless, it would also be useful to perform similar profiling on epithelial cells in the jejunum, ileum, and colon to understand which effects are region-specific versus global to the gut. While retinoic acid production (and eosinophil levels) is highest in the proximal small intestine and may be less affected in other regions, features like MHCII expression are likely to be regulated across the gut. Additionally, among epithelial cells, we found that stem cell and enterocyte transcriptional profiles were highly regulated by the microbiota, but other cell types including tuft cells and enteroendocrine cells were more similar across microbiota backgrounds. This could be because neither of our complex microbiota contained specific bacteria

that regulate these cells, because they are less sensitive to commensal microbial stimuli in general, or because of a regional specificity of cell regulation, which could also be investigated with sequencing of other distal gut segments.

One of our initial observations was that specific microbiota in IH mice increase epithelial turnover rate, proliferation, and MHCII expression. Whether this increased turnover rate is beneficial or harmful to the host could be context-dependent. We found that IH mice, and particularly IH PHIL mice, which had the highest turnover rate, are more susceptible to anti-CD3-induced intestinal injury. However, other studies have shown that an accelerated intestinal epithelial turnover rate promotes helminth parasite expulsion.[111] Thus, different compositions of the microbiota could favor host survival under different circumstances. A helminth infection model in Jax and IH mice, such as with *Nippostrongylus brasiliensis* that targets the proximal small intestine, could directly test if epithelial cell alterations affect parasite clearance. Furthermore, as SPF mice housed in animal facilities encounter fewer pathogens and have a more naïve immune response compared to wild or pet store mice[214,215], it would be interesting to measure turnover rate in mice with a more "natural" microbiota to understand what tradeoffs in fitness occur. Along this vein, in addition to the changes in turnover and MHCII expression, IH enterocytes also had reduced expression of many metabolic genes, including fatty acid metabolism, which could affect their nutrient absorption function. It would be interesting to determine if IH mice have a different metabolic phenotype compared to GF or Jax mice and if the shift towards an immune-skewed expression profile has metabolic costs for the host.

We also demonstrated a role for retinoic acid in supporting the survival of certain intestinal eosinophil populations. This finding adds to wide variety of immune-regulating effects of RA. The mechanisms by which RA promotes eosinophil survival require additional study. As we did not

observe a synergistic effect of RA and IL-5 in promoting eosinophil survival, it is possible that RA may activate some of the same survival pathways as IL-5. These could include inhibition of the pro-apoptotic protein Bid and activation of ERK and c-Myc signaling.[216] Furthermore, only some intestinal eosinophil populations were dependent on RA, suggesting that there is heterogeneity in intestinal eosinophil populations with the potential for different functional states or subsets. This interpretation would be in line with recent work investigating eosinophil functional states.[217] CD11c expression level has been described as a marker of different intestinal eosinophil populations, and *in vitro*, eosinophils can be polarized to type 1 or type 2 states upon IFN-γ or IL-4 stimulation, similar to macrophages.[218,219] Whether GF, Jax, and IH eosinophils have different functional properties and if these properties are regulated by RA could be studied via single cell RNA sequencing, though this poses technical difficulties for eosinophils. Commonly used droplet-based sequencing methods like 10X do not adequately capture eosinophils, possibly because the granulocytes are sensitive to the pressures imposed during cell encapsulation. We attempted to perform an alternate sequencing method, SeqWell[220], to sidestep this issue, but failed to recover sufficient high quality reads, and will need to further optimize this method. A more targeted approach could be to measure RAR target gene expression in eosinophils to see if any regulated genes could affect eosinophil function.

Additionally, we found that eosinophils act as a rheostat to tune epithelial responses to the microbiota. When IFN-γ and epithelial turnover promoting signals are present, eosinophils suppress them. This restriction appears beneficial to gut health, as IH PHIL mice with heightened proliferation are more susceptible to anti-CD3 induced intestinal injury. The role of eosinophils in regulating proliferation and repair fits with the Local Immunity And/or Remodeling/Repair (LIAR) hypothesis posited by Lee and colleagues.[50] It holds that eosinophils are recruited to sites

with high levels of cell proliferation and cell death, both in homeostasis and disease, where they modulate immunity and tissue remodeling. Determining how eosinophils regulate IELs to reduce their IFN-γ production and consequently epithelial MHCII expression and turnover would further elucidate their role in promoting tissue homeostasis.

From the microbial side, a future area of investigation could include the properties of *F. rodentium* that contribute to epithelial cell interactions. In the ileum and colon, *F. rodentium* can produce short chain fatty acids that suppress tumor growth.[22] It is possible that a similar effect holds in the duodenum, or that *F. rodentium* produces a different regulatory metabolite. However, we did not observe any effect of the short chain fatty acids propionate or butyrate on eosinophil abundance, so they may not be the regulatory molecules in our system. A metabolomics analysis of intestinal contents from IH, Jax, and *F. rodentium* monocolonized mice could identify metabolites of interest. Alternatively, *F. rodentium* could interact directly with epithelial cells, as it has been found in the mucus layer. Current studies indicate that epithelial cells exposed to *F. rodentium ex vivo* may downregulate RA producing enzymes, so additional experiments using conditioned media or killed bacteria could narrow down the means of interaction. A related question would be to determine what other bacteria could share these properties. *F. rodentium* alone does not recapitulate the entire effect of the IH microbiota, suggesting that other bacteria, including *B. pseudolongum* and others, are contributing as well. These other bacteria could act through a similar or distinct mechanism. Interestingly, another *Erysipelotrichaceae* family member was enriched in Jax mice, indicating that not all *Erysipelotrichaceae* share the capacities of *F. rodentium*. Colonization with other related bacteria, such as *Allobaculum stercoricanis*, could provide additional points of reference depending on if they also regulate RA enzyme expression.

Comparison of the genomes of regulatory vs non-regulatory species could then identify potential gene clusters involved.

Another point raised by our study is the importance of understanding individual contributions of gut microbiota members. Despite the presence of a complex microbiota in Jax mice, their epithelial cell and eosinophil phenotypes resembled those of GF mice. In some ways, this finding is reminiscent of the effect of segmented filamentous bacteria, which induce Th17 cells in the gut, particularly in the ileum.[8] In that study, Jax mice also more closely resembled GF mice in terms of their Th17 compartment. Later work identified the ability of SFB to attach to epithelial cells as critical for Th17 induction, and that other bacteria with attachment properties could act similarly.[221] Thus, determining the mechanism of *F. rodentium* interaction with epithelial cells as described above would aid in forming selection criteria to find other bacteria with similar capabilities.

As discussed in relation to *F. rodentium,* microbes can be sensed by the host in many ways, via canonical microbe-associated molecular patterns activating pattern recognition receptors, microbial metabolites, or direct contact with host cells. In Chapter 3, we demonstrate another instance of this detection in finding that TAS1R3 is required for the initial tuft cell response to the microbial metabolite succinate. One major outstanding question is the ligand responsible for TAS1R3 activation in tuft cells. Under homeostatic conditions, the ligand is unlikely to be microbial, as WT GF mice had higher tuft cell abundance than SPF *Tas1r3*$^{-/-}$ mice. Neither does the ligand necessarily appear to be a canonical TAS1R3 ligand or taste pathway activator, as the artificial sweetener sucralose and steviol glycoside rebaudioside A did not increase tuft cell levels. This second observation may not be surprising given that TAS1R1 and TAS1R2, the receptors with which TAS1R3 can form heterodimers to detect umami and sweet taste, are lowly expressed

in intestinal tuft cells. It is possible that TAS1R3 could dimerize with a non-canonical partner in tuft cells, allowing the detection of different ligands. TAS1R3 (and all type 1 taste receptors) are class C GPCRs, and tuft cells express GPRC5A and GPRC5C, two class C orphan receptors, at higher levels than other epithelial cells.[93] Such receptors may also be involved in tuft cell function, whether in concert with TAS1R3 or separately. Future work could involve screening a compound library on tuft cells with calcium flux activated by taste chemosensory components as a readout.

Additionally, how TAS1R3 controls tuft cell abundance, and what signaling pathways are involved, remain to be determined. The defect in tuft cells in *Tas1r3*$^{-/-}$ mice does not seem to be due to impaired differentiation, as *Tas1r3*$^{-/-}$ organoids stimulated with IL-13 have similar tuft cell frequencies as WT organoids. Thus, it may be possible that *Tas1r3*$^{-/-}$ tuft cells have decreased survival. RNA-sequencing of WT versus *Tas1r3*$^{-/-}$ tuft cells could identify potential altered pathways. As mice deficient in common taste receptor transduction pathway components normally activated downstream of TAS1R3, including TRPM5 and PLCB2, do not have reduced tuft cell frequency at baseline, it is possible that TAS1R3 in tuft cells can signal through an alternative pathway in additional to the canonical one. Further study of this intriguing possibility would be important for understanding cues required for tuft cell survival or induction as well as potential new TAS1R3 signaling mechanisms.

Whether TAS1R3 or other taste receptors could regulate tuft cells in other tissues is also of interest. Thymus, trachea, and gallbladder tuft cells express TAS1R3[103], so whether the receptor regulates tuft cell abundance in these sites could be investigated. Thymic and tracheal tuft cells also express type 2 taste receptors including TAS2R108, TAS2R137, and TAS2R138.[103] Although we did not find high expression of TAS2Rs in ileal tuft cells, other studies have shown an increased expression of certain TAS2Rs after parasite infection.[140] These receptors could act similarly to

TAS1R3 to control tuft cell homeostasis or be involved in the detection of environmental or pathogenic signals. The multiplicity of taste receptors expressed by tuft cells could act to tune their responses to both site and pathogen-specific signals.

Lastly, we observed differences in tuft cell frequency in different inbred mouse strains, with fewer tuft cells in Balb/c mice that have an inactivating mutation in *Tas1r3*. Polymorphisms are also common in the human *TAS1R3* gene, and alter perceptions of sweetness, in some instances possibly due to changes in expression levels of *TAS1R3*.[204] Given these observations, it would be interesting to investigate if *TAS1R3* polymorphisms also affect human tuft cell function and lead to variations in responsiveness to type 2 stimuli.

In summary, this dissertation dissects two contexts in which the intestinal epithelium integrates luminal signals in the gut to coordinate immune cell responses, which then feed back to the epithelium to remodel its composition and function. These findings illustrate the importance of considering the epithelium as a nexus point which is both a sensor and readout of microbial activity, and thus a crucial component of understanding microbiota-immune interactions. Another implication of this work is the importance of studying microbiota-epithelial-immune interplay at different sites. Retinoic acid production is highest in the proximal small intestine, making an understanding of how *F. rodentium* regulates its activity in the duodenum very relevant, whereas TAS1R3 expression and tuft cell response to *T. muris* is highest in the ileum. Thus, care should be taken to choose a physiologically relevant region when studying relationships between microbes and the host.

Beyond advancing our understanding of epithelial-immune interactions in gut homeostasis, these findings also have implications for human disease. In celiac disease, IEL-mediated killing of epithelial cells in the proximal small intestine is a major cause of disease pathology. Our finding

that eosinophils regulate IEL-IEC interactions in a microbiota-dependent manner suggests that examination of eosinophils and microbiota in celiac disease, both of which remain poorly understood, could be a promising angle to explore in disease biology. Additionally, reduced numbers of ileal tuft cells have been linked to inflammation in Crohn's disease[222], so understanding how TAS1R3 maintains tuft cells at baseline could lead to targets for IBD treatment. Thus, this work provides a foundation for study of microbiota-epithelial-immune interactions in both homeostasis and disease.

Appendix 1

Supplementary Materials

Figure S2.1

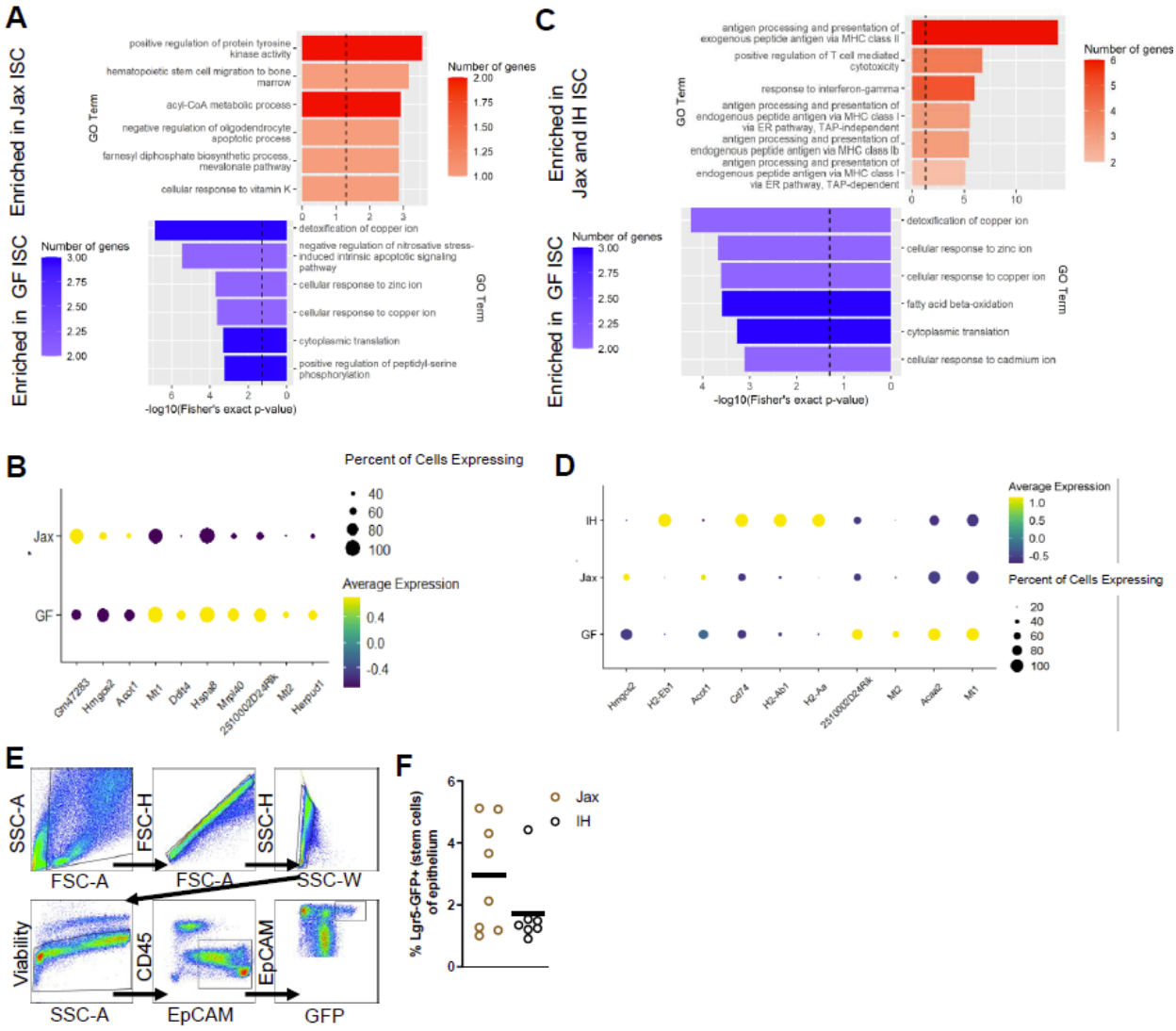

(A) GO categories for differentially expressed genes enriched in Jax vs GF ISCs (dashed line indicates threshold for p value = 0.05). **(B)** Top differentially expressed genes in Jax vs GF ISCs, ranked by significance. **(C)** GO categories for differentially expressed genes enriched in Jax vs GF ISCs (dashed line indicates threshold for p value = 0.05). **(D)** Top differentially expressed genes in Jax and IH vs GF ISCs, ranked by significance. **(E)** Flow cytometry gating strategy for epithelial cells. **(F)** Lgr5-GFP+ ISCs assessed by flow cytometry. Each symbol represents data from an individual mouse. Data are representative of 2 independent experiments.

Figure S2.2

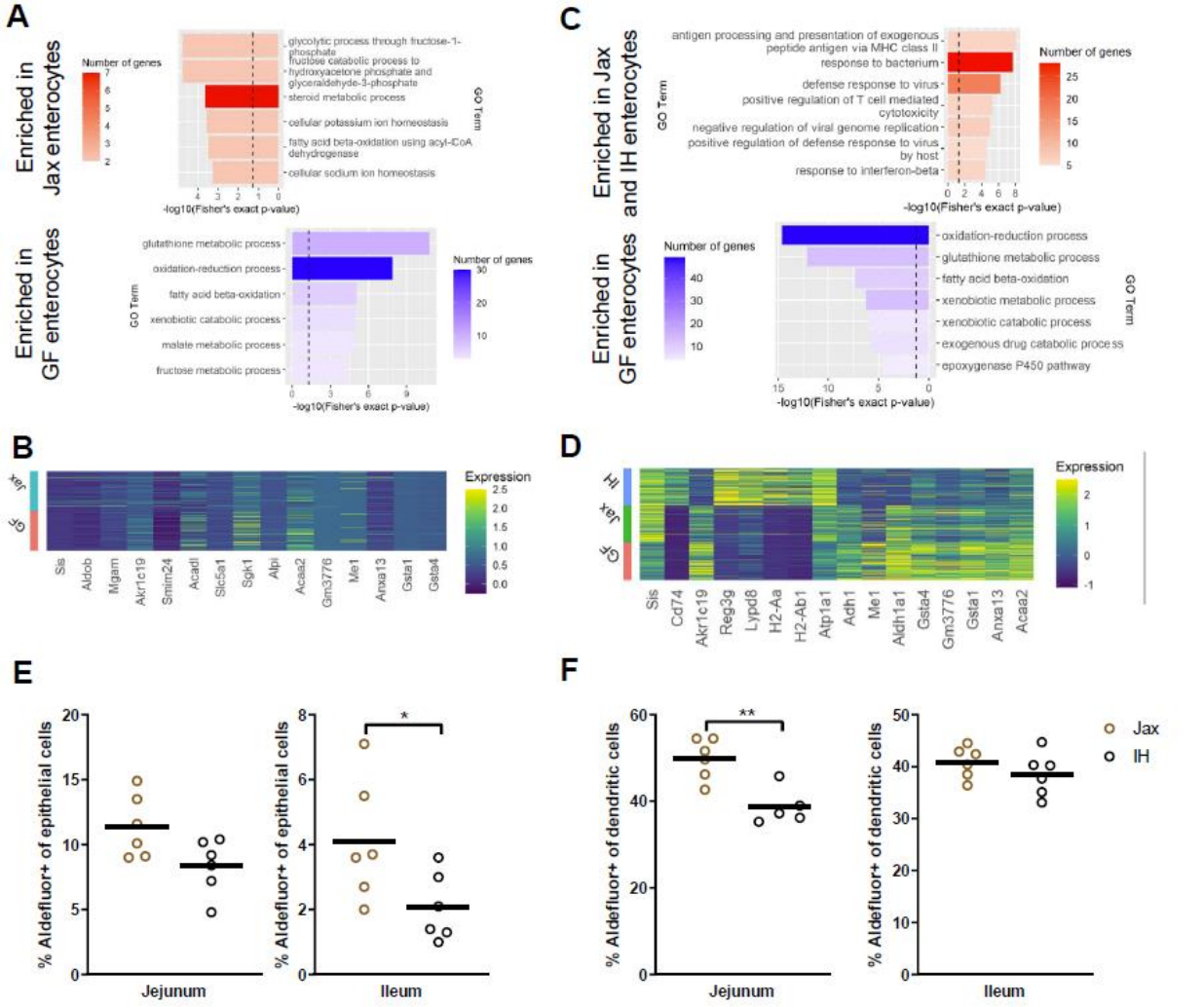

(A) GO categories for differentially expressed genes enriched in Jax vs GF enterocytes (dashed line indicates threshold for p value = 0.05). **(B)** Top differentially expressed genes in Jax vs GF enterocytes, ranked by significance. **(C)** GO categories for differentially expressed genes enriched in Jax vs GF enterocytes (dashed line indicates threshold for p value = 0.05). **(D)** Top differentially expressed genes in Jax and IH vs GF enterocytes, ranked by significance. **(E-F)** Measurement of Aldh enzyme activity via Aldefluor assay in epithelial cells ($EpCAM^+CD45^-$) or dendritic cells ($CD45^+CD11c^+MHCII^+CD64^-$). Gating strategy as in Fig. S1E and Fig. S3A. Each symbol (E-F) represents data from an individual mouse. Data reflect 3 independent experiments. Data are shown as mean with individual data points. *p < 0.05, **p < 0.01 Mann-Whitney U test.

Figure S2.3

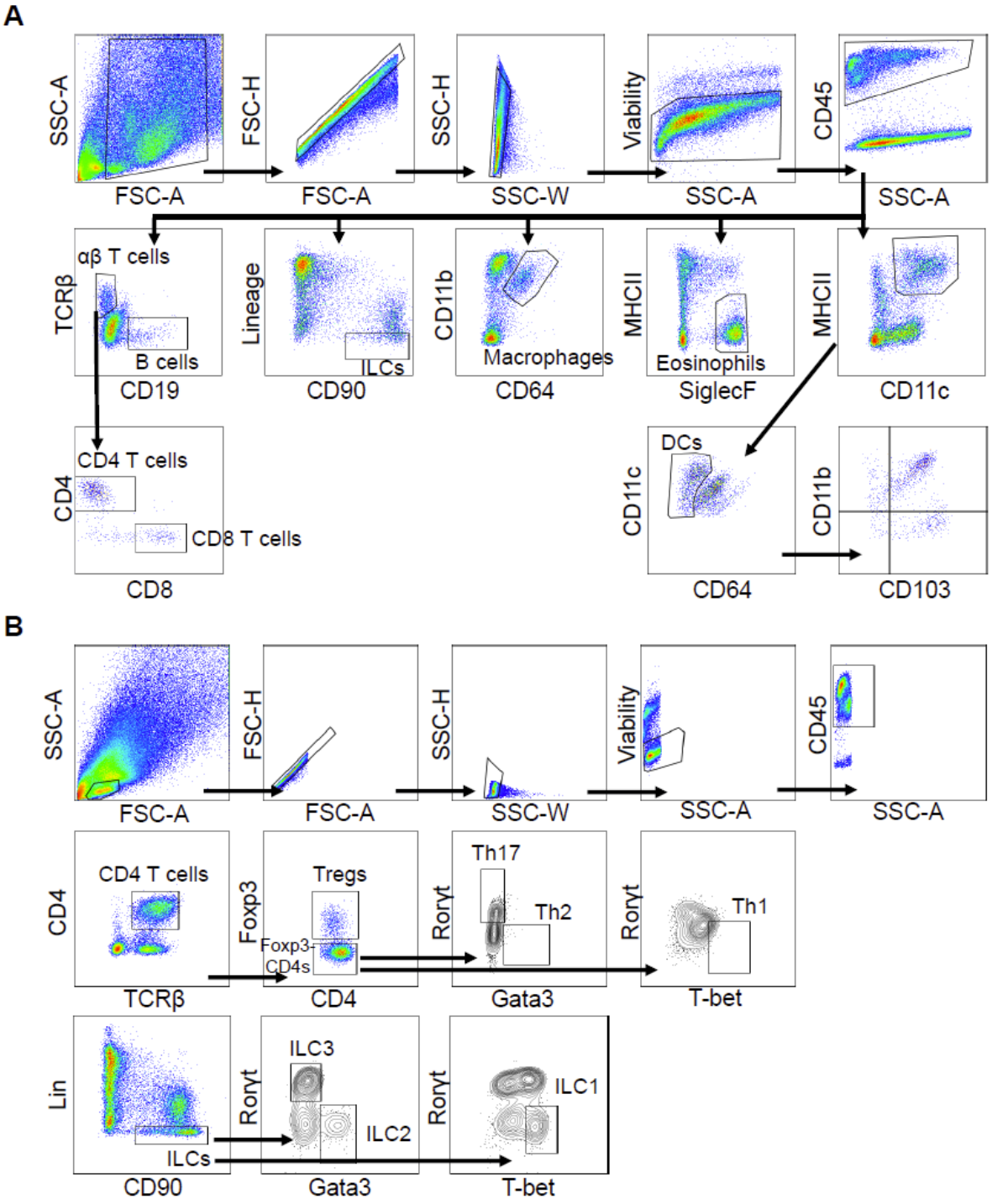

Flow cytometry gating strategies for **(A)** total immune cell populations and **(B)** CD4 T cell and ILC subsets.

Figure S2.4

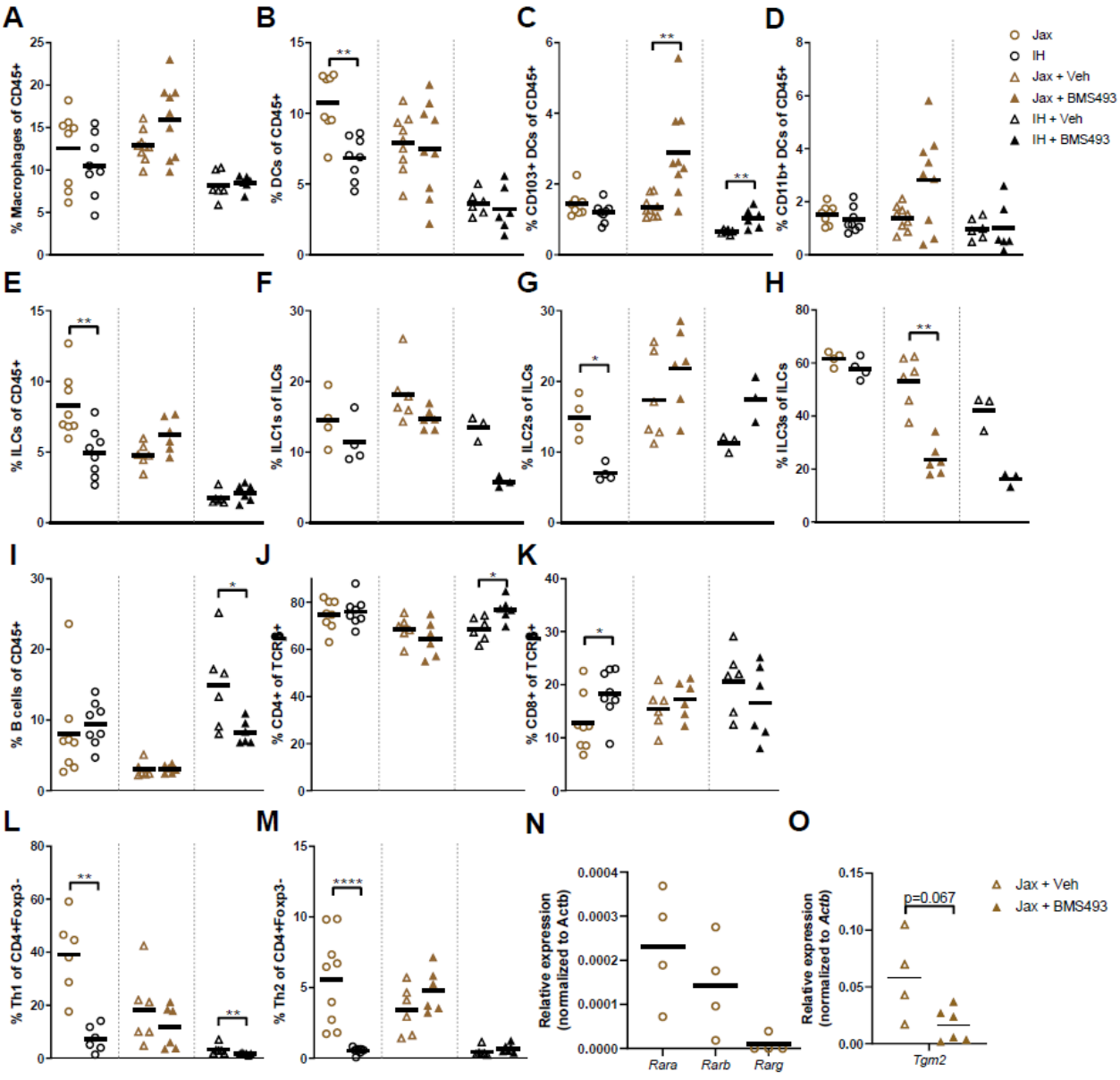

(A-M) Flow cytometry of lamina propria immune populations at steady state, or after treatment with 220µg RAR inhibitor BMS493 or vehicle (DMSO) for 8 days. **(N)** Retinoic acid receptor expression in sorted intestinal eosinophils from Jax mice. **(O)** Expression of RA target gene *Tgm2* in sorted intestinal eosinophils from mice treated for 8 days with BMS493 or vehicle (DMSO). Each symbol represents data from an individual mouse (A-M) or multiple mice pooled for sorting (N-O). Data reflect at least 2 independent experiments or are pooled from 2-3 experiments (K-M). Data are shown as mean with individual data points. *p < 0.05, **p < 0.01, ****p < 0.0001, Mann-Whitney U test.

Figure S2.5

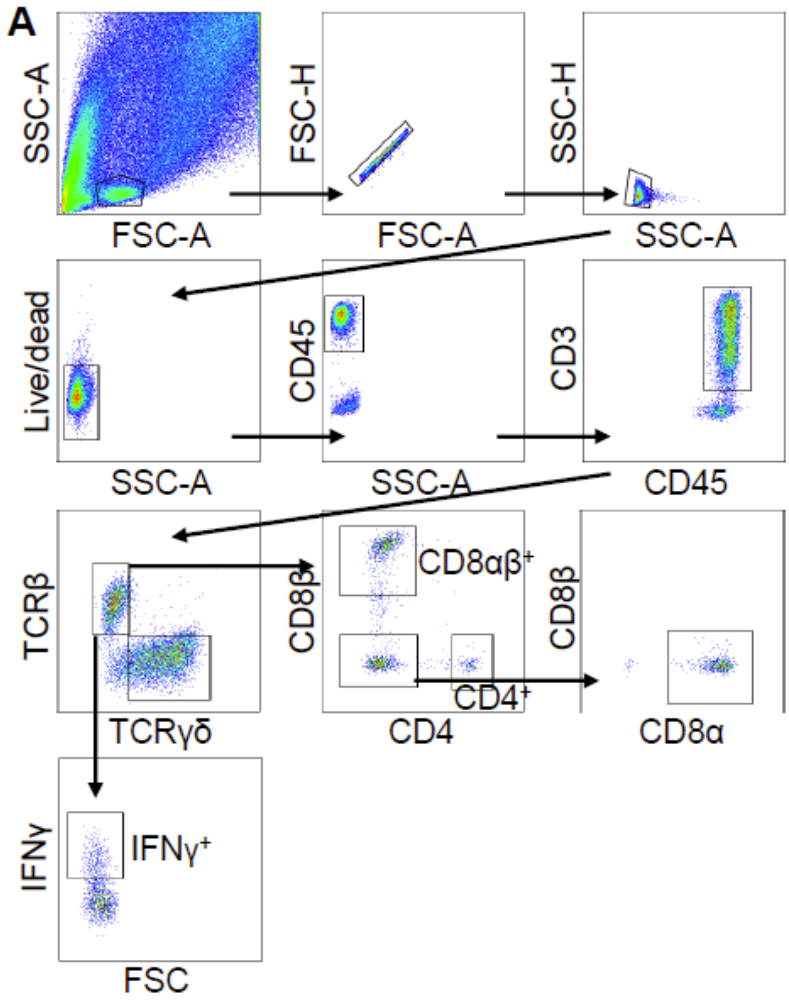

(A) Flow cytometry gating strategy for IEL populations.

Figure S2.6

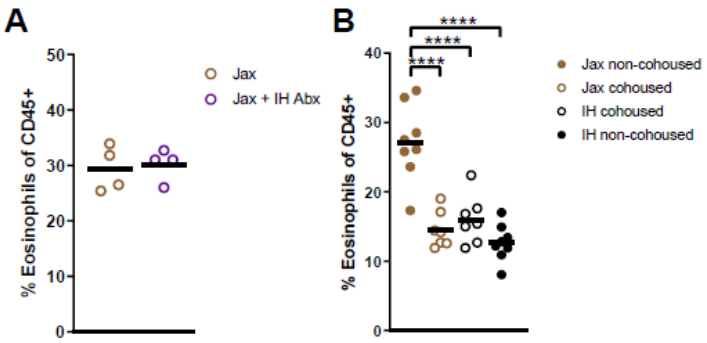

(A) Jax mice received transfer of microbiota from IH mice that were pre-treated for 2 weeks with broad-spectrum antibiotics (vancomycin, metronidazole, ampicillin, neomycin, and amphotericin B) and eosinophils were assessed by flow cytometry. **(B)** Jax and IH mice were either co-housed in the same cage or housed only with the same microbiota background mice for 2 weeks. Each symbol represents an individual mouse. Data are representative of 2 independent experiments. ****p < 0.0001, one-way ANOVA with Holm-Sidak's post-test (B).

Figure S2.7

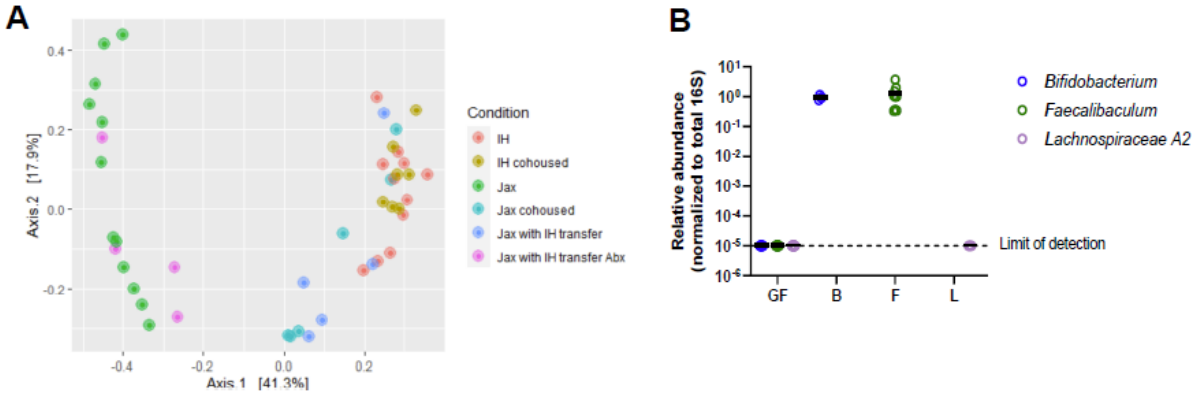

(A) Principal coordinates analysis of Bray-Curtis dissimilarity of stool 16S rRNA gene amplicon sequencing. **(B)** Colonization levels in stool of mono-colonized mice determined by qPCR. Each symbol represents data from stool from an individual mouse. Data are representative of 2 independent experiments.

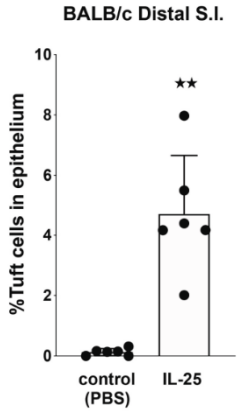

Figure S3.1. BALB/c mice expand distal SI tuft cells in response to IL-25. Tuft cell abundance determined by immunofluorescence after 1 week of IL-25 injection. Each symbol represents an individual mouse, and data are pooled from two independent experiments. Data are plotted as means with SEM. Two stars, $P < 0.01$. Mann-Whitney U test.

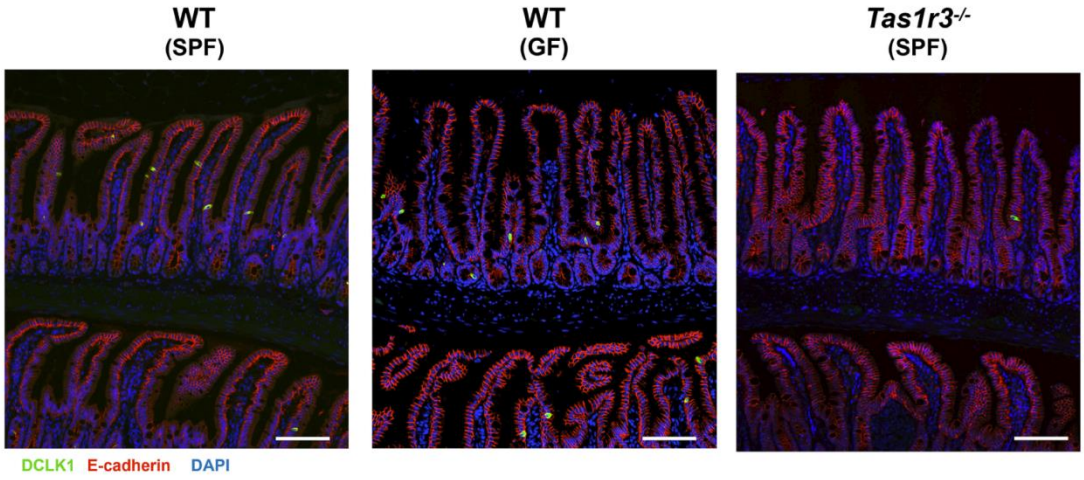

Figure S3.2. Distal SI tuft cells in C57BL6/J WT specific-pathogen-free (SPF), WT germ free (GF) and Tas1r3$^{-/-}$ (SPF) mice. Scale bars, 100 μm.

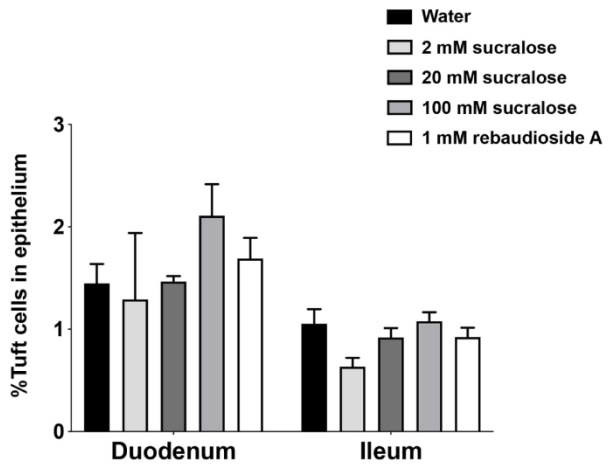

Figure S3.3. Taste pathway agonists do not expand intestinal tuft cells. Tuft cell abundance determined by flow cytometry after WT (*Gfi1b-eGFP/+*) C57BL/6J mice were fed sucralose or rebaudioside A in the drinking water at the indicated concentrations for 8 days. Data are representative of 2 to 8 biological replicates per group and plotted as means with SEM.

References

1. Sharma, R., Schumacher, U., Ronaasen, V. & Coates, M. Rat intestinal mucosal responses to a microbial flora and different diets. *Gut* **36**, 209–214 (1995).

2. Reinhardt, C. *et al.* Tissue factor and PAR1 promote microbiota-induced intestinal vascular remodelling. *Nature* **483**, 627–631 (2012).

3. Alam, M., Midtvedt, T. & Uribe, A. Differential Cell Kinetics in the Ileum and Colon of Germfree Rats. *Scand. J. Gastroenterol.* **29**, 445–451 (1994).

4. Sommer, F. & Bäckhed, F. The gut microbiota--masters of host development and physiology. *Nat. Rev. Microbiol.* **11**, 227–38 (2013).

5. Khoury, K. A., Floch, M. H. & Hersh, T. Small Intestinal Mucosal Cell Proliferation and Bacterial Flora in the Conventionalization of the Germfree Mouse. *J. Exp. Med.* **130**, 659–670 (1969).

6. Turnbaugh, P. J. *et al.* An obesity-associated gut microbiome with increased capacity for energy harvest. *Nature* **444**, 1027–1031 (2006).

7. Belkaid, Y. & Hand, T. W. Role of the microbiota in immunity and inflammation. *Cell* **157**, 121–141 (2014).

8. Ivanov, I. I. *et al.* Induction of intestinal Th17 cells by segmented filamentous bacteria. *Cell* **139**, 485–98 (2009).

9. Gaboriau-Routhiau, V. *et al.* The Key Role of Segmented Filamentous Bacteria in the Coordinated Maturation of Gut Helper T Cell Responses. *Immunity* **31**, 677–689 (2009).

10. Atarashi, K. *et al.* Induction of Colonic Regulatory T Cells by Indigenous Clostridium Species. *Science (80-.).* **331**, 337–341 (2011).

11. Round, J. L. & Mazmanian, S. K. Inducible Foxp3+ regulatory T-cell development by a commensal bacterium of the intestinal microbiota. *Proc. Natl. Acad. Sci.* **107**, 12204–12209 (2010).

12. Gury-BenAri, M. *et al.* The Spectrum and Regulatory Landscape of Intestinal Innate Lymphoid Cells Are Shaped by the Microbiome. *Cell* **166**, 1231-1246.e13 (2016).

13. Niess, J. H. & Adler, G. Enteric Flora Expands Gut Lamina Propria CX_3CR1^+ Dendritic Cells Supporting Inflammatory Immune Responses under Normal and Inflammatory Conditions. *J. Immunol.* **184**, 2026–2037 (2010).

14. Donaldson, G. P., Lee, S. M. & Mazmanian, S. K. Gut biogeography of the bacterial microbiota. *Nat. Rev. Microbiol.* **14**, 20–32 (2015).

15. Richard, M. L. & Sokol, H. The gut mycobiota: insights into analysis, environmental interactions and role in gastrointestinal diseases. *Nat. Rev. Gastroenterol. Hepatol. 2019 166* **16**, 331–345 (2019).

16. Li, Y., Handley, S. A. & Baldridge, M. T. The dark side of the gut: Virome-host interactions in intestinal homeostasis and disease. *J. Exp. Med.* **218**, (2021).

17. Chabé, M., Lokmer, A. & Ségurel, L. Gut Protozoa: Friends or Foes of the Human Gut Microbiota? *Trends Parasitol.* **33**, 925–934 (2017).

18. Geva-Zatorsky, N. *et al.* Mining the Human Gut Microbiota for Immunomodulatory Organisms. *Cell* **168**, 1–16 (2017).

19. Palm, N. W. *et al.* Immunoglobulin A coating identifies colitogenic bacteria in inflammatory bowel disease. *Cell* **158**, 1000–1010 (2014).

20. Cox, L. M. *et al.* Altering the intestinal microbiota during a critical developmental window has lasting metabolic consequences. *Cell* **158**, 705 (2014).

21. Miyauchi, E. *et al.* Gut microorganisms act together to exacerbate inflammation in spinal cords. *Nature* **585**, 102–106 (2020).

22. Zagato, E. *et al.* Endogenous murine microbiota member Faecalibaculum rodentium and its human homologue protect from intestinal tumour growth. *Nat. Microbiol.* **5**, (2020).

23. Fung, T. C. *et al.* Intestinal serotonin and fluoxetine exposure modulate bacterial colonization in the gut. *Nat. Microbiol.* **4**, 2064 (2019).

24. Szarka, L. A. & Camilleri, M. Methods for the Assessment of Small-Bowel and Colonic Transit. *Semin. Nucl. Med.* **42**, 113–123 (2012).

25. Martinez-Guryn, K., Leone, V. & Chang, E. B. Regional Diversity of the Gastrointestinal Microbiome. *Cell Host Microbe* **26**, 314–324 (2019).

26. Battle, M. A. *et al.* GATA4 is essential for jejunal function in mice. *Gastroenterology* **135**, (2008).

27. Earley, Z. M. *et al.* GATA4 regionalizes intestinal metabolism and barrier function to prevent immunopathology. *bioRxiv* 2021.10.28.466194 (2021) doi:10.1101/2021.10.28.466194.

28. Kim, K. S. *et al.* Dietary antigens limit mucosal immunity by inducing regulatory T cells in the small intestine. *Science (80-.).* **351**, 858–863 (2016).

29. Mowat, A. M. & Agace, W. W. Regional specialization within the intestinal immune system. *Nat. Rev. Immunol. 2014 1410* **14**, 667–685 (2014).

30. Agace, W. W. & McCoy, K. D. Regionalized Development and Maintenance of the Intestinal Adaptive Immune Landscape. *Immunity* **46**, 532–548 (2017).

31. Denning, T. L. *et al.* Functional Specializations of Intestinal Dendritic Cell and Macrophage Subsets That Control Th17 and Regulatory T Cell Responses Are Dependent on the T Cell/APC Ratio, Source of Mouse Strain, and Regional Localization. *J. Immunol.* **187**, 733–747 (2011).

32. Villablanca, E. J. *et al.* MyD88 and retinoic acid signaling pathways interact to modulate gastrointestinal activities of dendritic cells. *Gastroenterology* **141**, 176–185 (2011).

33. Klebanoff, C. A. *et al.* Retinoic acid controls the homeostasis of pre-cDC–derived splenic

and intestinal dendritic cells. *J. Exp. Med.* **210**, 1961–1976 (2013).

34. Mora, J. R. *et al.* Generation of Gut-Homing IgA-Secreting B Cells by Intestinal Dendritic Cells. *Science (80-.).* **314**, 1157–1160 (2006).

35. Lindner, C. *et al.* Age, microbiota, and T cells shape diverse individual IgA repertoires in the intestine. *J. Exp. Med.* **209**, 365–377 (2012).

36. Bunker, J. J. *et al.* Natural polyreactive IgA antibodies coat the intestinal microbiota. *Science (80-.).* **358**, (2017).

37. Di Marco Barros, R. *et al.* Epithelia Use Butyrophilin-like Molecules to Shape Organ-Specific γδ T Cell Compartments. *Cell* **167**, 203-218.e17 (2016).

38. Martinez-Guryn, K. *et al.* Small Intestine Microbiota Regulate Host Digestive and Absorptive Adaptive Responses to Dietary Lipids. *Cell Host Microbe* **23**, 458-469.e5 (2018).

39. Sayin, S. I. *et al.* Gut Microbiota Regulates Bile Acid Metabolism by Reducing the Levels of Tauro-beta-muricholic Acid, a Naturally Occurring FXR Antagonist. *Cell Metab.* **17**, 225–235 (2013).

40. Kay, A. B. The early history of the eosinophil. *Clin. Exp. Allergy* **45**, 575–582 (2015).

41. Acharya, K. R. & Ackerman, S. J. Eosinophil granule proteins: Form and function. *J. Biol. Chem.* **289**, 17406–17415 (2014).

42. Frigas, E., Loegering, D. A. & Gleich, G. J. Cytotoxic effects of the guinea pig eosinophil major basic protein on tracheal epithelium. *Lab. Invest.* **42**, 35–43 (1980).

43. Soragni, A. *et al.* Toxicity of Eosinophil MBP Is Repressed by Intracellular Crystallization and Promoted by Extracellular Aggregation. *Mol. Cell* **57**, 1011–1021 (2015).

44. Abu-Ghazaleh, R. I., Gleich, G. J. & Prendergast, F. G. Interaction of eosinophil granule major basic protein with synthetic lipid bilayers: a mechanism for toxicity. *J. Membr. Biol.* **128**, 153–64 (1992).

45. Lacy, P. *et al.* Divergence of mechanisms regulating respiratory burst in blood and sputum eosinophils and neutrophils from atopic subjects. *J. Immunol.* **170**, 2670–9 (2003).

46. Yang, D. *et al.* Eosinophil-derived neurotoxin (EDN), an antimicrobial protein with chemotactic activities for dendritic cells. *Blood* **102**, 3396–3403 (2003).

47. Yang, D. *et al.* Eosinophil-derived neurotoxin acts as an alarmin to activate the TLR2–MyD88 signal pathway in dendritic cells and enhances Th2 immune responses. *J. Exp. Med.* **205**, 79–90 (2008).

48. Yousefi, S. *et al.* Catapult-like release of mitochondrial DNA by eosinophils contributes to antibacterial defense. *Nat. Med.* **14**, 949–953 (2008).

49. Weller, P. F. & Spencer, L. A. Functions of tissue-resident eosinophils. *Nat. Rev.*

Immunol. (2017) doi:10.1038/nri.2017.95.

50. Lee, J. J., Jacobsen, E. A., Mcgarry, M. P., Schleimer, R. P. & Lee, N. A. Eosinophils in health and disease : the LIAR hypothesis. *Clin. Exp. Allergy* **40**, 563–575 (2010).

51. Filley, W. V, Holley, K. E., Kephart, G. M. & Gleich, G. J. Identification by immunofluorescence of eosinophil granule major basic protein in lung tissues of patients with bronchial asthma. *Lancet (London, England)* **2**, 11–6 (1982).

52. Raheem, M., Leach, S. T., Day, A. S. & Lemberg, D. A. The pathophysiology of eosinophilic esophagitis. *Front. Pediatr.* **2**, 41 (2014).

53. Lampinen, M. *et al.* Eosinophil granulocytes are activated during the remission phase of ulcerative colitis. *Gut* **54**, 1714–1720 (2005).

54. Davoine, F. & Lacy, P. Eosinophil cytokines, chemokines, and growth factors: Emerging roles in immunity. *Front. Immunol.* **5**, 1–17 (2014).

55. Svensson-Frej, M. Immunobiology of intestinal eosinophils - A dogma in the changing? *J. Innate Immun.* **3**, 565–576 (2011).

56. Flood-Page, P. *et al.* A study to evaluate safety and efficacy of mepolizumab in patients with moderate persistent asthma. *Am. J. Respir. Crit. Care Med.* **176**, 1062–1071 (2007).

57. Mishra, A., Hogan, S. P., Lee, J. J., Foster, P. S. & Rothenberg, M. E. Fundamental signals that regulate eosinophil homing to the gastrointestinal tract. *J. Clin. Invest.* **103**, 1719–1727 (1999).

58. Yu, Y.-R. A. *et al.* A Protocol for the Comprehensive Flow Cytometric Analysis of Immune Cells in Normal and Inflamed Murine Non-Lymphoid Tissues. *PLoS One* **11**, e0150606 (2016).

59. Wu, D. *et al.* Eosinophils Sustain Adipose Alternatively Activated Macrophages Associated with Glucose Homeostasis. *Science (80-.).* **332**, 243–247 (2011).

60. Qiu, Y. *et al.* Eosinophils and type 2 cytokine signaling in macrophages orchestrate development of functional beige fat. *Cell* **157**, 1292–308 (2014).

61. Chu, V. T. *et al.* Eosinophils promote generation and maintenance of immunoglobulin-A-expressing plasma cells and contribute to gut immune homeostasis. *Immunity* **40**, 582–593 (2014).

62. Jung, Y. *et al.* IL-1β in eosinophil-mediated small intestinal homeostasis and IgA production. *Mucosal Immunol.* **8**, 930–942 (2015).

63. Chu, V. T. *et al.* Eosinophils are required for the maintenance of plasma cells in the bone marrow. *Nat. Immunol.* **12**, 151–159 (2011).

64. Sugawara, R. *et al.* Small intestinal eosinophils regulate Th17 cells by producing IL-1 receptor antagonist. *J. Exp. Med.* **213**, 555–567 (2016).

65. Heredia, J. E. *et al.* Type 2 innate signals stimulate fibro/adipogenic progenitors to

facilitate muscle regeneration. *Cell* **153**, 376–88 (2013).

66. Goh, Y. P. S. *et al.* Eosinophils secrete IL-4 to facilitate liver regeneration. *Proc. Natl. Acad. Sci.* **110**, 9914–9919 (2013).

67. Vicetti Miguel, R. D. *et al.* IL-4–secreting eosinophils promote endometrial stromal cell proliferation and prevent *Chlamydia* -induced upper genital tract damage. *Proc. Natl. Acad. Sci.* **114**, E6892–E6901 (2017).

68. Chu, D. K. *et al.* Indigenous enteric eosinophils control DCs to initiate a primary Th2 immune response in vivo. *J. Exp. Med.* **211**, 1657–72 (2014).

69. Arnold, I. C. *et al.* Eosinophils suppress Th1 responses and restrict bacterially induced gastrointestinal inflammation. *J. Exp. Med.* jem.20172049 (2018) doi:10.1084/jem.20172049.

70. Clutterbuck, E. J., Hirst, E. M. & Sanderson, C. J. Human interleukin-5 (IL-5) regulates the production of eosinophils in human bone marrow cultures: comparison and interaction with IL-1, IL-3, IL-6, and GMCSF. *Blood* **73**, 1504–12 (1989).

71. Collins, P. D., Marleau, S., Griffiths-Johnson, D. A., Jose, P. J. & Williams, T. J. Cooperation between interleukin-5 and the chemokine eotaxin to induce eosinophil accumulation in vivo. *J. Exp. Med.* **182**, 1169–74 (1995).

72. Takemura, N. *et al.* Eosinophil depletion suppresses radiation-induced small intestinal fibrosis. *Sci. Transl. Med.* **10**, eaan0333 (2018).

73. Griseri, T. *et al.* Granulocyte Macrophage Colony-Stimulating Factor-Activated Eosinophils Promote Interleukin-23 Driven Chronic Colitis. *Immunity* **43**, 187–200 (2015).

74. Jiménez-Saiz, R. *et al.* Microbial Regulation of Enteric Eosinophils and Its Impact on Tissue Remodeling and Th2 Immunity. *Front. Immunol.* **11**, (2020).

75. Guan, Q. A Comprehensive Review and Update on the Pathogenesis of Inflammatory Bowel Disease. *J. Immunol. Res.* **2019**, (2019).

76. Loktionov, A. Eosinophils in the gastrointestinal tract and their role in the pathogenesis of major colorectal disorders. *http://www.wjgnet.com/* **25**, 3503–3526 (2019).

77. Ahrens, R. *et al.* Intestinal macrophage/epithelial cell-derived CCL11/eotaxin-1 mediates eosinophil recruitment and function in pediatric ulcerative colitis. *J. Immunol.* **181**, 7390–7399 (2008).

78. Jacobs, I. *et al.* Role of Eosinophils in Intestinal Inflammation and Fibrosis in Inflammatory Bowel Disease: An Overlooked Villain? *Front. Immunol.* **12**, 4355 (2021).

79. Smyth, C. M. *et al.* Activated Eosinophils in Association with Enteric Nerves in Inflammatory Bowel Disease. *PLoS One* **8**, (2013).

80. Masterson, J. C. *et al.* Eosinophil-mediated signalling attenuates inflammatory responses in experimental colitis. *Gut* **64**, 1236–1247 (2015).

81. Karmele, E. P. *et al.* Anti-IL-13Rα2 therapy promotes recovery in a murine model of inflammatory bowel disease. *Mucosal Immunol.* **12**, 1174–1186 (2019).

82. O'Shea, K. M. *et al.* Pathophysiology of Eosinophilic Esophagitis. *Gastroenterology* **154**, 333 (2018).

83. Blanchard, C. *et al.* A striking local esophageal cytokine expression profile in eosinophilic esophagitis. *J. Allergy Clin. Immunol.* **127**, (2011).

84. Dellon, E. S. The Esophageal Microbiome in Eosinophilic Esophagitis. *Gastroenterology* **151**, 364–365 (2016).

85. Prizment, A. E. *et al.* Tumor eosinophil infiltration and improved survival of colorectal cancer patients: Iowa Women's Health Study. *Mod. Pathol.* **29**, 516–27 (2016).

86. Prizment, A. E., Anderson, K. E., Visvanathan, K. & Folsom, A. R. Inverse association of eosinophil count with colorectal cancer incidence: Atherosclerosis Risk in Communities Study. *Cancer Epidemiol. Biomarkers Prev.* **20**, 1861 (2011).

87. Reichman, H. *et al.* Activated Eosinophils Exert Antitumorigenic Activities in Colorectal Cancer. *Cancer Immunol. Res.* 1–14 (2019) doi:10.1158/2326-6066.CIR-18-0494.

88. Arnold, I. C. *et al.* The GM-CSF-IRF5 signaling axis in eosinophils promotes antitumor immunity through activation of type 1 T cell responses. *J. Exp. Med.* **217**, (2020).

89. Khoury, P. *et al.* Revisiting the NIH Taskforce on the Research needs of Eosinophil-Associated Diseases (RE-TREAD). *J. Leukoc. Biol.* **104**, 69–83 (2018).

90. Allaire, J. M. *et al.* The Intestinal Epithelium: Central Coordinator of Mucosal Immunity. *Trends Immunol.* **39**, 677–696 (2018).

91. Hooper, L. V. Epithelial Cell Contributions to Intestinal Immunity. in *Advances in Immunology* vol. 126 129–172 (Academic Press, 2015).

92. Solis, A. G., Klapholz, M., Zhao, J. & Levy, M. The bidirectional nature of microbiome-epithelial cell interactions. *Curr. Opin. Microbiol.* **56**, 45–51 (2020).

93. Haber, A. L. *et al.* A single-cell survey of the small intestinal epithelium. *Nature* **551**, 333–339 (2017).

94. Elmentaite, R. *et al.* Cells of the human intestinal tract mapped across space and time. *Nature* **597**, 250–255 (2021).

95. Peterson, L. W. & Artis, D. Intestinal epithelial cells: regulators of barrier function and immune homeostasis. *Nat. Rev. Immunol.* **14**, 141–53 (2014).

96. McDole, J. R. *et al.* Goblet cells deliver luminal antigen to CD103+ dendritic cells in the small intestine. *Nature* **483**, 345–349 (2012).

97. Soderholm, A. T. & Pedicord, V. A. Intestinal epithelial cells: at the interface of the microbiota and mucosal immunity. *Immunology* vol. 158 267–280 (2019).

98. Larsen, S. B., Cowley, C. J. & Fuchs, E. Epithelial cells: liaisons of immunity. *Curr. Opin. Immunol.* **62**, 45–53 (2020).

99. Hall, J. A., Grainger, J. R., Spencer, S. P. & Belkaid, Y. The Role of Retinoic Acid in Tolerance and Immunity. *Immunity* **35**, 13–22 (2011).

100. Tuganbaev, T. *et al.* Diet Diurnally Regulates Small Intestinal Microbiome-Epithelial-Immune Homeostasis and Enteritis. *Cell* 1–19 (2020) doi:10.1016/j.cell.2020.08.027.

101. Howitt, M. R. *et al.* Tuft cells, taste-chemosensory cells, orchestrate parasite type 2 immunity in the gut. *Science (80-.).* **351**, 1329–1333 (2016).

102. Schneider, C. *et al.* A Metabolite-Triggered Tuft Cell-ILC2 Circuit Drives Small Intestinal Remodeling. *Cell* 1–14 (2018) doi:10.1016/j.cell.2018.05.014.

103. Nadjsombati, M. S. *et al.* Detection of Succinate by Intestinal Tuft Cells Triggers a Type 2 Innate Immune Circuit. *Immunity* **49**, 33-41.e7 (2018).

104. van der Flier, L. G. & Clevers, H. Stem Cells, Self-Renewal, and Differentiation in the Intestinal Epithelium. *Annu. Rev. Physiol.* **71**, 241–260 (2009).

105. Okada, T. *et al.* Microbiota-derived lactate accelerates colon epithelial cell turnover in starvation-refed mice. *Nat. Commun.* **4**, 1654 (2013).

106. Lee, Y.-S. *et al.* Microbiota-Derived Lactate Accelerates Intestinal Stem-Cell-Mediated Epithelial Development. *Cell Host Microbe* **24**, 833-846.e6 (2018).

107. Park, J. *et al.* Promotion of Intestinal Epithelial Cell Turnover by Commensal Bacteria: Role of Short-Chain Fatty Acids. *PLoS One* **11**, e0156334 (2016).

108. Sun, L. *et al.* Type I Interferons Link Viral Infection to Enhanced Epithelial Turnover and Repair. *Cell Host Microbe* **17**, 85–97 (2015).

109. Nishiyama, Y. *et al.* Homeostatic regulation of intestinal villous epithelia by B lymphocytes. *J. Immunol.* **168**, 2626–33 (2002).

110. Komano, H. *et al.* Homeostatic regulation of intestinal epithelia by intraepithelial gamma delta T cells. *Proc. Natl. Acad. Sci. U. S. A.* **92**, 6147–51 (1995).

111. Cliffe, L. J. *et al.* Accelerated intestinal epithelial cell turnover: A new mechanism of parasite expulsion. *Science (80-.).* **308**, 1463–1465 (2005).

112. Larange, A. & Cheroutre, H. Retinoic Acid and Retinoic Acid Receptors as Pleiotropic Modulators of the Immune System. *Annu. Rev. Immunol.* **34**, 369–394 (2016).

113. Bang, Y.-J. *et al.* Serum amyloid A delivers retinol to intestinal myeloid cells to promote adaptive immunity. *Science (80-.).* **373**, (2021).

114. Czarnewski, P., Das, S., Parigi, S. M. & Villablanca, E. J. Retinoic acid and its role in modulating intestinal innate immunity. *Nutrients* vol. 9 (2017).

115. Iwata, M. *et al.* Retinoic Acid Imprints Gut-Homing Specificity on T Cells. *Immunity* **21**,

527–538 (2004).

116. Kim, M. H., Taparowsky, E. J. & Kim, C. H. Retinoic Acid Differentially Regulates the Migration of Innate Lymphoid Cell Subsets to the Gut. *Immunity* **43**, 107–119 (2015).

117. Mucida, D. *et al.* Reciprocal TH17 and Regulatory T Cell Differentiation Mediated by Retinoic Acid. *Science (80-.).* **317**, 256–260 (2007).

118. Wang, C., Kang, S. G., Esch, H. H., Love, P. E. & Kim, C. H. Retinoic acid determines the precise tissue tropism of inflammatory Th17 cells in the intestine. *J. Immunol.* **184**, 5519 (2010).

119. Xiao, S. *et al.* Retinoic acid increases Foxp3+ regulatory T cells and inhibits development of Th17 cells by enhancing TGF-β-driven Smad3 signaling and inhibiting IL-6 and IL-23 receptor expression. *J. Immunol.* **181**, 2277 (2008).

120. Hall, J. A. *et al.* Essential role for retinoic acid in the promotion of CD4+ T cell effector responses via retinoic acid receptor alpha. *Immunity* **34**, 435 (2011).

121. Cha, H.-R. *et al.* Downregulation of Th17 Cells in the Small Intestine by Disruption of Gut Flora in the Absence of Retinoic Acid. *J. Immunol.* **184**, 6799–6806 (2010).

122. Takahashi, H. *et al.* TGF-β and retinoic acid induce miR-10a, which targets Bcl-6 and constrains helper T cell plasticity. *Nat. Immunol.* **13**, 587 (2012).

123. Reis, B. S., Rogoz, A., Costa-Pinto, F. A., Taniuchi, I. & Mucida, D. Mutual expression of Runx3 and ThPOK regulates intestinal CD4+ T cell immunity. *Nat. Immunol.* **14**, 271 (2013).

124. Spencer, S. P. *et al.* Adaptation of Innate Lymphoid Cells to a Micronutrient Deficiency Promotes Type 2 Barrier Immunity. *Science* **343**, 432 (2014).

125. Grizotte-Lake, M. *et al.* Commensals Suppress Intestinal Epithelial Cell Retinoic Acid Synthesis to Regulate Interleukin-22 Activity and Prevent Microbial Dysbiosis. *Immunity* **49**, 1103-1115.e6 (2018).

126. McDonald, B. D., Jabri, B. & Bendelac, A. Diverse developmental pathways of intestinal intraepithelial lymphocytes. *Nat. Rev. Immunol.* **18**, 1–12 (2018).

127. Faria, A. M. C., Reis, B. S. & Mucida, D. Tissue adaptation: Implications for gut immunity and tolerance. *J. Exp. Med.* **214**, 1211 (2017).

128. Bilate, A. M. *et al.* T Cell Receptor Is Required for Differentiation, but Not Maintenance, of Intestinal CD4 + Intraepithelial Lymphocytes. *Immunity* **53**, 1001-1014.e20 (2020).

129. Denning, T. L. *et al.* Mouse TCRalphabeta+CD8alphaalpha intraepithelial lymphocytes express genes that down-regulate their antigen reactivity and suppress immune responses. *J. Immunol.* **178**, 4230–4239 (2007).

130. Hoytema van Konijnenburg, D. P. *et al.* Intestinal Epithelial and Intraepithelial T Cell Crosstalk Mediates a Dynamic Response to Infection. *Cell* 1–12 (2017) doi:10.1016/j.cell.2017.08.046.

131. Ismail, A. S. *et al.* γδ intraepithelial lymphocytes are essential mediators of host-microbial homeostasis at the intestinal mucosal surface. *Proc. Natl. Acad. Sci. U. S. A.* **108**, 8743–8748 (2011).

132. Yu, Q. *et al.* MyD88-dependent signaling for IL-15 production plays an important role in maintenance of CD8 alpha alpha TCR alpha beta and TCR gamma delta intestinal intraepithelial lymphocytes. *J. Immunol.* **176**, 6180–6185 (2006).

133. Abadie, V., Discepolo, V. & Jabri, B. Intraepithelial lymphocytes in celiac disease immunopathology. *Semin. Immunopathol.* (2012) doi:10.1007/s00281-012-0316-x.

134. Trier, J. S., Allan, C. H., Marcial, M. A. & Madara, J. L. Structural features of the apical and tubulovesicular membranes of rodent small intestinal tuft cells. *Anat. Rec.* **219**, 69–77 (1987).

135. Gerbe, F. *et al.* Intestinal epithelial tuft cells initiate type 2 mucosal immunity to helminth parasites. *Nature* **529**, 226–30 (2016).

136. Bezençon, C. *et al.* Murine intestinal cells expressing Trpm5 are mostly brush cells and express markers of neuronal and inflammatory cells. *J. Comp. Neurol.* **509**, 514–525 (2008).

137. von Moltke, J., Ji, M., Liang, H.-E. & Locksley, R. M. Tuft-cell-derived IL-25 regulates an intestinal ILC2–epithelial response circuit. *Nature* **529**, 221–225 (2015).

138. McGinty, J. W. *et al.* Tuft-Cell-Derived Leukotrienes Drive Rapid Anti-helminth Immunity in the Small Intestine but Are Dispensable for Anti-protist Immunity. *Immunity* **0**, 528-541.e7 (2020).

139. Lei, W. *et al.* Activation of intestinal tuft cell-expressed Sucnr1 triggers type 2 immunity in the mouse small intestine. *Proc. Natl. Acad. Sci.* 201720758 (2018) doi:10.1073/pnas.1720758115.

140. Luo, X.-C. *et al.* Infection by the parasitic helminth *Trichinella spiralis* activates a Tas2r-mediated signaling pathway in intestinal tuft cells. *Proc. Natl. Acad. Sci.* **116**, 5564–5569 (2019).

141. Janssen, S. *et al.* Bitter taste receptors and α-gustducin regulate the secretion of ghrelin with functional effects on food intake and gastric emptying. *Proc. Natl. Acad. Sci.* **108**, 2094–2099 (2011).

142. Liszt, K. I. *et al.* Human intestinal bitter taste receptors regulate innate immune responses and metabolic regulators in obesity. *J. Clin. Invest.* **132**, (2022).

143. Okumura, R. & Takeda, K. Roles of intestinal epithelial cells in the maintenance of gut homeostasis. *Exp. Mol. Med.* **49**, e338 (2017).

144. Goto, Y. *et al.* Innate lymphoid cells regulate intestinal epithelial cell glycosylation. *Science* **345**, 1254009 (2014).

145. Rausch, P. *et al.* Colonic mucosa-associated microbiota is influenced by an interaction of

crohn disease and FUT2 (Secretor) genotype. *Proc. Natl. Acad. Sci. U. S. A.* **108**, 19030–19035 (2011).

146. Cadwell, K. *et al.* A key role for autophagy and the autophagy gene Atg16l1 in mouse and human intestinal Paneth cells. *Nature* **456**, 259–263 (2008).

147. Okumura, R. *et al.* Lypd8 promotes the segregation of flagellated microbiota and colonic epithelia. *Nature* **532**, 117–121 (2016).

148. Meresse, B. *et al.* Coordinated induction by IL15 of a TCR-independent NKG2D signaling pathway converts CTL into lymphokine-activated killer cells in celiac disease. *Immunity* **21**, 357–66 (2004).

149. Terrazzano, G. *et al.* Gliadin regulates the NK-dendritic cell cross-talk by HLA-E surface stabilization. *J. Immunol.* **179**, 372–381 (2007).

150. Fodde, R. & Brabletz, T. Wnt/beta-catenin signaling in cancer stemness and malignant behavior. *Curr. Opin. Cell Biol.* **19**, 150–158 (2007).

151. Kastl, A. J., Terry, N. A., Wu, G. D. & Albenberg, L. G. The Structure and Function of the Human Small Intestinal Microbiota: Current Understanding and Future Directions. *Cell. Mol. Gastroenterol. Hepatol.* **9**, 33–45 (2020).

152. Barsouk, A., Rawla, P., Barsouk, A. & Thandra, K. C. Epidemiology of Cancers of the Small Intestine: Trends, Risk Factors, and Prevention. *Med. Sci.* **7**, 46 (2019).

153. Sivan, A. *et al.* Commensal Bifidobacterium promotes antitumor immunity and facilitates anti-PD-L1 efficacy. *Science (80-.).* **350**, 1084–1089 (2015).

154. Skoskiewicz, M. J., Colvin, R. B., Schneeberger, E. E. & Russell, P. S. Widespread and selective induction of major histocompatibility complex-determined antigens in vivo by gamma interferon. *J. Exp. Med.* **162**, 1645–1664 (1985).

155. Li, F., Dai, L. & Niu, J. GPX2 silencing relieves epithelial–mesenchymal transition, invasion, and metastasis in pancreatic cancer by downregulating Wnt pathway. *J. Cell. Physiol.* **235**, 7780–7790 (2020).

156. Florian, S. *et al.* Loss of GPx2 increases apoptosis, mitosis, and GPx1 expression in the intestine of mice. *Free Radic. Biol. Med.* **49**, 1694–1702 (2010).

157. Jiao, Y., Wang, Y., Guo, S. & Wang, G. Glutathione peroxidases as oncotargets. *Oncotarget* **8**, 80093 (2017).

158. Kumar, S., Sandell, L. L., Trainor, P. A., Koentgen, F. & Duester, G. Alcohol and Aldehyde Dehydrogenases: Retinoid Metabolic Effects in Mouse Knockout Models. *Biochim. Biophys. Acta* **1821**, 198 (2012).

159. Germain, P. *et al.* Differential Action on Coregulator Interaction Defines Inverse Retinoid Agonists and Neutral Antagonists. *Chem. Biol.* **16**, 479–489 (2009).

160. Ueki, S. *et al.* Retinoic Acids Are Potent Inhibitors of Spontaneous Human Eosinophil Apoptosis. *J. Immunol.* **181**, 7689–7698 (2008).

161. Moore, W. T., Murtaugh, M. P. & Davies, P. J. A. Retinoic Acid-induced Expression of Tissue Transglutaminase in Mouse Peritoneal Macrophages. *J. Biol. Chem.* **259**, 12794–12802 (1984).

162. Takatsu, K. & Nakajima, H. IL-5 and eosinophilia. *Curr. Opin. Immunol.* **20**, 288–294 (2008).

163. Merger, M. *et al.* Defining the roles of perforin, Fas/FasL, and tumour necrosis factor alpha in T cell induced mucosal damage in the mouse intestine. *Gut* **51**, 155–163 (2002).

164. Nava, P. *et al.* Interferon-γ Regulates Intestinal Epithelial Homeostasis through Converging β-Catenin Signaling Pathways. *Immunity* **32**, 392–402 (2010).

165. Carroll, T. D., Newton, I. P., Chen, Y., Blow, J. J. & Näthke, I. Lgr5+ intestinal stem cells reside in an unlicensed G1 phase. *J. Cell Biol.* **217**, 1667 (2018).

166. Segata, N. *et al.* Metagenomic biomarker discovery and explanation. *Genome Biol.* **12**, R60 (2011).

167. Cox, L. M. *et al.* Description of two novel members of the family Erysipelotrichaceae: Ileibacterium valens gen. nov., sp. nov. and Dubosiella newyorkensis, gen. nov., sp. nov., from the murine intestine, and emendation to the description of Faecalibacterium rodentium. *Int. J. Syst. Evol. Microbiol.* **67**, 1247–1254 (2017).

168. Chang, D.-H. *et al.* Faecalibaculum rodentium gen. nov., sp. nov., isolated from the faeces of a laboratory mouse. *Antonie Van Leeuwenhoek* **108**, 1309–1318 (2015).

169. Biton, M. *et al.* T Helper Cell Cytokines Modulate Intestinal Stem Cell Renewal and Differentiation. *Cell* **175**, 1307-1320.e22 (2018).

170. Woo, V. *et al.* Commensal segmented filamentous bacteria-derived retinoic acid primes host defense to intestinal infection. *Cell Host Microbe* 1–13 (2021) doi:10.1016/j.chom.2021.09.010.

171. Eriguchi, Y. *et al.* Essential role of IFN-γ in T cell–associated intestinal inflammation. *JCI Insight* **3**, (2018).

172. Tanoue, T. *et al.* A defined commensal consortium elicits CD8 T cells and anti-cancer immunity. *Nature* **565**, 600–605 (2019).

173. Shah, K., Ignacio, A., McCoy, K. D. & Harris, N. L. The emerging roles of eosinophils in mucosal homeostasis. *Mucosal Immunol.* 1–10 (2020) doi:10.1038/s41385-020-0281-y.

174. Lee, J. J. *et al.* Defining a link with asthma in mice congenitally deficient in eosinophils. *Science (80-.).* **305**, 1773–1776 (2004).

175. Sasajima, N. *et al.* Role of intestinal Bifidobacterium pseudolongum in dietary fructo-oligosaccharide inhibition of 2,4-dinitrofluorobenzene-induced contact hypersensitivity in mice. *Br. J. Nutr.* **103**, 539–548 (2010).

176. Stuart, T. *et al.* Comprehensive Integration of Single-Cell Data. *Cell* **177**, 1888-1902.e21 (2019).

177. Finak, G. *et al.* MAST: a flexible statistical framework for assessing transcriptional changes and characterizing heterogeneity in single-cell RNA sequencing data. *Genome Biol. 2015 161* **16**, 1–13 (2015).

178. Alexa, A., Rahnenführer, J. & Lengauer, T. Improved scoring of functional groups from gene expression data by decorrelating GO graph structure. *Bioinformatics* **22**, 1600–1607 (2006).

179. Lobel, L., Cao, Y. G., Fenn, K., Glickman, J. N. & Garrett, W. S. Diet posttranslationally modifies the mouse gut microbial proteome to modulate renal function. *Science* **369**, 1518–1524 (2020).

180. Thompson, L. R. *et al.* A communal catalogue reveals Earth's multiscale microbial diversity. *Nat. 2017 5517681* **551**, 457–463 (2017).

181. Comeau, A. M., Douglas, G. M. & Langille, M. G. I. Microbiome Helper: a Custom and Streamlined Workflow for Microbiome Research. *mSystems* **2**, (2017).

182. Caporaso, J. G. *et al.* QIIME allows analysis of high-throughput community sequencing data. *Nat. Methods* **7**, 335–336 (2010).

183. Quast, C. *et al.* The SILVA ribosomal RNA gene database project: improved data processing and web-based tools. *Nucleic Acids Res.* **41**, D590 (2013).

184. McMurdie, P. J. & Holmes, S. phyloseq: An R Package for Reproducible Interactive Analysis and Graphics of Microbiome Census Data. *PLoS One* **8**, e61217 (2013).

185. McKenzie, G. J., Bancroft, A., Grencis, R. K. & McKenzie, A. N. J. A distinct role for interleukin-13 in Th2-cell-mediated immune responses. *Curr. Biol.* **8**, 339–342 (1998).

186. Zhang, Y. *et al.* Coding of sweet, bitter, and umami tastes: different receptor cells sharing similar signaling pathways. *Cell* **112**, 293–301 (2003).

187. Hoft, D. F., Lynch, R. G. & Kirchhoff, L. V. Kinetic analysis of antigen-specific immune responses in resistant and susceptible mice during infection with Trypanosoma cruzi. *J. Immunol.* **151**, 7038–47 (1993).

188. Filbey, K. J. *et al.* Innate and adaptive type 2 immune cell responses in genetically controlled resistance to intestinal helminth infection. *Immunol. Cell Biol.* **92**, 436–48 (2014).

189. Reed, D. R. *et al.* Polymorphisms in the Taste Receptor Gene (Tas1r3) Region Are Associated with Saccharin Preference in 30 Mouse Strains. *J. Neurosci.* **24**, 938 (2004).

190. Max, M. *et al.* Tas1r3, encoding a new candidate taste receptor, is allelic to the sweet responsiveness locus Sac. *Nat. Genet.* **28**, 58–63 (2001).

191. Hass, N., Schwarzenbacher, K. & Breer, H. T1R3 is expressed in brush cells and ghrelin-producing cells of murine stomach. *Cell Tissue Res.* **339**, 493–504 (2010).

192. Deckmann, K. *et al.* Bitter triggers acetylcholine release from polymodal urethral chemosensory cells and bladder reflexes. *Proc. Natl. Acad. Sci. U. S. A.* **111**, 8287–8292

(2014).

193. Yan, K. S. *et al.* Intestinal Enteroendocrine Lineage Cells Possess Homeostatic and Injury-Inducible Stem Cell Activity. *Cell Stem Cell* **21**, 78-90.e6 (2017).

194. Chaudhari, N. & Roper, S. D. The cell biology of taste. *Journal of Cell Biology* vol. 190 285–296 (2010).

195. Kojima, I. *et al.* Return of the glucoreceptor: Glucose activates the glucose-sensing receptor T1R3 and facilitates metabolism in pancreatic β-cells. *J. Diabetes Investig.* **6**, 256 (2015).

196. Philippaert, K. *et al.* Steviol glycosides enhance pancreatic beta-cell function and taste sensation by potentiation of TRPM5 channel activity. *Nat. Commun.* **8**, 14733 (2017).

197. Reimann, F. *et al.* Glucose sensing in L cells: a primary cell study. *Cell Metab.* **8**, 532–539 (2008).

198. Koehler, J. A. *et al.* GLP-1R agonists promote normal and neoplastic intestinal growth through mechanisms requiring Fgf7. *Cell Metab.* **21**, 379–391 (2015).

199. Drucker, D. J., Ehrlich, P., Asa, S. L. & Brubaker, P. L. Induction of intestinal epithelial proliferation by glucagon-like peptide 2. *Proc. Natl. Acad. Sci. U. S. A.* **93**, 7911–7916 (1996).

200. Kokrashvili, Z., Mosinger, B. & Margolskee, R. F. T1r3 and alpha-gustducin in gut regulate secretion of glucagon-like peptide-1. *Ann. N. Y. Acad. Sci.* **1170**, 91–94 (2009).

201. Westphalen, C. B. *et al.* Long-lived intestinal tuft cells serve as colon cancer-initiating cells. *J. Clin. Invest.* **124**, 1283–1295 (2014).

202. Jang, H. J. *et al.* Gut-expressed gustducin and taste receptors regulate secretion of glucagon-like peptide-1. *Proc. Natl. Acad. Sci. U. S. A.* **104**, 15069–15074 (2007).

203. Bezençon, C., le Coutre, J. & Damak, S. Taste-signaling proteins are coexpressed in solitary intestinal epithelial cells. *Chem. Senses* **32**, 41–49 (2007).

204. Fushan, A. A., Simons, C. T., Slack, J. P., Manichaikul, A. & Drayna, D. Allelic Polymorphism within the TAS1R3 Promoter is Associated with Human Taste Sensitivity to Sucrose. *Curr. Biol.* **19**, 1288 (2009).

205. Damak, S. *et al.* Detection of sweet and umami taste in the absence of taste receptor T1r3. *Science (80-.).* **301**, 850–853 (2003).

206. Damak, S. *et al.* Trpm5 Null Mice Respond to Bitter, Sweet, and Umami Compounds. *Chem. Senses* **31**, 253–264 (2006).

207. Toma, I. *et al.* Succinate receptor GPR91 provides a direct link between high glucose levels and renin release in murine and rabbit kidney. *J. Clin. Invest.* **118**, (2008).

208. Camberis, M., Le Gros, G. & Urban, J. Animal model of Nippostrongylus brasiliensis and Heligmosomoides polygyrus. *Curr. Protoc. Immunol.* **Chapter 19**, (2003).

209. Miyoshi, H. & Stappenbeck, T. S. In vitro expansion and genetic modification of gastrointestinal stem cells in spheroid culture. *Nat. Protoc.* **8**, 2471–82 (2013).

210. Picelli, S. *et al.* Full-length RNA-seq from single cells using Smart-seq2. *Nat. Protoc. 2013 91* **9**, 171–181 (2014).

211. Langmead, B., Trapnell, C., Pop, M. & Salzberg, S. L. Ultrafast and memory-efficient alignment of short DNA sequences to the human genome. *Genome Biol.* **10**, 1–10 (2009).

212. Li, B. & Dewey, C. N. RSEM: Accurate transcript quantification from RNA-Seq data with or without a reference genome. *BMC Bioinformatics* **12**, 1–16 (2011).

213. Love, M. I., Huber, W. & Anders, S. Moderated estimation of fold change and dispersion for RNA-seq data with DESeq2. *Genome Biol.* **15**, 1–21 (2014).

214. Beura, L. K. *et al.* Normalizing the environment recapitulates adult human immune traits in laboratory mice. *Nature* **532**, 512–516 (2016).

215. Huggins, M. A. *et al.* Microbial Exposure Enhances Immunity to Pathogens Recognized by TLR2 but Increases Susceptibility to Cytokine Storm through TLR4 Sensitization. *Cell Rep.* **28**, 1729-1743.e5 (2019).

216. Kouro, T. & Takatsu, K. IL-5- and eosinophil-mediated inflammation: from discovery to therapy. *Int. Immunol.* **21**, 1303–1309 (2009).

217. Masterson, J. C., Menard-Katcher, C., Larsen, L. D., Furuta, G. T. & Spencer, L. A. Heterogeneity of Intestinal Tissue Eosinophils: Potential Considerations for Next-Generation Eosinophil-Targeting Strategies. *Cells* **10**, 426 (2021).

218. Larsen, L. D., Dockstader, K., Olbrich, C. L., Cartwright, I. M. & Spencer, L. A. Modulation of surface CD11c expression tracks plasticity in murine intestinal tissue eosinophils. *J. Leukoc. Biol.* (2022) doi:10.1002/JLB.3HI0821-432RR.

219. Dolitzky, A. *et al.* Transcriptional Profiling of Mouse Eosinophils Identifies Distinct Gene Signatures Following Cellular Activation. *Front. Immunol.* **12**, 802839 (2021).

220. Hughes, T. K. *et al.* Second-Strand Synthesis-Based Massively Parallel scRNA-Seq Reveals Cellular States and Molecular Features of Human Inflammatory Skin Pathologies. *Immunity* **53**, 878-894.e7 (2020).

221. Atarashi, K. *et al.* Th17 Cell Induction by Adhesion of Microbes to Intestinal Epithelial Cells. *Cell* **163**, 367–380 (2015).

222. Banerjee, A. *et al.* Succinate Produced by Intestinal Microbes Promotes Specification of Tuft Cells to Suppress Ileal Inflammation. *Gastroenterology* **159**, 2101-2115.e5 (2020).